Journal of Medicinal Chemistry

pubs.acs.org/jmc Article

Discovery of a Novel Bromodomain and Extra Terminal Domain (BET) Protein Inhibitor, I-BET282E, Suitable for Clinical Progression

Published as part of the Journal of Medicinal Chemistry special issue "Epigenetics 2022".

Katherine L. Jones,* Dominic M. Beaumont, Sharon G. Bernard, Rino A. Bit, Simon P. Campbell, Chun-wa Chung, Leanne Cutler, Emmanuel H. Demont, Kate Dennis, Laurie Gordon, James R. Gray, Michael V. Haase, Antonia J. Lewis, Scott McCleary, Darren J. Mitchell, Susanne M. Moore, Nigel Parr, Olivia J. Robb, Nicholas Smithers, Peter E. Soden, Colin J. Suckling, Simon Taylor, Ann L. Walker, Robert J. Watson, and Rab K. Prinjha

Cite This: *J. Med. Chem.* 2021, 64, 12200−12227 Read Online

ACCESS | Metrics & More | Article Recommendations | Supporting Information

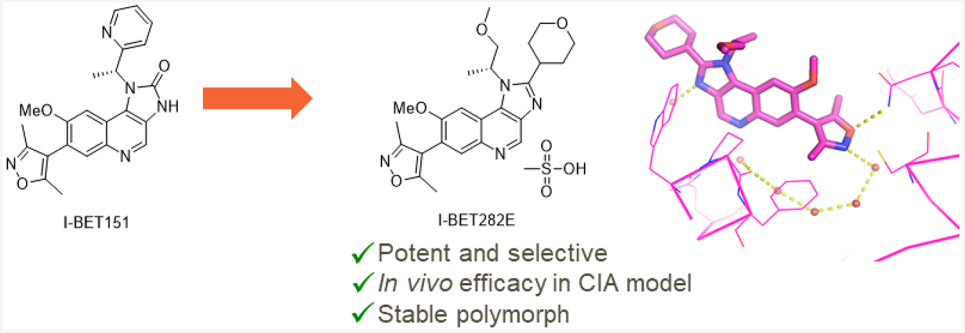

ABSTRACT: The functions of the bromodomain and extra terminal (BET) family of proteins have been implicated in a wide range of diseases, particularly in the oncology and immuno-inflammatory areas, and several inhibitors are under investigation in the clinic. To mitigate the risk of attrition of these compounds due to structurally related toxicity findings, additional molecules from distinct chemical series were required. Here we describe the structure- and property-based optimization of the *in vivo* tool molecule I-BET151 toward I-BET282E, a molecule with properties suitable for progression into clinical studies.

INTRODUCTION

As a result of a wide range of disease-relevant biology, there has been significant interest in the inhibition of functions of the bromodomain and extra terminal (BET) family of proteins by small molecule inhibitors of their bromodomains. Bromodomains are ∼110 amino acid structural domains within proteins that were first reported in 1992.[1,2] Structural and site-directed mutagenesis studies of the bromodomain of P300/CBP-associated factor (PCAF) provided evidence that the bromodomain interacts specifically with acetylated lysine residues, an epigenetic histone modification that is important for transcription.[3] The acetylation of lysine residues on histone tails has a direct effect on the structure of chromatin. This is due to the neutralization of the charge present on lysine amino acid side chains at physiological pH. This results in activated states of chromatin, as the DNA is more accessible to transcription factors.[4]

There are 46 known human bromodomain-containing proteins, which contain a total of 61 bromodomain sequence domains.[5] Proteins containing bromodomains can be classified into several families, one of which is the "bromodomain (B) and extra−terminal (ET)", or BET, proteins. In humans, there are four BET proteins (BRD2, BRD3, BRD4, and BRDT) which exhibit similar gene arrangements, domain organizations, and some functional properties; each of these proteins contains two bromodomains (BD1 and BD2) and one ET domain.[6] The four BET proteins have all been shown to bind acetylated lysines, although their preference for which lysine mark, and on which histone, differs. There is over 75% homology between each of the *N*-terminals (BD1) and each of the *C*-terminals (BD2) across the BET family proteins, although only approximately 44% homology between the *N*-terminal and *C*-terminal bromodomain within the same

Received: May 11, 2021
Published: August 13, 2021

https://doi.org/10.1021/acs.jmedchem.1c00855
J. Med. Chem. 2021, 64, 12200−12227

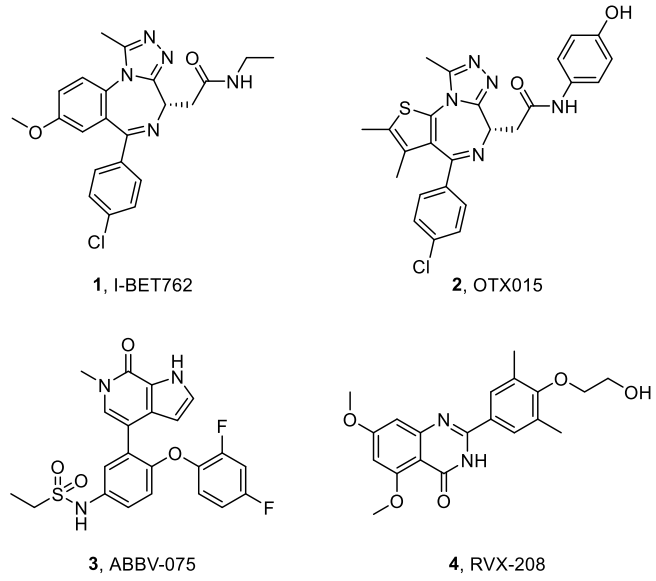

Figure 1. Selected BET bromodomain inhibitors currently being progressed in clinical trials.

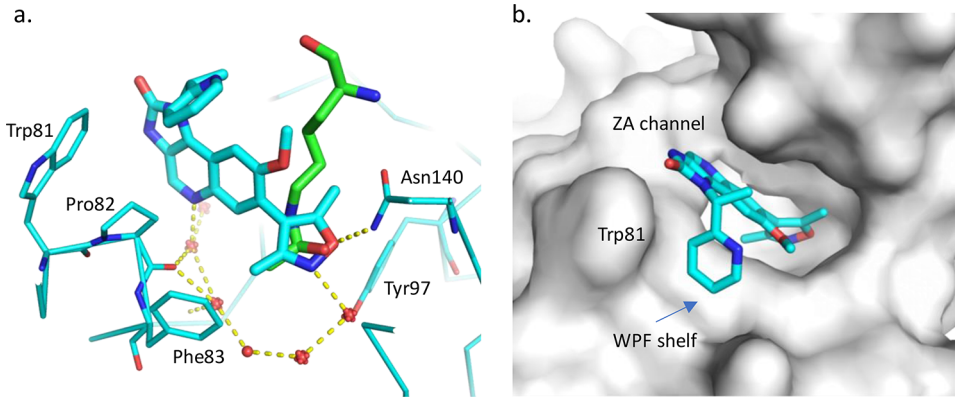

Figure 2. I-BET151 bound to the *N*-terminal bromodomain of BRD4 with key residues labeled (PDB: 3ZYU, cyan). (a) I-BET151 shown in stick format overlaid with acetylated lysine residue of peptide from PDB: 2DVQ (green). (b) Solvent-accessible protein surface of BRD4 with WPF shelf highlighted. (PDB: 3ZYU) overlaid with acetylated lysine residue of peptide from PDB: 2DVQ.

protein.[7] However, in all cases, the amino acid residues critical for binding acetylated lysine residues are conserved.

Published research has provided a rationale for targeting BET proteins in cancer. A cell-penetrant small molecule inhibitor of the BET family of bromodomains, (+)-JQ1, was shown to have antitumor efficacy in xenograft models of nuclear protein in testes (NUT) midline carcinoma (NMC).[8] NMC is characterized by a recurrent t(15;19) chromosomal translocation and the expression of a fusion protein containing NUT and BRD3/4. Subsequent to the initial research on (+)-JQ1, it has been shown that BET inhibitors may have therapeutic potential in a wider range of cancers. BET inhibitors have been shown to down regulate key genes in cell-proliferation such as c-Myc, and have shown efficacy in *in vivo* models of multiple myeloma, prostate cancer, neuroblastoma, and leukemia.[9−14]

As well as their potential utility as anticancer agents, strong evidence has also been provided for targeting BET bromodomains in inflammation. Work within our own laboratories showed that a potent, selective inhibitor of the BET family of bromodomains, I-BET762 (**1**, Figure 1), has anti-inflammatory potential.[15] I-BET762, which has a similar structure, as well as *in vitro* potency and selectivity profile, to (+)-JQ1 was shown to disrupt chromatin complexes responsible for the expression of key inflammatory genes in activated macrophages. Additionally, in an *in vivo* model of LPS-induced endotoxic shock, administration of I-BET762 both 1 h prior and 1.5 h after stimulation prevented or delayed the death of the mice.

Outside the oncology and immuno-inflammatory areas, it has been shown that BRD4 has a role in virus-induced pathogenesis and is a potential target for drug development with a view to controlling HPV-induced human diseases, including genital warts, skin tumors, and cervical cancers.[16,17] In addition, whole-body disruption of BRD2 in mice led to severe obesity while avoiding the development of Type 2 diabetes and enhancing glucose tolerance. This suggests that the BET family of proteins may also be relevant in metabolic diseases.[18]

A number of BET bromodomain inhibitors have already been reported as having progressed to clinical trials (Figure 1).[19,20] Those with disclosed chemical structures included I-BET762 (**1**) from within our laboratories,[21] the structurally related Oncoethix inhibitor OTX015 (**2**),[22] and the structurally distinct Abbvie inhibitor ABBV-075 (**3**)[23] being progressed for oncology indications, and the structurally

https://doi.org/10.1021/acs.jmedchem.1c00855
J. Med. Chem. 2021, 64, 12200−12227

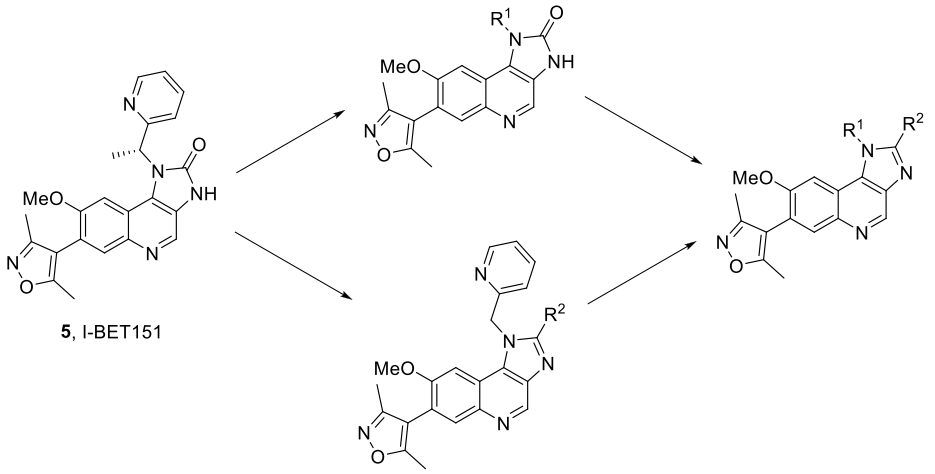

Figure 3. Medicinal chemistry design strategy for optimization of I-BET151.

distinct pan-BD2 biased Resverlogix inhibitor RVX-208 (**4**),[24,25] being assessed in a range of cardiovascular diseases.

Recent literature has begun to elucidate the phenotype of inhibitors of only the first or second bromodomains of the BET proteins.[26] However, given the wide range of profound effects across biological pathways relevant to many different therapeutic areas, the potential of pan-BET bromodomain inhibition remains worthy of serious investigation. To enhance the probability of success in providing novel medicines to patients, multiple clinically enabled molecules of diverse chemotypes are of significant value.[27] This helps to minimize the risk of off-target toxicity associated with any clinical candidate (since the selectivity profile of any molecule cannot be fully assessed via proteomics) or any developability issue associated with the compound itself (such as a reactive metabolite, lack of a stable crystalline form, limited solubility, or a risk of genotoxicity). In this manuscript, we describe the identification of I-BET282E, a structurally distinct pan-BET bromodomain inhibitor with properties suitable for progression into clinical studies.

RESULTS AND DISCUSSION

In parallel with our clinical investigations with I-BET762, chemotypes with alternative structural features acting as the acetyl lysine mimetic were developed. Key among these were compounds of the dimethylisoxazole family, exemplified by I-BET151 (**5**, Figure 3).[28] Here, the dimethylisoxazole moiety acted as the acetyl lysine mimetic, with the pyridine bound within the WPF shelf and the quinoline ring system in the ZA channel. The dimethylisoxazole motif is widely established within small molecule bromodomain inhibitors, most extensively in the BET[29−33] and CBP[34] proteins.

Compound Design and Biological Activities. Key parameters of the profile of I-BET151 (**5**, Figure 3) and I-BET762 (**1**, Figure 1) are compared in Table 1. As previously reported,[28] I-BET151 is a molecule with encouraging cellular potency, as measured in peripheral blood mononuclear cells (PBMCs), but its activity in the human whole blood assay can be improved upon. This could be achieved either by increasing biochemical potency or reducing the drop-off from the biochemical to cellular assays. Solubility in the biologically relevant fasted state simulated intestinal fluid (FaSSIF) assay is limited, and values much greater than 100 μg/mL from crystalline material would be targeted to mitigate attrition in clinical development. A potential strategy to achieve this would be through lowering the aromatic ring count, with no increase in lipophilicity (as measured by clogP).[35,36] Compound **5** shows low turnover in rat hepatocytes which translates into good exposure following oral administration in vivo.[28] Turnover of compound **5** in human hepatocytes is below the lowest level of quantification of the assay, which is encouraging. This is in sharp contrast to data in the dog which indicated the likelihood that high hepatic clearance will be seen *in vivo*. This will have to be discharged as it will be essential to use this species in preclinical safety studies to enable comparison with the data generated for I-BET762. It is also of note that the modest CYP activity of I-BET151 (**5**) will require improvement to minimize the risk of drug−drug interactions in clinical settings.

Table 1. Comparison of the Developability Profiles of I-BET151 and I-BET762[21,28]

		I-BET762 (**1**)	I-BET151 (**5**)
clogP		2.4	2.3
PBMC pIC_{50}[a]		6.5	6.7
HWB pIC_{50}[a]		6.2	5.9
FaSSIF solubility (μg/mL)		122	66
CYP inhibition IC_{50} (μM)	2C9	>50	9.9
	3A4 (DEF)[b]	>50	9.7
CL_i (hepatocytes, mL/min/g liver)	rat	<0.86	<0.86
	dog	<1.7	9.8
	human	<0.86	<0.86

[a]LPS-stimulated PMBC/HWB assay, measuring IL-6. [b]DEF refers to the probe substrate used to determine the CYP3A4 inhibition profile.

As the protein target was not known at the time the medicinal chemistry to discover I-BET151 was performed, this compound was optimized from the 7-isoxazoquinoline series without access to X-ray crystallographic data. With access to the X-ray crystal structure of I-BET151 bound to the *N*-terminal bromodomain of BRD4 (Figure 2), we devised a medicinal chemistry strategy for further optimization.

Inspection of the X-ray data, and of previous SAR, identified the areas of binding which contributed to potency. The dimethylisoxazole of I-BET151 bound into the acetylated lysine binding site of the bromodomain via a bridging water molecule to the hydroxyl of Tyr97.[29,30] This structural water

https://doi.org/10.1021/acs.jmedchem.1c00855
J. Med. Chem. 2021, 64, 12200−12227

Table 2. R^1-Subsituent SAR on the I-BET151 Core

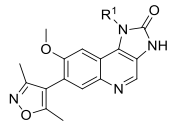

General structure

Compound	R^1	clogP	BRD4-BD1 pIC_{50}[a]	LLE[b]	PBMC pIC_{50}[a]
5		2.3	7.6	5.3	6.7
6	^{i}Pr	3.3	5.9	2.6	5.5
7	^{i}Bu	3.2	6.1	2.9	6.0
8[c]		4.3	6.9	2.6	6.9
9		3.4	6.2	2.8	6.4
10[c]		2.1	6.2	4.1	5.8
11[c]		2.8	6.2	3.4	5.4
12[c]		2.0	6.6	4.6	5.9
13	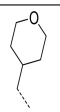	2.7	7.0	4.3	6.7
14[c]	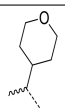	3.1	6.8	3.7	6.7
15		1.4	5.8	4.4	5.8
16		1.1	5.7	4.6	4.8
17	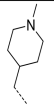	1.4	5.9	4.5	5.5
18		2.2	6.1	3.9	5.8

https://doi.org/10.1021/acs.jmedchem.1c00855
J. Med. Chem. 2021, 64, 12200−12227

Table 2. continued

[a]Expressed as a mean of at least two experimental replicates. [b]LLE is calculated as BRD4-BD1 pIC_{50} − clogP. [c]Compounds are a 1:1 mixture of enantiomers.

Table 3. R^2-Subsituent SAR on the Des-Methyl I-BET151 Core

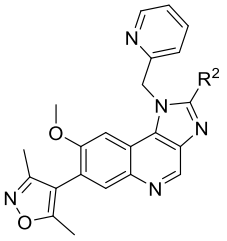

General structure

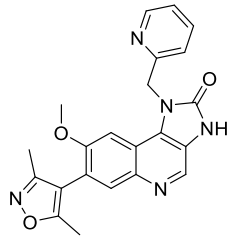

19

Compound	R^2	clogP	BRD4-BD1 pIC_{50}[a]	LLE[b]	PBMC pIC_{50}[a]
19	-	2.0	6.8	4.8	6.3
20	Me	1.7	7.4	5.7	7.4
21	Et	2.3	7.5	5.2	6.8
22	^{n}Pr	2.8	7.6	4.8	6.9
23	^{i}Pr	2.7	7.4	4.7	6.8
24	NH_2	1.4	7.4	6.0	6.8
25	$NHCH_2CH_2OCH_3$	2.9	7.5	4.6	7.0
26	CH_2OCH_3	1.5	7.2	5.7	6.4
27		1.7	7.2	5.5	6.6

[a]Expressed as a mean of at least two experimental replicates. [b]LLE is calculated as BRD4-BD1 pIC_{50} − clogP.

was part of a network of water molecules in the acetylated lysine binding site. As this was a critical interaction for potency, the dimethylisoxazole was not modified. The pyridine group is bound into the lipophilic "WPF shelf" region of the protein which consists of the side chains of Trp81 (W), Pro82 (P), and Phe83 (F). To access the WPF shelf, the vector from the imidazoquinoline core was critical, and therefore we did not make any alterations to the triaryl core structure. However, although this was identified as a lipophilic region, the X-ray structure did not suggest any reason why the substituent interacting with the WPF shelf needed to be aromatic. This was therefore an area open to optimization, for example, by replacement of the pyridine with cyclic and acyclic alkyl, ether, and amine substituents. The crystallographic data also identified the imidazoquinolinone 2-position as a vector where further substitution would be tolerated; therefore, this could be investigated as a handle for modulating the physicochemical properties of the molecule. Indeed, as recently published work carried out concurrently within our laboratories shows, substitution with a small ether group in this position increased potency.[37] The medicinal chemistry strategy was to optimize both substituents independently, followed by the combination of favored groups into compounds which

https://doi.org/10.1021/acs.jmedchem.1c00855
J. Med. Chem. 2021, 64, 12200−12227

Table 4. Optimized Molecules Combining Favored R^1- and R^2-Substituents

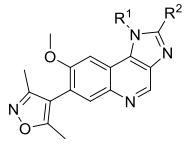

General structure

Compound	R^1	R^2	clogP	BRD4-BD1 pIC_{50}[a]	LLE[b]	PBMC pIC_{50}[a]	HWB (IL-6) pIC_{50}[a]
28[d]	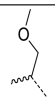		1.5	6.7	5.2	6.2	-[c]
29			1.5	7.1	5.6	6.4	-[c]
30			2.4	6.9	4.5	6.5	5.7
31[d]			1.7	7.0	5.3	6.9	6.4
32 (I-BET282)			1.7	7.4	5.7	7.0	6.5
33	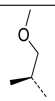		1.7	6.8	5.1	6.3	6.5
34[d]			2.0	7.5	5.5	7.0	6.7
35			2.5	7.5	5.0	7.4	6.6
36			1.8	7.4	5.6	7.6	6.6
37			2.5	7.9	5.4	7.5	6.8
25[e]	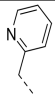		2.9	7.5	4.6	7.0	6.4

[a]Expressed as a means of at least two experimental replicates. [b]LLE is calculated as BRD4-BD1 pIC_{50} − clogP. [c]Not tested. [d]Compounds are a 1:1 mixture of enantiomers. [e]Compound **25** from Table 3 included to show HWB data.

would be assessed as potential preclinical candidate molecules (Figure 3).

The substituents designed for the imidazoquinolone R^1-position were chosen to reduce the aromatic ring count by

https://doi.org/10.1021/acs.jmedchem.1c00855
J. Med. Chem. 2021, 64, 12200−12227

replacement of the pyridine (Table 2). Because of the lipophilicity of the WPF shelf, several small alkyl (compounds **6**–**9**) and ether (compounds **10**–**15**) substituents were designed. The biochemical potency of compounds at the first bromodomain of BRD4 was measured using a TR-FRET assay, where the second bromodomain of BRD4 was mutated (Y390A) to prevent compound binding. Lipophilic ligand efficiencies (LLEs)[38] of the alkyl compounds **6**–**9** were significantly lower than that of I-BET151; all LLEs were between 2.6 and 2.9, indicating that potency was driven by lipophilic interactions. Compound **10**, the ether analogue of compound **8**, had reduced potency; however, there was a significant increase in LLE from 2.6 to 4.0. This higher LLE was consistent across all ethers, with the 4-tetrahydropyranyl analogues **13** and **14** standing out in terms of higher potency. Also synthesized were a small number of amines (compounds **16**–**18**) as the pyridine of I-BET151 suggested a basic center could be tolerated in the WPF shelf region of the protein. However, these compounds all showed a significant reduction in potency over I-BET151, and basic substituents were not investigated further. The key advantage of non-aryl R^1-substituents was seen in the LPS-stimulated PBMC assay, where in almost all examples there was a lower drop-off between the biochemical and cellular assays. This was particularly striking for compounds **13** and **14**. Overall, the optimization of the R^1-substituent resulted in the identification of several non-aryl pyridine replacements, with the ether-containing substituents giving a particularly advantageous balance between good cellular potency and low lipophilicity.

The opportunity for substitution in the imidazoquinoline R^2-position, as hypothesized using the X-ray crystal structure, was confirmed by exploring a small set of alkyl substituents (**20**–**23**) on the simplified des-methyl analogue **19** of I-BET151 (Table 3). These conveyed a significant increase in potency over the imidazolone **19**, and the isopropyl **23** showed that branching was tolerated. In compounds **20**–**22**, LLE was either maintained or increased versus compound **19**. On the basis of these examples, heteroalkyl groups such as amines **24**–**25** and ethers **26**–**27** were introduced. Both the amines showed increased biochemical and cellular potency over the baseline compound **19**, and as for the R^1-substituent, the ethers maintained the cellular potency of compound **19** while reducing lipophilicity.

Using the results generated for the individual R^1- and R^2-substituent changes (Tables 2 and 3), a set of analogues were synthesized combining the most promising substituents (Table 4). In addition, two additional amine R^2-substituents were added (dimethylamino **35** and morpholino **36**) to maintain the amine functionality of **24** and **25** while reducing hydrogen bond donor count to give an increased chance of good passive permeability.[39] *In silico* profiling prior to synthesis was used to prioritize targets with low predicted lipophilicity.

While having reasonable biochemical potency, compounds with the small methoxymethyl R^2-substituents (**28**–**29**) had poor cellular potency. This poor cellular potency was also seen for analogue **30**. Compound **31** had a promising biochemical and cellular potency and showed minimal potency drop-off into the LPS-stimulated human whole blood (HWB) assay. This compound was therefore separated into the single enantiomers **32** and **33** using chiral HPLC. Of these, the *R*-enantiomer **32** was preferred due to its higher biochemical potency. Compounds with the 4-tetrahydropyranyl R^1-substituent (**34**–**36**) were among the most potent analogues, reflecting its observed higher potency in initial SAR studies (Table 2), as was the compound containing an aryl R^1-substituent (**37**).

Of the optimized compounds, three were identified as the most likely to deliver the desired preclinical profile. These included bis-ether **32**, the dimethylamino substituted **35**, and the pyridyl analogues **37**. The pyridyl analogue **25** (Table 3) also showed suitable potency in the HWB assay and was further profiled. These preferred compounds were selected based on their biochemical and cellular potency; additionally, compounds **34** and **36** were deprioritized due to challenges associated with their synthesis, which precluded a rapid and cost-effective large-scale preparation. The CYP2C9 and 3A4 inhibition profiles of the lead compounds were generated (Table 5). Compounds **35** and **37** were discounted for further progression due to the lower but significant level of CYP inhibition. Ultimately, compound **32** was selected over compound **25** due to its lower aromatic ring count and the associated lower risk of toxicity.[35]

Table 5. CYP2C9 and 3A4 Profiles of Lead Compounds in Comparison with I-BET151

	CYP inhibition IC_{50} (μM)	
compound	2C9	3A4(VG)[a]
5	9.9	9.7
32	>50	25.1
35	1.3	10
25	31.6	15.8
37	7.9	7.9

[a]VG refers to the probe substrate used to determine the CYP3A4 inhibition profile.

Compound Synthesis. The synthesis of compounds was built upon key quinoline-isoxazole intermediates whose synthesis have been previously described.[23] These intermediates were then diversified to provide access to the compounds described within this manuscript.

Modifications of the R^1-position of the imidazoquinolinone (Table 2), compounds **6**–**18**, were installed in two steps (Scheme 1) from the 4-chloroquinoline intermediate **39**.[23] Compound **39** underwent nucleophilic aromatic substitution (S_NAr) with the appropriate aliphatic amines giving intermediates **40**–**52**. These were converted to final products **6**–**18** via a Hoffman-type rearrangement using hypervalent iodine and potassium hydroxide.[40] This was followed, in the case of compound **16**, by deprotection of the piperidine.

The majority of modifications of the R^2-position of the imidazoquinoline (Table 3), compounds **20**–**23**, and **26**–**27**, were installed from the quinoline diamine **53**[23] via amide formation and acid-mediated cyclization (Scheme 2). The remaining compounds were prepared directly from the quinoline diamine **53** (Scheme 3). Compound **19** was prepared using a Hoffman-type rearrangement, compound **24** using cyanic bromide, and compound **25** using 1-isothiocyanato-2-methoxyethane followed by EDC.

To combine the preferred groups at the R^1- and R^2-positions of the imidazoquinoline, the key 3-nitro,4-chloro intermediate **63** was prepared (Scheme 4). The acid of compound **60**[23] was decarboxylated by addition to refluxing diphenyl ether to give compound **61**. Compound **61** was nitrated to give compound **62**, which was chlorinated using phosphorus oxychloride, to give compound **63**.

https://doi.org/10.1021/acs.jmedchem.1c00855
J. Med. Chem. 2021, 64, 12200−12227

Scheme 1. Access to Compounds with Diverse R^1 Functionality[a]

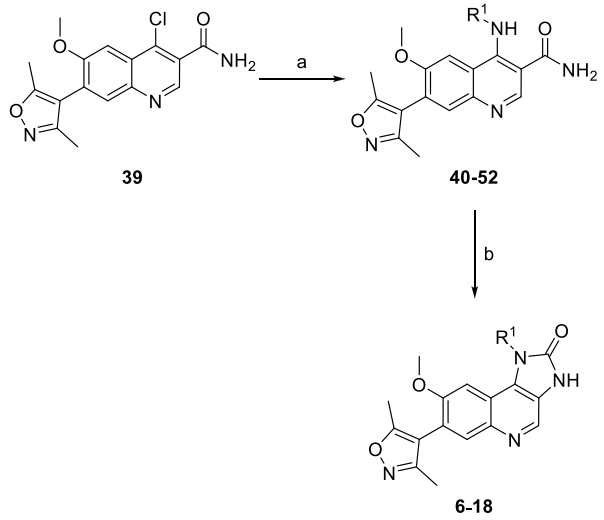

[a]Reagents and conditions: (a) R^1NH_2, DIPEA, NMP, 100−120 °C, 14−100%; (b) $PhI(OAc)_2$, KOH, MeOH, 0 °C, 6−89%, followed by TFA, DCM, r.t., 83% for compound **16**.

Scheme 2. Access to Compounds with C-Linked R^2 Functionality[a]

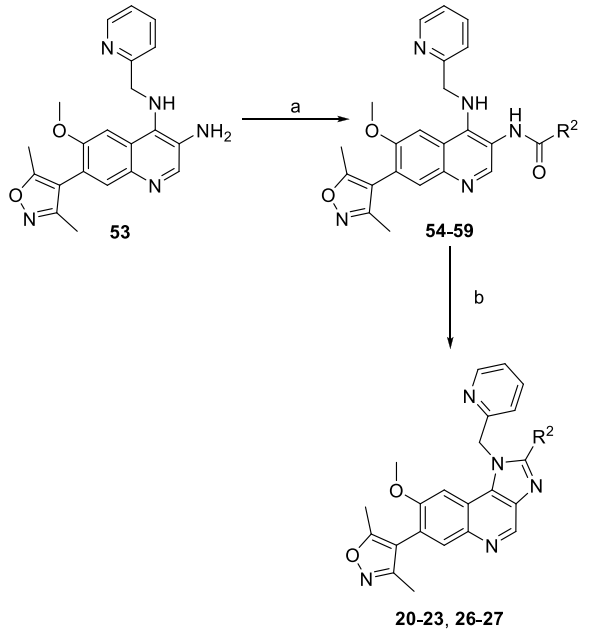

[a]Reagents and conditions: (a) $(R^2CO)_2O/R^2COCl$, pyridine, DCM, r.t., 59−72%, or R^2COOH, HATU, DIPEA, or NEt_3, DCM, r.t., 61−82%; (b) AcOH reflux, 26−79%.

The chloro-nitro intermediate **63** was converted to the final compounds **28**−**29**, **31**, and **34**, via nucleophilic aromatic substitution, reduction of the nitro group, amide formation, and acid-mediated cyclization (Scheme 5). Compound **31** was separated into its constituent enantiomers **32** and **33** by chiral HPLC.

Using intermediates prepared as above (Scheme 5), the remaining compounds were synthesized via a range of bespoke conditions to access the desired substituents (Scheme 6). Compound **30** was prepared using a one-step reductive

Scheme 3. Access to Compounds with Heteroatom Linked R^2 Functionality[a]

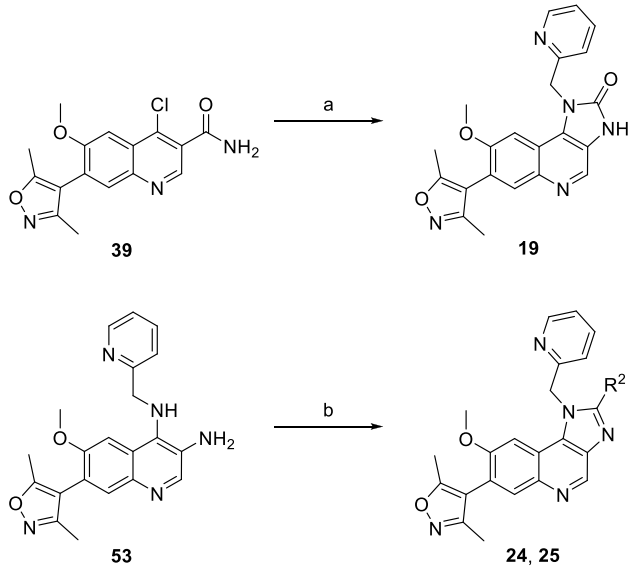

[a]Reagents and conditions: (a) (i) pyridin-2-ylmethanamine, CH_3CN, reflux; (ii) $PhI(O(CO)CF_3)_2$, CH_3CN, 50 °C, 54% over two steps; (b) **24**: BrCN, EtOH, 60 °C, 32%, **25**: (i) $MeO(CH_2)_2NCS$, EtOH, 60 °C, (ii) EDC, THF 60 °C, 2%.

Scheme 4. Access to Key Intermediate 62[a]

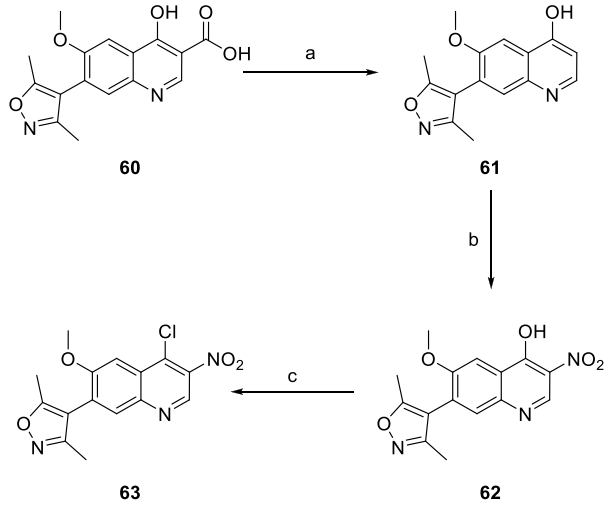

[a]Reagents and conditions: (a) Ph_2O, reflux, 88%; (b) HNO_3, propionic acid, 100 °C, 72%; (c) $POCl_3$, 120 °C, 75%.

cyclization as a more rapid alternative to the two-step route used to prepare earlier compounds. Compound **36** was synthesized from the imidazolone **13** via formation of the heteroaryl chloride, and compound **35** was formed using a commercially available starting material to insert the dimethylamino substituent. Primary aryl amine **37** was accessed using a thiocyanate to form the thiourea, followed by cyclization mediated by EDC.

Preclinical Developability Profile. Compound **32**, hereon named I-BET282, showed an excellent preclinical developability profile. The compound was tested against an in-house developability panel of 38 unrelated proteins representing key safety considerations, and only a weak inhibition of the hERG potassium ion channel (pIC_{50} 4.4−

https://doi.org/10.1021/acs.jmedchem.1c00855
J. Med. Chem. 2021, 64, 12200−12227

Scheme 5. General Route to Compounds with Diverse R^1 and R^2 Functionality[a]

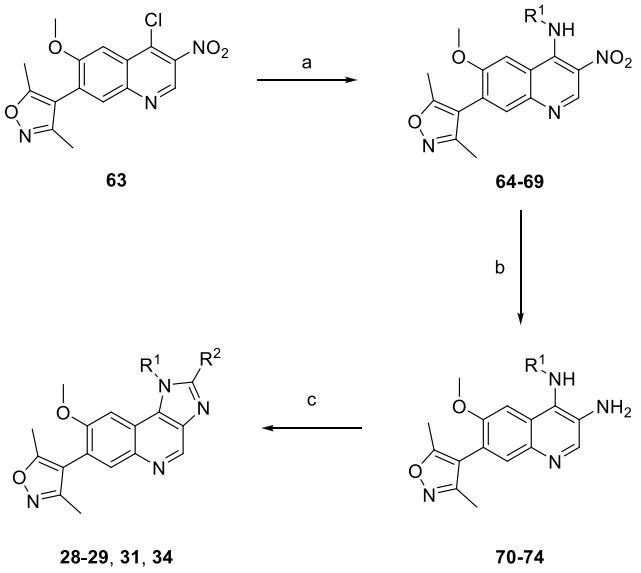

[a]Reagents and conditions: (a) R^1NH_2, DIPEA, NMP, 100 °C, 19−85% or R^1NH_2, 1,4-dioxane, r.t., 73−92%; (b) H_2, 10% Pd/C EtOAc, EtOH 20 °C 93−96% or $SnCl_2$, EtOH, 40 °C 36−96%; (c) (i) R^2COCl, pyridine, DCM r.t. or R^2COOH, HATU, DIPEA, DMF, r.t.; (ii) AcOH 120 °C; or pTSA, toluene, reflux; or NH_3, $(NH_4)_2HCO_3$, acetonitrile, r.t. 15−74%.

Scheme 6. Access to Compounds with Diverse R^1 and R^2 Functionality Which Were Not Prepared via the General Method[a]

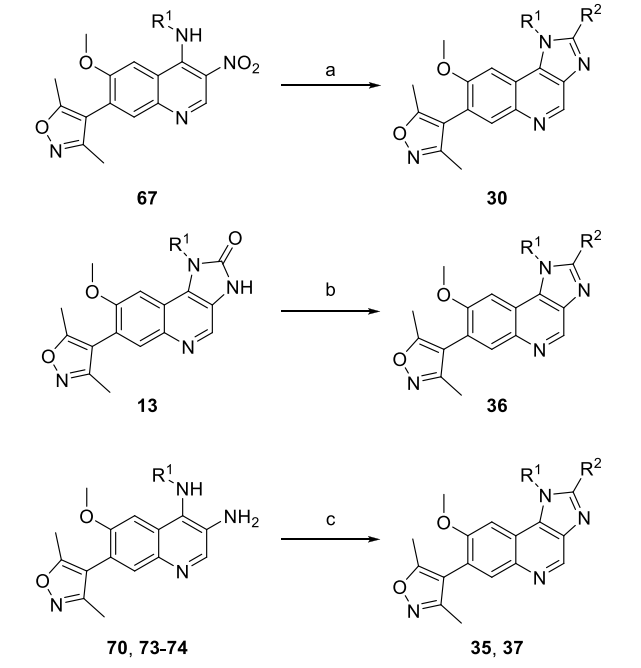

[a]Reagents and conditions: (a) $Na_2S_2O_4$, EtOH, H_2O, R^2COH, 100 °C, 27%; (b) (i) $POCl_3$, PCl_5, 120 °C, (ii) morpholine, NMP, 120 °C, 2%; (c) **35**: *N*-(dichloromethylene)-*N*-methylmethanaminium chloride, MeCN, 120 °C, 77%; **37**: (i) 1-isothiocyanato-2-methoxyethane, EtOH, 60 °C, (ii) EDC, THF, 60 °C, 19%.

5.1 in a variety of assay formats) was identified as a cause for further investigation. The weak hERG inhibition was further investigated using an *ex vivo* rabbit wedge model; the data supported further progression with a 40-fold margin to concentrations in the range expected in humans for cardiovascular findings in this assay system. X-ray crystallographic data in the first bromodomain of BRD4 showed that the compound had a similar binding mode to I-BET151 (Figure 4a,b), as well as GSK788 (Figure 4c,d) which was developed concurrently within our laboratories.[37] As with I-BET151, the dimethylisoxazole bound to the acetyl lysine binding site of the bromodomain, with a direct hydrogen bond to Asn140 and a water-mediated hydrogen bond to Tyr97. The methoxymethyl of the branched imidazoquinoline *N*-substituent bound into the WPF shelf region, with the α-methyl interacting with the lipophilic surface of Leu92. The THP substituent exited through the ZA channel formed by Trp81 and Leu92, showing excellent shape complementarity with the protein surface. In contrast to the BD1 selective GSK788,[37] I-BET282 has no equivalent to the pyrrolidine that interacts with D145 of the "Asp-His" BD1/BD2 selectivity switch (Figure 4d). Consequently, D145 in the I-BET282 structure adopts a conformation swung away from the ligand, giving rise to a more extended WPF shelf, and as a result we expected I-BET282 to maintain equivalent potency against BD1 and BD2 domains.

I-BET282 was confirmed to be a pan-inhibitor of all eight BET bromodomains, and selectivity over other representative bromodomain-containing proteins was also established (see Supporting Information). As the closest off-target, and as a result of the potential for associated toxicity,[41] the selectivity over the bromodomain of CBP was established definitively by biophysical techniques. Thermal shift data showed binding to the bromodomain of CBP (ΔT_m = 3.4 °C cf. ΔT_m = 9.9 °C for BRD4), which was confirmed using isothermal titration calorimetry (ITC). I-BET282 bound to the bromodomain of CBP with an affinity constant determined to be 1.73 ± 0.17 μM by ITC, a 36-fold window to BRD4 as measured by the same technique (47.5 ± 25 nM).

I-BET282 showed a low potential to inhibit CYP proteins *in vitro*, with no evidence of time-dependent inhibition of 2D6 or 3A4 (Table 6). *In vitro* hepatocyte clearance was low across mouse, rat, and human; encouragingly, a significant increase in metabolic stability in dog hepatocytes for I-BET282 (2.4 mL/min/g liver) compared with I-BET151 (9.8 mL/min/g liver) indicated the pharmacokinetics of I-BET282 in the dog may be appropriate for use as a preclinical safety species. I-BET282 had high *in vitro* passive permeability (346 nm/s in MDCK cells) and a moderate free fraction in blood consistent across all species investigated (f_{ub} 0.1−0.2).

The pharmacokinetic profile of the compound was assessed in three preclinical species: mouse, rat, and dog (Table 7). Total blood clearance was low in the mouse and rat (<25% hepatic blood flow, HBF) and higher in the dog (68% HBF). The rate of total clearance *in vivo* was consistent with the pattern of clearance determined in hepatocytes *in vitro* providing confidence that I-BET282 had the potential for low/moderate clearance in humans. Renal clearance determined in rats was negligible at <1% of total clearance, so the major route of elimination was assumed to be metabolism. Volume of distribution was moderate across all species indicating distribution to the tissues. Elimination half-life was considered moderate across all preclinical species indicating the potential for once or twice daily administration in humans. Oral bioavailability of the free base in a suspension formulation

https://doi.org/10.1021/acs.jmedchem.1c00855
J. Med. Chem. 2021, 64, 12200−12227

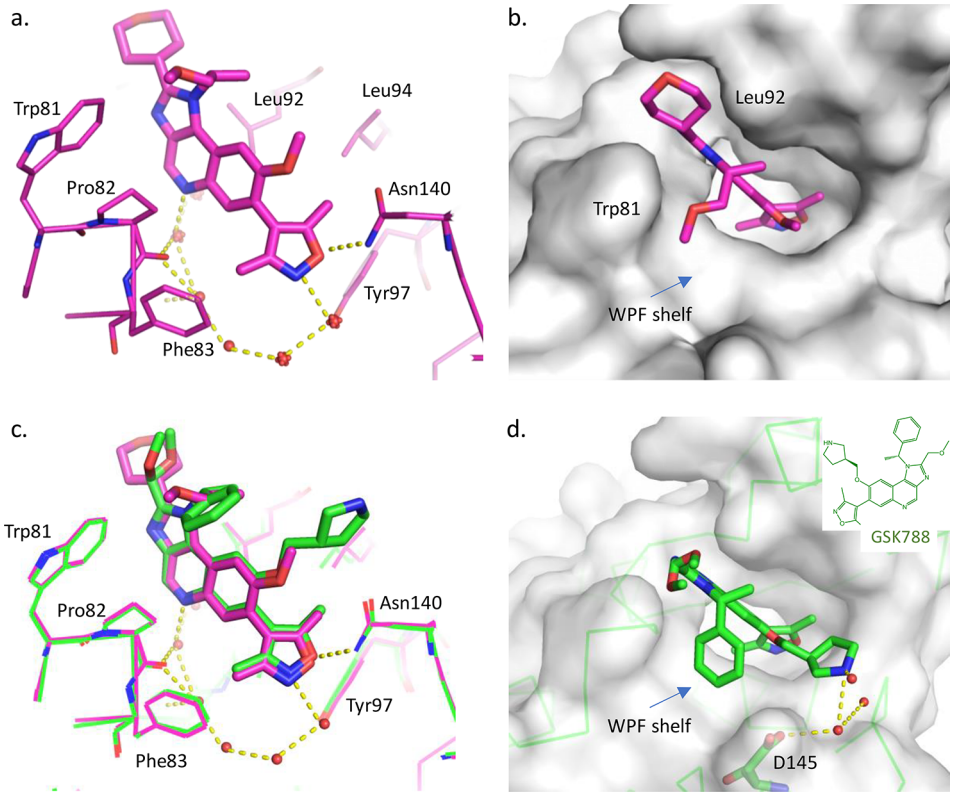

Figure 4. I-BET282 bound to the *N*-terminal bromodomain of BRD4 with key residues labeled (PDB: 7O18, magenta). (a) I-BET282 shown in stick format. (b) Solvent-accessible protein surface of BRD4 with the WPF shelf highlighted. (c, d) Show overlay with GSK788 (PDB: 6SWN, green).

Table 6. CYP2C9 and 3A4 Profiles of Lead Compound I-BET282

assay	test system	mouse	rat	dog	human
metabolic stability (mL/min/g liver)	hepatocytes	<0.86	<0.86	2.4	<0.86
free fraction (f_{ub})[a]	blood	0.10	0.16	0.24	0.17
CYP inhibition profile IC_{50} (μM)[b,c]	singly expressed P450 enzymes	CYP1A2 ER: > 50 CYP2C9 FCA: > 50 CYP2C19 BMC: > 50 CYP2D6 MMC: > 50 CYP3A4 VR: > 50 CYP3A4 VG: > 20			
time-dependent P450 inhibition[c]	singly expressed P450 enzymes	CYP2D6 MMC - no inhibition of CYP2D6 CYP3A4 DEF[c] - no inhibition of CYP3A4, but an increase in IC_{50} 7BQ[c]- could not be determined			

[a]Mean value determined at 100 ng/mL and 1000 ng/mL. [b]Expressed as an average of at least two experimental replicates. [c]ER, FCA, BMC, MMC, VR, VG, DEF, and 7BQ refer to the probe substrates used to determine the CYP inhibition profiles.

Table 7. Pharmacokinetic Profile of I-BET282 in Male CD1 Mice, Male Wistar Han Rats, and Male Beagle Dogs

parameters	mouse[a]	rat[a]	dog[a]
doses i.v.[b], p.o.[c] (mg/kg)	1.4, 3	1, 3	1, 3
Cl_b (mL/min/kg)	23 ± 8	20 ± 6	27 ± 6
% LBF	19	22	68
V_{ss} (L/kg)	1.9 ± 0.1	2.2 ± 0.5	3.1 ± 0.1
$t_{1/2}$ (iv, h)	1.2 ± 0.5	1.4 ± 0.3	1.8 ± 0.2
F, po %	51 ± 15	74 ± 9	31 ± 12

[a]Values are mean, $n = 3 \pm$ SD. [b]i.v. dose was 1 h infusion in DMSO and (10%, w/v) Kleptose HPB in saline (2%:98% (v/v)). [c]p.o. dose vehicle: 1% (w/v) methylcellulose (400 cps) (aq).

ranged between 31% in dogs to 74% in rats. This was broadly consistent with the extent of first-pass extraction in the respective species though with some evidence of absorption limitations, particularly in the mouse. Overall, the DMPK profile was suitable for further development offering the potential for an orally available, low-moderate clearance molecule in humans.

During the preparation of large-scale batches of the free base I-BET282 (compound **32**), powder X-ray diffraction studies (see Supporting Information) revealed multiple crystalline forms. This was undesirable as the presence of multiple crystalline forms can have significant impact during late-stage drug development as well as on marketed drugs.[42] Additionally, the new stable "Form 2" material had a lower measured fasted state solubility of 130 μg/mL, reduced from 480 μg/mL for the "Form 1" material.[43] The low solubility of "Form 2", as well as its multiple crystalline forms, led to concerns over the long-term development of the free base. A salt screen was therefore performed to improve the physical properties of the material which identified the mesylate salt compound **75**, hereon named I-BET282E. Closed samples of the mesylate I-BET282E were stable under three-month accelerated storage conditions. As salt formation impacts the kinetic, rather than thermodynamic, solubility of a compound,[44] the mesylate salt I-BET282E showed a significantly improved dissolution rate

https://doi.org/10.1021/acs.jmedchem.1c00855
J. Med. Chem. 2021, 64, 12200−12227

than the free base of I-BET282, resulting in a 20-fold solubility increase at 30 min (1.8 mg/mL for I-BET282E, 92 μg/mL for I-BET282 Form 2). Additionally, only one crystalline form was observed during polymorph screening of the mesylate I-BET282E. The mesylate salt was therefore selected as the salt form of choice for ongoing preclinical development activities.

Prior to progression into these studies, the oral exposure of I-BET282E administered as the mesylate salt was compared with that following administration as the free base (Table 8).

Table 8. Pharmacokinetic Profile of I-BET282 and I-BET282E in Male Wistar Han Rats and Male Beagle Dogs on Oral Dosing[a]

	rat		dog	
parameter	I-BET282	I-BET282E	I-BET282	I-BET282E
dose (mg/kg)	1	1	5	5
AUC_{0-t} (ng·h/mL)	467 ± 213	348 ± 89	367 ± 122	885 ± 150
C_{max} (ng/mL)	125 ± 34	101 ± 19	177 ± 51	578 ± 182
T_{max} (h)	1	1	0.75	0.375

[a]All doses were administered as an oral suspension prepared in 1% hydroxypropylmethyl cellulose (w/v) in water. Key: Values are mean ± SD, n = 3 for rat, and n = 4 for dog AUC_{0-t} = Area under the plasma concentration−time curve from 0 h to last quantifiable time point. C_{max} = maximum observed plasma concentration. T_{max} = time at which C_{max} is observed and is reported as median.

In the rat, C_{max} and AUC were comparable, whereas in the dog an approximate 3-fold increase in both C_{max} and AUC was observed. These data confirmed that the mesylate salt provided at least equivalent exposure to the free base in preclinical species.

Further to its excellent pharmacokinetic profile, I-BET282E also showed *in vivo* efficacy in a rat model of collagen-induced arthritis (Figure 5). Briefly, the arthritis was established in 4−5 week old female Wistar rats using intradermal injection of bovine collagen and boosted 7 days later with a combination of collagen, muramyl dipeptide (MDP), and incomplete Freund's adjuvant. Compounds were dosed in a peri-onset schedule from day 12 when the rats showed the first signs of arthritis until day 21 when the arthritis was fully established. Dosing with I-BET282E showed a dose-dependent inhibition of clinical score with significant inhibition observed at 3 and 1 mg/kg. Similarly, analysis of microcomputed tomography (CT) scans demonstrated a dose-dependent inhibition of bone resorption and remodeling at the same doses. Dosing of I-BET282E at 3 mg/kg resulted in a more pronounced efficacy than I-BET151 at 3 mg/kg, which was similar to I-BET282E dosed at 1 mg/kg. Both BET inhibitors were well tolerated over the period of the *in vivo* study, as demonstrated by a general improvement in the maintenance of body weight by the highest dosed groups compared to the vehicle control group. We believe the improved pharmacology of I-BET282E over I-BET151 is driven by potency and bioavailability as the

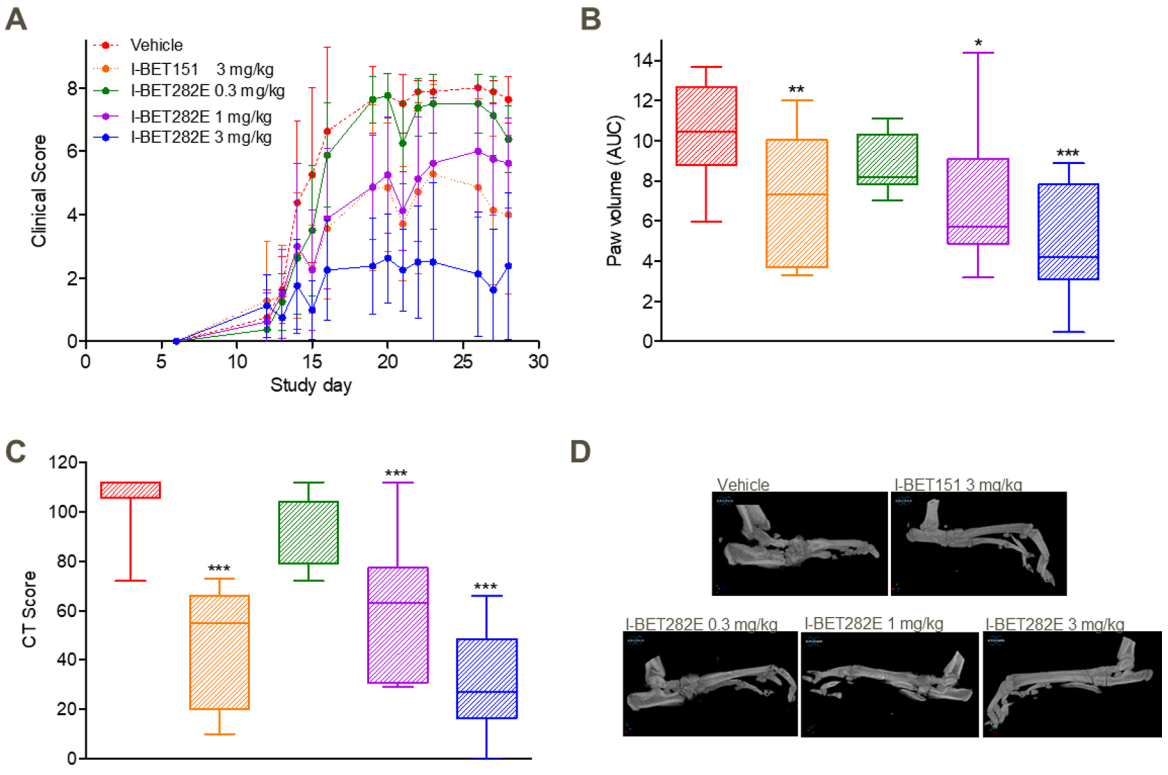

Figure 5. Effects of I-BET282E in the rat collagen-induced arthritis (CIA) model. Arthritis was induced in female Lewis rats by intradermal injection of bovine type II collagen on Day 0 followed by an intradermal booster injection of bovine type II collagen and MDP on day 7. Rats were administered either vehicle, I-BET151 (3 mg/kg) or I-BET282E (0.3, 1, or 3 mg/kg) p.o. once daily from day 12 (at onset of symptoms) until day 28, i.e., for 16 days. (A) The effects of I-BET282E on clinical scores of the hind limbs was visually assessed daily from day 6−28. (B) The effects of I-BET282E on hind paw volumes was measured via plethysmography on days 12−26, data expressed as AUC. Colors were assigned to doses as in panel A. (C) The effects of I-BET282E on the number of affected bones and overall severity score were determined by micro computed tomography (CT). Colors were assigned to doses as in panel A. (D) Effects of I-BET282E on new bone growth illustrated by CT images. Data are expressed as mean ± SD, n = 7−8/group. *p < 0.05, **p < 0.01, ***p < 0.001 compared with the vehicle control group.

https://doi.org/10.1021/acs.jmedchem.1c00855
J. Med. Chem. 2021, 64, 12200−12227

preference for BD1 compared to BD2 is similar for both compounds (~2.5 fold and ~5 fold respectively).

CONCLUSION

Late-stage optimization of I-BET151, with the aim of increasing cellular potency and improving the pharmacokinetic profile, identified I-BET282E as a molecule with the potential for progression into *in vivo* studies. This compound showed an excellent selectivity profile, a pharmacokinetic profile offering the potential for an orally available, low-moderate clearance molecule in humans, as well as *in vivo* efficacy in a model of collagen-induced arthritis. The pharmacokinetic profile in dogs was also suitable for this species to be used in preclinical safety studies. Formation of the mesylate salt improved the polymorph and solubility profile and delivered a molecule suitable for progression into preclinical development, and ultimately I-BET282E was progressed into a clinical dose escalation study in subjects with advanced or recurrent solid tumors.[45] During the course of this study, a number of emerging reports highlighted that despite the high level of structural diversity of BET inhibitors progressed in clinical trials, dose limiting safety signals showed strong commonalities (in particular thrombocytopenia, fatigue, and GI toxicity (mainly diarrhea)), suggesting pharmacology-driven signals in the majority of cases[46] even if an unexpected and atypical safety profile has also been reported.[47] On the basis of these data and the emerging safety profile of I-BET762 (Figure 1, compound **1**) from Phase I trials, the progression of a back-up molecule was considered unnecessary leading to the termination of I-BET282E in 2017.

EXPERIMENTAL SECTION

The human biological samples were sourced ethically, and their research use was in accord with the terms of the informed consents under an IRB/EC approved protocol.

Chemistry Methods and Characterization for Compounds. All commercial chemicals and solvents used were of reagent grade and used without further purification. Where compounds were hydrogenated using an H-cube, a Thales H-cube continuous−flow hydrogenation reactor was used, where hydrogen is generated *in situ*. Thales disposable catalyst cartridges were used, either the CatCart 30 (30 mm cartridge, containing 140 mg of 10% Pd/C catalyst) or the CatCart 70 (70 mm cartridge, containing 350 mg of 10% Pd/C catalyst). Reactions heated under microwave conditions were heated in a Biotage Initiator microwave. Unless otherwise stated, the initial absorption was set as "high", and 15 s of prestirring was applied before heating commenced. Hydrophobic frit cartridges by ISOLUTE, which contain a frit selectively permeable to organic solutions, were used for separation of organic phases from aqueous phases under gravity. ISOLUTE aminopropyl and SCX cartridges were used for scavenging SPE protocols. Column chromatography was carried out either using manual or automated flash chromatography systems using silica SPE cartridges. The names of the compounds were obtained using ChemDraw. Mass-directed autopreparative high-performance liquid chromatography (MDAP) were conducted either with a formic acid modifier "MDAP (formic acid)" or an ammonium bicarbonate modifier "MDAP (high pH)". Method using formic acid modifier: "MDAP (formic acid)". LC conditions: The HPLC analysis was conducted on either a Sunfire C_{18} column (100 mm × 19 mm, i.d. 5 μm packing diameter) or a Sunfire C_{18} column (150 mm × 30 mm, i.d. 5 μm packing diameter) at ambient temperature. The solvents employed were A = 0.1% v/v solution of formic acid in water; B = 0.1% v/v solution of formic acid in acetonitrile. The purification was run as a gradient (A:B) over either 15 or 25 min, with a flow rate of 20 mL/min (100 mm × 19 mm, i.d. 5 μm packing diameter) or 40 mL/min (150 mm × 30 mm, i.d. 5 μm packing diameter). The UV detection was a summed signal from wavelength of 210 to 350 nm. MS conditions: The mass spectrometry was conducted on a Waters ZQ mass spectrometer, with an ionization mode of alternate-scan positive and negative electrospray. The scan range was 100−1000 AMU, the scan time was 0.50 s, and the interscan delay was 0.20 s. Method using ammonium bicarbonate modifier: "MDAP (high pH)". The method was as for MDAP (formic acid), except the solvents employed were A = 10 mM ammonium bicarbonate in water, adjusted to pH 10 with ammonia solution; B = acetonitrile. The purity of compounds tested in *in vitro* and *in vivo* assays was of greater than 95% using interpretation of a combination of LCMS and ^{1}H NMR data, unless stated otherwise. LCMS were conducted either with a formic acid modifier "LCMS (formic acid)", trifluoroacetic acid modifier "LCMS (TFA)", or ammonium bicarbonate modifier "LCMS (high pH)". Method using formic acid modifier: "LCMS (formic acid)". LC conditions: The UPLC analysis was conducted on an Acquity UPLC BEH C_{18} column (50 mm × 2.1 mm, i.d. 1.7 μm packing diameter) at 40 °C. The solvents employed were A = 0.1% v/v solution of formic acid in water; B = 0.1% v/v solution of formic acid in acetonitrile. The gradient (A:B) employed was from 97:3 to 3:97 over 2 min. The UV detection was a summed signal from wavelength of 210 to 350 nm. MS conditions: The mass spectrometry was conducted on a Waters ZQ mass spectrometer, with an ionization mode of alternate-scan positive and negative electrospray. The scan range was 100−1000 AMU, the scan time was 0.27 s, and the interscan delay was 0.10 s. Method using trifluoroacetic acid modifier: "LCMS (TFA)". The method was as for LCMS (formic acid), except the solvents employed were A = 0.1% v/v solution of trifluoroacetic acid in water; B = 0.1% v/v solution of trifluoroacetic acid in acetonitrile. Method using ammonium bicarbonate modifier: "LCMS (high pH)". The method was as for LCMS (formic acid), except the solvents employed were A = ammonium hydrogen carbonate in water adjusted to pH 10 with ammonia solution; B = acetonitrile. High-resolution mass spectrometry chromatography and analysis conditions: An Agilent 1100 liquid chromatograph equipped with a model G1367A autosampler, a model G1312A binary pump, and a HP1100 model G1315B diode array detector was used. The method used was generic for all experiments. All separations were achieved using a C_{18} reversed phase column (100 × 2.1 mm, 3 μm particle size) or equivalent. Gradient elution was carried out with the mobile phases as (A) water containing 0.1% (v/v) TFA and (B) acetonitrile containing 0.1% (v/v) TFA. The conditions for the gradient elution were initially 0% B, increasing linearly to 95% B over 8 min, remaining at 95% B for 0.5 min, then decreasing linearly to 0% B over 0.1 min followed by an equilibration period of 1.49 min prior to the next injection. The flow rate was 1 mL/min, split to source, and the temperature controlled at 40 °C with an injection volume of between 2 to 5 μL. Mass spectrometry conditions: Positive ion mass spectra were acquired using a Thermo LTQ-Orbitrap FT mass spectrometer, equipped with an ESI interface, over a mass range of 100−1100 Da, with a scan time of 1 s. The elemental composition was calculated using Xcalibur software and processed using RemoteAnalyzer (Spectral Works Ltd.) for the $[M + H]^+$ and the mass error quoted as ppm. Unless otherwise specified, ^{1}H and ^{13}C NMR spectra were recorded at 400 and 101 MHz respectively, and chemical shifts are given in ppm (δ) relative to tetramethylsilane (TMS) as an internal standard. Chemical shifts are given to the nearest 0.01 ppm (^{1}H NMR) or 0.1 ppm (^{13}C NMR), and coupling constants are given to the nearest 0.1 Hz. NMR spectra were recorded at room temperature unless otherwise stated. Infrared (IR) spectra were recorded using a PerkinElmer Spectrum One FT-IR spectrometer, and key well-defined peaks were recorded in cm^{-1}. Optical rotation measurements were recorded using a Jasco P-1030 polarimeter. The concentration was recorded in g/mL, path length in mm, and temperature in °C.

*7-(3,5-Dimethyl-4-isoxazolyl)-1-(1-methylethyl)-8-(methyloxy)-1,3-dihydro-2H-imidazo[4,5-c]quinolin-2-one (**6**).* 7-(3,5-Dimethyl-4-isoxazolyl)-4-[(1-methylethyl)amino]-6-(methyloxy)-3-quinolinecarboxamide **40** (188 mg, 0.53 mmol) was suspended in methanol (10 mL), and potassium hydroxide (44.6 mg, 0.796 mmol) was

https://doi.org/10.1021/acs.jmedchem.1c00855
J. Med. Chem. 2021, 64, 12200−12227

added. The mixture was stirred for 20 min, then cooled in an ice bath, and iodobenzene diacetate (222 mg, 0.69 mmol) added. The reaction mixture was stirred at 0 °C for 2 h. The reaction mixture was concentrated *in vacuo*. The residue was taken up in DCM and purified by column chromatography (silica), eluted using 1−10% of MeOH in DCM. The appropriate fractions were combined and concentrated *in vacuo* to give an orange oil (113 mg). The oil was taken up in dichloromethane (∼1 mL), and 1 M hydrochloric acid (0.31 mL, 0.31 mmol) was added. The solvent was removed under a stream of nitrogen to give the title compound (117 mg, 0.29 mmol, 54% yield) as a brown solid.

LCMS (formic acid): rt = 0.69 min, MH^+ = 353.

^{1}H NMR (CD_3OD, 400 MHz) δ 1.85 (d, 6H, J = 6.8 Hz) 2.23 (s, 3H) 2.40 (s, 3H) 4.11 (s, 3H) 5.38−5.48 (m, 1H) 7.81 (s, 1H) 7.98 (s, 1H) 8.74 (s, 1H).

*7-(3,5-Dimethyl-4-isoxazolyl)-8-(methyloxy)-1-(2-methylpropyl)-1,3-dihydro-2H-imidazo[4,5-c]quinolin-2-one (**7**).* 7-(3,5-Dimethyl-4-isoxazolyl)-6-(methyloxy)-4-[(2-methylpropyl)amino]-3-quinolinecarboxamide **41** (762 mg, 1.03 mmol) was taken up in methanol (20 mL). Potassium hydroxide (87 mg, 1.55 mmol) was added, and the mixture stirred for 20 min. The mixture was cooled in an ice bath, and iodobenzene diacetate (433 mg, 1.34 mmol) was added. The mixture was stirred at 0 °C for 2 h. The reaction mixture was concentrated *in vacuo*. The residue was loaded in DCM and purified by column chromatography (silica), eluted using 1−10% MeOH in DCM. The appropriate fractions were concentrated *in vacuo*. Dichloromethane (∼0.5 mL) and 1 M hydrochloric acid (0.46 mL, 0.46 mmol) were added, and the solvent removed under a stream of nitrogen to give the title compound (117 mg, 0.26 mmol, 25% yield) as a brown solid.

LCMS (formic acid): rt = 0.76 min, MH^+ = 367.

^{1}H NMR ($CDCl_3$, 400 MHz) δ 1.15 (br s, 6H) 2.25 (br s, 3H) 2.41 (br s, 4H) 4.02 (br s, 3H) 4.24 (s, 2H) 7.50 (br s, 1H) 8.17 (br s, 1H) 9.09 (br s, 1H).

*7-(3,5-Dimethylisoxazol-4-yl)-8-methoxy-1-(pentan-2-yl)-1H-imidazo[4,5-c]quinolin-2(3H)-one (**8**).* 7-(3,5-Dimethylisoxazol-4-yl)-6-methoxy-4-(pentan-2-ylamino)quinoline-3-carboxamide **42** (483 mg, 1.26 mmol) was taken up in methanol (20 mL). Potassium hydroxide (106 mg, 1.89 mmol) was added, and the mixture was stirred for 20 min. The mixture was cooled in an ice bath, and iodobenzene diacetate (529 mg, 1.64 mmol) was added. The reaction was stirred at 0 °C for 2 h. The reaction mixture was concentrated *in vacuo*. The residue was loaded in the minimum amount of DCM and purified by column chromatography (silica), eluted using 1−10% MeOH in DCM. The appropriate fractions were combined and concentrated *in vacuo* to give the title compound (352 mg, 0.88 mmol, 70% yield) as an orange oil.

LCMS (formic acid): rt = 0.83 min, MH^+ = 381.

^{1}H NMR ($CDCl_3$,400 MHz) δ 0.98 (t, 2H, J = 7.3 Hz) 1.35−1.56 (m, 1H) 1.82 (d, 1H, J = 6.8 Hz) 2.00−2.11 (m, 1H) 2.13 (s, 1H) 2.24 (s, 2H) 2.38 (s, 2H) 3.98 (s, 1H) 7.56 (br s, 1H) 7.97 (s, 1H) 8.79 (s, 1H).

*1-(Cyclopropylmethyl)-7-(3,5-dimethylisoxazol-4-yl)-8-methoxy-1H-imidazo[4,5-c]quinoline-2(3H)-one (**9**).* To a suspension of 4-((cyclopropylmethyl)amino)-7-(3,5-dimethylisoxazol-4-yl)-6-methoxyquinoline-3-carboxamide **43** (365 mg, 1.00 mmol) in MeOH (4 mL) was added potassium hydroxide (84 mg, 1.49 mmol), and the reaction mixture stirred at room temperature for 20 min. The reaction mixture was cooled to 0 °C (ice/water bath), iodobenzene diacetate (417 mg, 1.23 mmol) was added, and the reaction mixture was stirred at 0 °C for a further 2 h. The reaction mixture was blown down under a stream of nitrogen. A portion (100 mg) of the crude material was dissolved in DMSO (1 mL) and purified by MDAP (high pH). The solvent was blown down a stream of nitrogen to give the title compound (22 mg, 0.06 mmol, 6% yield). The remaining crude material (902 mg) was retained without purification.

LCMS (formic acid): rt = 0.73 min, MH^+ = 365.

^{1}H NMR (DMSO-d_6, 393 K, 400 MHz): δ 0.46−0.51 (m, 2H), 0.55−0.61 (m, 2H), 1.36−1.46 (m, 1H), 2.14 (s, 3H), 2.33 (s, 3H), 3.99 (s, 3H), 4.29 (d, J = 6.3 Hz, 2H), 7.67 (s, 1H), 7.84 (s, 1H), 8.58 (s, 1H), 10.87−10.99 (br s, 1H).

*7-(3,5-Dimethylisoxazol-4-yl)-8-methoxy-1-(1-methoxypropan-2-yl)-1H-imidazo[4,5-c]quinolin-2(3H)-one (**10**).* 7-(3,5-Dimethylisoxazol-4-yl)-6-methoxy-4-((1-methoxypropan-2-yl)amino)quinoline-3-carboxamide **44** (116 mg, 0.30 mmol) and potassium hydroxide (25 mg, 0.45 mmol) were taken up in methanol (5 mL) and stirred at room temperature for 20 min. The reaction mixture was cooled in an ice bath, and iodobenzene diacetate (126 mg, 0.39 mmol) was added. The mixture was stirred at 0 °C for 2 h. The reaction mixture was concentrated *in vacuo* and purified by MDAP (formic acid). The appropriate fractions were blown down under a stream of nitrogen, taken up in methanol, and purified by SCX, and eluted with methanol and then 2 M NH_3 in MeOH. The appropriate fractions were concentrated *in vacuo* to give the title compound (44 mg, 0.10 mmol, 34% yield) as a yellow residue.

LCMS (formic acid): rt = 0.68 min, MH^+ = 383,

^{1}H NMR (CD_3OD, 400 MHz) δ 1.71−1.74 (d, 3H, J = 6.3 Hz), 2.19 (s, 3H), 2.36 (s, 3H), 3.37 (s, 3H), 3.80−3.84 (m, 1H), 4.01 (s, 3H), 4.26−4.31 (m, 1H), 5.29−5.35 (m, 1H), 7.76 (s, 1H), 7.85 (s, 1H), 8.55 (s, 1H).

*7-(3,5-Dimethylisoxazol-4-yl)-8-methoxy-1-((tetrahydrofuran-3-yl)methyl)-1H-imidazo[4,5-c]quinoline-2(3H)-one (**11**).* To a suspension of 7-(3,5-dimethylisoxazol-4-yl)-6-methoxy-4-(((tetrahydrofuran-3-yl)methyl)amino)quinoline-3-carboxamide **39** (667 mg, 1.68 mmol) in methanol (5 mL) was added potassium hydroxide (142 mg, 2.52 mmol), and the reaction mixture was stirred for 20 min at room temperature. The reaction mixture was cooled in an ice/water bath, iodobenzene diacetate (704 mg, 2.19 mmol) added, and the reaction mixture was stirred at 0 °C for a further 2 h. The reaction mixture was blown down under a stream of nitrogen. The sample was loaded in methanol/dichloromethane (and the column dried in a vacuum oven) and purified by column chromatography (silica), eluted using 0−10% MeOH in DCM. The appropriate fractions were combined and dried under a stream of nitrogen to give the title compound (558 mg, 1.42 mmol, 84% yield) as a pale brown foam.

LCMS (formic acid): rt = 0.65 min, MH^+ = 395.

^{1}H NMR (DMSO-d_6, 393 K, 400 Hz): δ 1.80−1.90 (m, 1H), 2.01−2.11 (m, 1H), 2.14 (s, 3H), 2.33 (s, 3H), 2.85−2.98 (m, 1H), 3.66−3.77 (m, 3H), 3.87−3.93 (m, 1H), 3.99 (s, 3H), 4.29−4.40 (m, 2H), 7.57 (s, 1H), 7.84 (s, 1H), 8.58 (s, 1H), 10.90−11.31 (br s, 1H).

*7-(3,5-Dimethylisoxazol-4-yl)-8-methoxy-1-((tetrahydro-2H-pyran-3-yl)methyl)-1H-imidazo[4,5-c]quinoline-2(3H)-one (**12**).* To a suspension of 7-(3,5-dimethylisoxazol-4-yl)-6-methoxy-4-(((tetrahydro-2*H*-pyran-3-yl)methyl)amino)quinoline-3-carboxamide **46** (610 mg, 1.49 mmol) in methanol (5 mL) was added potassium hydroxide (125 mg, 2.23 mmol), and the reaction mixture was stirred at room temperature for 20 min. The reaction mixture was cooled in an ice/water bath, iodobenzene diacetate (622 mg, 1.93 mmol) added, and the reaction mixture was stirred at 0 °C for 2 h. The reaction mixture was blown down under a stream of nitrogen. The sample was loaded in methanol/dichloromethane (and the column dried in a vacuum oven) and purified by column chromatography (silica, 100 g), eluted using 0−100% EtOAc in cyclohexane followed by 0−10% MeOH in DCM. The appropriate fractions were combined and dried under a stream of nitrogen to give the title compound (407 mg, 1.00 mmol, 67% yield) as a pale brown foam.

LCMS (formic acid): rt = 0.69 min, MH^+ = 409.

^{1}H NMR (d_6-DMSO, 393 K, 400 MHz): δ 1.43−1.53 (m, 2H), 1.65−1.75 (m, 1H), 1.79−1.87 (m, 1H), 2.12 (s, 3H), 2.14−2.26 (m, 1H), 2.31 (s, 3H), 3.37−3.48 (m, 2H), 3.64−3.79 (m, 2H), 3.96 (s, 3H), 4.23 (m, 2H), 7.50 (s, 1H), 7.82 (s, 1H), 8.55 (s, 1H), 10.91−11.24 (br s, 1H).

*7-(3,5-Dimethylisoxazol-4-yl)-8-methoxy-1-((tetrahydro-2H-pyran-4-yl)methyl)-1H-imidazo[4,5-c]quinoline-2(3H)-one (**13**).* To a suspension of 7-(3,5-dimethylisoxazol-4-yl)-6-methoxy-4-(((tetrahydro-2*H*-pyran-4-yl)methyl)amino)quinoline-3-carboxamide **47** (1.7 g, 4.14 mmol) in MeOH (15 mL) was added potassium hydroxide (0.35 g, 6.21 mmol), and the reaction mixture was stirred at room temperature for 20 min. The reaction mixture was cooled in an ice/water bath, iodobenzene diacetate (1.73 g, 5.38 mmol) was added, and the reaction mixture was stirred at 0 °C for 2 h. The reaction

https://doi.org/10.1021/acs.jmedchem.1c00855
J. Med. Chem. 2021, 64, 12200−12227

mixture was blown down under a stream of nitrogen. The residue was loaded as a suspension in MeOH and DCM (and the column dried in a vacuum oven) and purified by SPE (silica, 100 g) using 0−20% MeOH in DCM. The appropriate fractions were combined and dried under a stream of nitrogen to give the title compound (1.50 g, 3.67 mmol, 89% yield) as a pale brown foam.

LCMS (formic acid): rt = 0.66 min, MH^+ = 409.

^{1}H NMR (DMSO-d_6, 400 MHz): δ 1.34−1.48 (m, 2H), 1.60 (d, J = 11.1 Hz, 2H), 2.14 (s, 3H), 2.17−2.25 (m, 1H), 2.33 (s, 3H), 3.22−3.28 (m, 2H), 3.84 (dd, J = 11.4, 2.0 Hz, 2H), 3.97 (s, 3H), 4.23 (d, J = 7.3 Hz, 2H), 7.46 (s, 1H), 7.87 (s, 1H), 8.57 (s, 1H), 11.45−11.58 (br s, 1H).

^{13}C NMR (d_6-DMSO, 300 K): δ 10.4, 11.4, 30.2, 36.7, 46.9, 55.6, 66.4, 99.0, 112.2, 115.6, 120.6, 122.0, 128.3, 132.1, 133.0, 139.7, 154.3, 155.0, 159.1, 166.1.

IR (neat): 1694 (urea), 1597 (aryl), 1228 (aryl ether), 841 (aryl C−H) cm^{-1}.

M.p.: 233−238 °C.

HRMS: $C_{22}H_{25}N_4O_4$ MH^+ requires 409.1870, found MH^+ 409.1870.

*7-(3,5-Dimethylisoxazol-4-yl)-8-methoxy-1-(1-(tetrahydro-2H-pyran-4-yl)ethyl)-1H-imidazo[4,5-c]quinoline-2(3H)-one (**14**).* To a suspension of 7-(3,5-dimethylisoxazol-4-yl)-6-methoxy-4-((1-(tetrahydro-2*H*-pyran-4-yl)ethyl)amino)quinoline-3-carboxamide **48** (169 mg, 0.40 mmol) in MeOH (2 mL) was added potassium hydroxide (34 mg, 0.60 mmol), and the reaction mixture was stirred at room temperature for 20 min. The reaction mixture was cooled to 0 °C (ice/water bath), iodobenzene diacetate (167 mg, 0.52 mmol) was added, and the reaction mixture was stirred at 0 °C for a further 2 h. The reaction mixture was blown down under a stream of nitrogen and MDAP (formic acid and high pH). The solvent was dried under a stream of nitrogen to give the title compound (41 mg, 0.10 mmol, 24% yield).

LCMS (formic acid): rt = 0.71 min, MH^+ = 423.

^{1}H NMR (DMSO-d_6, 393 K, 400 MHz): δ 1.20−1.31 (m, 1H), 1.31−1.38 (m, 1H), 1.39−1.52 (m, 1H), 1.66 (d, J = 7.1 Hz, 3H), 1.85−1.94 (m, 1H), 2.12 (s, 3H), 2.30 (s, 3H), 2.55−2.68 (m, 1H), 3.21 (dt, J = 11.6, 2.5 Hz, 1H), 3.37 (dt, J = 11.4, 2.8 Hz, 1H), 3.72−3.79 (m, 1H), 3.92−3.96 (m, 4H), 4.66−4.76 (m, 1H), 7.53 (s, 1H), 7.82 (s, 1H), 8.11−8.14 (br s, 1H) 8.54 (s, 1H).

*7-(3,5-Dimethyl-4-isoxazolyl)-8-(methyloxy)-1-(tetrahydro-2H-pyran-4-yl)-1,3-dihydro-2H-imidazo[4,5-c]quinolin-2-one (**15**).* 7-(3,5-Dimethyl-4-isoxazolyl)-6-(methyloxy)-4-(tetrahydro-2*H*-pyran-4-ylamino)-3-quinolinecarboxamide **39** (0.34 g, 0.86 mmol) and potassium hydroxide (0.072 g, 1.29 mmol) were dissolved in methanol (10 mL), the mixture was cooled in an ice bath, and then iodobenzene diacetate (0.36 g, 1.12 mmol) was added, and the mixture was stirred for 3 h. The reaction mixture was evaporated *in vacuo*. The residue was dissolved in DCM and purified by silica column and then eluted with 0−50% 2 M methanolic ammonia/DCM. The product-containing fractions were evaporated *in vacuo* to give a brown gum. The product was triturated with EtOAc (3 mL) to give a pale yellow solid, which was collected by filtration and washed with ether (5 mL) to give the title compound (0.23 g, 0.58 mmol, 68% yield) as pale yellow powder.

LCMS (formic acid): rt = 0.64 min, MH^+ = 395.

^{1}H NMR ($CDCl_3$, 400 MHz) δ 2.02−2.09 (m, 2H), 2.26 (s, 3H), 2.40 (s, 3H), 2.95−3.05 (m, 2H), 3.66−3.72 (m, 2H), 4.03 (s, 3H), 4.28−4.36 (m, 2H), 5.12−5.27 (br s, 1H), 7.17−7.30 (br s, 1H), 7.97 (s, 1H), 8.76 (s, 1H), 10.10−10.19 (br s, 1H).

*7-(3,5-Dimethyl-4-isoxazolyl)-8-(methyloxy)-1-(4-piperidinyl)-1,3-dihydro-2H-imidazo[4,5-c]quinolin-2-one (**16**).* 1,1-Dimethylethyl 4-{[3-(aminocarbonyl)-7-(3,5-dimethyl-4-isoxazolyl)-6-(methyloxy)-4-quinolinyl]amino}-1-piperidinecarboxylate **50** (0.50 g, 1.01 mmol) was dissolved in methanol (5 mL), and then potassium hydroxide (0.085 g) was added, the mixture was cooled to 0 °C, and iodobenzene diacetate (0.422 g, 1.31 mmol) was added. The mixture was stirred for 4 h and then evaporated *in vacuo*. The residue was dissolved in DCM (5 mL), loaded onto a 25 g silica column, and eluted with 0−10% 2 M methanolic ammonia/DCM. Product-containing fractions were evaporated *in vacuo* to give a pale yellow glass. The glass was triturated with a mixture of EtOAc (5 mL) and cyclohexane (5 mL), and then the solvent evaporated *in vacuo* to give a beige solid (247 mg). TFA (2 mL, 26.0 mmol) was added to a solution of this solid (200 mg) in DCM (10 mL), and the mixture was stirred for 2 h and then evaporated *in vacuo*. The residue was dissolved in methanol (10 mL) and purified by SCX, washed with methanol (50 mL), and then eluted with 2 M methanolic ammonia (30 mL). The eluant was evaporated *in vacuo* to give the title compound (133 mg, 0.34 mmol, 42% yield) as gray solid.

LCMS (formic acid): rt = 0.42 min, MH^+ = 394.

^{1}H NMR ($CDCl_3$, 400 MHz) δ 2.08−2.22 (m, 2H), 2.25 (s, 3H), 2.40 (s, 3H), 2.92−3.24 (m, 4H), 3.50−3.69 (m, 2H), 4.02 (s, 3H), 4.96−5.08 (m, 1H), 7.45−7.77 (br s, 1H) 7.97 (s, 1H), 8.76 (s, 1H). The two NH were not observed.

*7-(3,5-Dimethyl-4-isoxazolyl)-8-(methyloxy)-1-[(1-methyl-4-piperidinyl)methyl]-1,3-dihydro-2H-imidazo[4,5-c]quinolin-2-one (**17**).* 7-(3,5-Dimethyl-4-isoxazolyl)-6-(methyloxy)-4-{[(1-methyl-4-piperidinyl)methyl]amino}-3-quinolinecarboxamide **51** (250 mg, 0.59 mmol), potassium hydroxide (50 mg, 0.89 mmol), and iodobenzene diacetate (247 mg, 0.77 mmol) were dissolved in methanol at 0 °C, and the mixture was stirred for 3 h, then evaporated *in vacuo*. The residue was dissolved in DCM (3 mL) and loaded onto a 25g silica column and then eluted with 0−10% 2 M methanolic ammonia/DCM. Product-containing fractions were evaporated *in vacuo* to give an amber solid. The product was suspended in hot EtOAc (3 mL) and then cooled to room temperature and filtered, and the solid was washed with EtOAc (3 mL) to give the title compound (181 mg, 0.43 mmol, 73% yield) as a beige solid.

LCMS (formic acid): rt = 0.80 min, MH^+ = 422.

^{1}H NMR ($CDCl_3$, 400 MHz) δ 1.62−1.85 (m, 4H), 1.93−2.15 (m, 3H), 2.25 (s, 3H), 2.30 (s, 3H), 2.40 (s, 3H), 2.92−3.00 (m, 2H), 3.98 (s, 3H), 4.30−4.36 (m, 2H), 7.41 (s, 1H), 7.95 (s, 1H), 8.76 (s, 1H), 10.23−10.44 (br s, 1H).

*1-(2-(Dimethylamino)ethyl)-7-(3,5-dimethylisoxazol-4-yl)-8-methoxy-1H-imidazo[4,5-c]quinolin-2(3H)-one (**18**).* 4-((2-(Dimethylamino)ethyl)amino)-7-(3,5-dimethylisoxazol-4-yl)-6-methoxyquinoline-3-carboxamide **52** (501 mg, 1.31 mmol) and potassium hydroxide (110 mg, 1.96 mmol) were taken up in methanol (20 mL) and stirred at room temperature for 20 min. The reaction mixture was cooled in an ice bath and iodobenzene diacetate (547 mg, 1.70 mmol) was added, and the mixture was stirred at 0 °C for 3 h. The reaction mixture was concentrated *in vacuo*. The residue was taken up in dichloromethane and purified by silica column chromatography, eluted with 1−10% MeOH in DCM. The appropriate fractions were combined and concentrated *in vacuo* to give the title compound (234 mg, 0.58 mmol, 45% yield) as a yellow oil.

LCMS (formic acid): rt = 0.46 min, MH^+ = 382.

^{1}H NMR ($CDCl_3$, 400 MHz) δ 2.25 (s, 3H) 2.40 (s, 3H) 2.42 (s, 6H) 2.88 (t, 2H, J = 7.5 Hz) 4.01 (s, 3H) 4.54 (t, 2H, J = 7.5 Hz) 7.61 (s, 1H) 7.94 (s, 1H) 8.73 (s, 1H) 10.09 (br s, 1H).

*7-(3,5-Dimethylisoxazol-4-yl)-8-methoxy-1-(pyridin-2-ylmethyl)-1,3-dihydro-2H-imidazo[4,5-c]quinolin-2-one (**19**).* A flask was charged with 4-chloro-7-(3,5-dimethylisoxazol-4-yl)-6-methoxyquinoline-3-carboxamide **39** (6.0 g, 18 mmol) and pyridin-2-ylmethanamine (4.23 g, 39.1 mmol) then was filled with CH_3CN (100 mL), and the resulting mixture was stirred at reflux for 4 h and then was cooled to room temperature and concentrated *in vacuo*. The residue was dissolved in water, and the aqueous phase was extracted with DCM. The combined organics were dried over Na_2SO_4 and concentrated *in vacuo* to give 7-(3,5-dimethylisoxazol-4-yl)-6-methoxy-4-((pyridin-2-ylmethyl)amino)quinoline-3-carboxamide (5.84 g, 14.5 mmol) which was used in the next step without further purification. This crude material was suspended in CH_3CN and then was treated at room temperature with phenyl-λ^3-iodanediyl bis(2,2,2-trifluoroacetate) (19.4 g, 45.0 mmol), and the resulting mixture was stirred at 50 °C for 12 h and then was cooled to room temperature and concentrated *in vacuo*. The residue was dissolved in water, and the aqueous phase was extracted with DCM. The combined organics

https://doi.org/10.1021/acs.jmedchem.1c00855
J. Med. Chem. 2021, 64, 12200−12227

were dried over Na_2SO_4 and concentrated *in vacuo*. Purification of the residue by flash chromatography on silica gel (eluent: 95/5 EtOAc/MeOH) gave after trituration with CH_3CN/Et_2O the title compound (3.90 g, 54% over two steps) as a beige powder.

LCMS (formic acid): rt = 0.71 min, MH^+ = 402.

^{1}H NMR (DMSO-d_6, 400 MHz) δ 2.09 (s, 3H), 2.30 (s, 3H), 3.74 (s, 3H) 5.75 (s, 2H), 7.33−7.37 (m, 1H), 7.49−7.56 (m, 2H), 7.82−7.88 (m, 1H), 7.94 (s, 1H), 8.48−8.53 (m, 1H), 8.88 (s, 1H), 12.33 (br s, 1H).

*7-(3,5-Dimethyl-4-isoxazolyl)-2-methyl-8-(methyloxy)-1-(2-pyridinylmethyl)-1H-imidazo[4,5-c]quinoline (**20**).* A solution of *N*-(7-(3,5-dimethylisoxazol-4-yl)-6-methoxy-4-((pyridin-2-ylmethyl)-amino)quinolin-3-yl)acetamide **54** (80 mg, 0.19 mmol) in glacial acetic acid (1 mL) was refluxed for 2 h. The reaction mixture was cooled, and the solvent was evaporated. The residue was chromatographed using 2−10% methanol in dichloromethane to give the title compound (37 mg, 0.09 mmol, 48% yield) as a colorless solid.

LCMS (formic acid): rt = 0.65 min, MH^+ = 400.

^{1}H NMR (DMSO-d_6, 400 MHz): δ 2.07 (s, 3H), 2.28 (s, 3H), 2.76 (s, 3H), 3.74 (s, 3H), 6.08 (s, 2H), 7.30−7.38 (m, 2H), 7.48 (s, 1H), 7.82 (dt, 1H, J = 10.0 Hz, 4.0 Hz), 7.91 (s, 1H), 8.53 (d, 1H, J = 10.0 Hz), 9.03 (s, 1H).

*7-(3,5-Dimethyl-4-isoxazolyl)-2-ethyl-8-(methyloxy)-1-(2-pyridinylmethyl)-1H-imidazo[4,5-c]quinoline (**21**).* Glacial acetic acid (2 mL) was added to *N*-{7-(3,5-dimethyl-4-isoxazolyl)-6-(methyloxy)-4-[(2-pyridinylmethyl)amino]-3-quinolinyl}propanamide **55** (100 mg, 0.18 mmol), and the mixture was refluxed for 2 h. The solvent was evaporated, and the residue was chromatographed using 2−10% methanol in dichloromethane, followed by trituration with diethyl ether to give the title compound (40 mg, 0.10 mmol, 42% yield) as an off-white solid.

LCMS (formic acid): rt = 0.70 min, MH^+ = 414.

^{1}H NMR ($CDCl_3$, 400 MHz): δ 1.56 (t, 3H, J = 12.0 Hz), 2.15 (s, 3H), 2.32 (s, 3H), 3.10 (q, 2H, J = 12.0 Hz), 3.63 (s, 3H), 5.93 (s, 2H), 6.78 (d, 1H, J = 10.0 Hz), 7.23−7.34 (m, 2H), 7.64 (dt, 1H, J = 10.0 Hz, 4.0 Hz), 7.99 (s, 1H), 8.70 (d, 1H, J = 4.0 Hz), 9.23 (s, 1H).

*7-(3,5-Dimethyl-4-isoxazolyl)-8-(methyloxy)-2-propyl-1-(2-pyridinylmethyl)-1H-imidazo[4,5-c]quinoline (**22**).* Glacial acetic acid (2 mL) was added to *N*-{7-(3,5-dimethyl-4-isoxazolyl)-6-(methyloxy)-4-[(2-pyridinylmethyl)amino]-3-quinolinyl}butanamide **56** (45 mg, 0.1 mmol), and the mixture was refluxed for 2 h. The reaction mixture was cooled to room temperature, and the solvent was evaporated. The residue was chromatographed in 2−5% methanol in dichloromethane and then triturated with hexane/diethyl ether to give the title compound (23 mg, 0.054 mmol, 53% yield) as an off-white solid.

LCMS (formic acid): rt = 0.75 min, MH^+ = 428.

^{1}H NMR (DMSO-d_6, 400 MHz): δ 1.04 (t, 3H, J = 12.0 Hz), 1.82−1.93 (m, 2H), 2.07 (s, 3H), 2.27 (s, 3H), 3.06 (q, 2H, J = 12.0 Hz), 3.70 (s, 3H), 6.08 (s, 1H), 7.27 (d, 1H, J = 12.0 Hz), 7.30−7.34 (m, 2H), 7.45 (s, 1H), 7.80 (dt, 1H, J = 10.0 Hz, 4.0 Hz), 7.90 (s, 1H), 8.50−8.54 (m, 1H), 9.06 (s, 1H).

*7-(3,5-Dimethyl-4-isoxazolyl)-2-(1-methylethyl)-8-(methyloxy)-1-(2-pyridinylmethyl)-1H-imidazo[4,5-c]quinoline (**23**).* Glacial acetic acid (2 mL) was added to *N*-{7-(3,5-dimethyl-4-isoxazolyl)-6-(methyloxy)-4-[(2-pyridinylmethyl)amino]-3-quinolinyl}-2-methylpropanamide **57** (50 mg, 0.11 mmol), and the mixture refluxed for 2 h. The reaction mixture was cooled to room temperature, and the solvent was evaporated. The residue was chromatographed using 2−5% methanol in dichloromethane, and the product was triturated with hexane/diethyl ether to give the title compound (25 mg, 0.06 mmol, 52% yield) as an off-white solid.

LCMS (formic acid): rt = 0.74 min, MH^+ = 428.

^{1}H NMR (DMSO-d_6, 400 MHz): δ 1.39 (d, 6H, J = 12.0 Hz), 2.07 (s, 3H), 2.27 (s, 3H), 3.52−3.60 (m, 1H), 3.66 (s, 3H), 6.12 (s, 2H), 7.22 (d, 1H, J = 12.0 Hz), 7.29−7.34 (m, 1H), 7.40 (s, 1H), 7.80 (dt, 1H, J = 10.0 Hz, 4.0 Hz), 7.90 (s, 1H,), 8.51−8.54 (m, 1H), 9.07 (s, 1H).

*7-(3,5-Dimethylisoxazol-4-yl)-8-methoxy-1-(pyridin-2-ylmethyl)-1H-imidazo[4,5-c]quinolin-2-amine (**24**).* 7-(3,5-Dimethylisoxazol-4-yl)-6-methoxy-N^4-(pyridin-2-ylmethyl)quinoline-3,4-diamine **53** (35 mg, 0.09 mmol) and cyanic bromide (9.9 mg, 0.09 mmol) were heated in ethanol (5 mL) for 5 h at 60 °C and then evaporated *in vacuo* to give a dark brown solid. This was purified by MDAP (high pH) to give the title compound (12 mg, 0.03 mmol, 32% yield) as a pale yellow solid.

LCMS (formic acid): rt = 0.61 min, MH^+ = 401.

^{1}H NMR (CD_3OD, 400 MHz) δ 2.24 (s, 3H), 2.42 (s, 3H), 3.83 (s, 3H), 6.00 (s, 2H), 7.33 (d, J = 8.1 Hz, 1H), 7.46−7.50 (m, 2H), 7.89−7.94 (m, 2H), 8.72−8.76 (m, 1H), 8.89 (s 1H).

*7-(3,5-Dimethylisoxazol-4-yl)-8-methoxy-N-(2-methoxyethyl)-1-(pyridine-2-ylmethyl)-1H-imidazo[4,5-c]quinoline-2-amine (**25**).* To a solution of 7-(3,5-dimethylisoxazol-4-yl)-6-methoxy-N^4-(pyridine-2-ylmethyl)quinoline-3,4-diamine **25** (875 mg, 2.33 mmol) in EtOH (50 mL) was added 1-isothiocyanato-2-methoxyethane (0.51 mL, 4.66 mmol), and the reaction mixture was heated at 60 °C for 6 h. The solvent was evaporated under reduced pressure. EDC (894 mg, 4.66 mmol) and THF (50 mL) were added, and the reaction mixture was stirred at 60 °C for 1 h, followed by stirring at room temperature overnight. The solvent was removed under reduced pressure. The sample was loaded in MeOH/DCM (and the column dried in a vacuum oven) and purified by SPE (silica, 100 g) using a gradient of 0−10% (2 M ammonia in MeOH) in DCM. The appropriate fractions were combined and evaporated under reduced pressure to give a brown gum (310 mg). A portion (40 mg) of this gum was dissolved in DMSO (1 mL) and purified by MDAP (high pH). The solvent was blown down a stream of nitrogen to give the title compound (23 mg, 0.05 mmol, 2% yield) as a white solid.

LCMS (formic acid): rt = 0.68 min, MH^+ = 459.

^{1}H NMR (DMSO-d_6, 393 K): δ 2.08 (s, 3H), 2.27 (s, 3H), 3.35 (s, 3H), 3.63−3.71 (m, 4H), 3.73 (s, 3H), 5.83 (s, 2H), 6.77−6.88 (br m, 1H), 7.24 (d, J = 7.8 Hz, 1H), 7.27−7.35 (m, 1H), 7.45 (s, 1H), 7.72−7.83 (m, 2H), 8.58 (d, J = 4.3 Hz, 1H), 8.81 (s, 1H).

^{13}C NMR (DMSO-d_6, 303 K): δ 10.3, 11.3, 42.5, 55.4, 58.0, 70.5, 98.8, 112.5, 116.8, 118.5, 120.8, 123.0, 131.7, 132.5, 131.7, 132.5, 136.7, 138.8, 139.5, 149.5, 154.3, 155.5, 156.5, 159.1, 165.7.

IR (neat): 3233 (imine NH), 1611 (aryl), 1572 (aryl), 1221 (aryl ether), 777 (aryl C−H) cm^{-1}.

M.p.: 245−252 °C.

HRMS: ($C_{25}H_{27}N_6O_3$) requires MH^+ 459.2145, found MH^+ 459.2151.

7-(3,5-Dimethyl-4-isoxazolyl)-8-(methyloxy)-2-[(methyloxy)-methyl]-1-(2-pyridinylmethyl)-1*H*-imidazo[4,5-*c*]quinoline (**26**).

Glacial acetic acid (2 mL) was added to *N*-{7-(3,5-dimethyl-4-isoxazolyl)-6-(methyloxy)-4-[(2-pyridinylmethyl)amino]-3-quinolinyl}-2-(methyloxy)acetamide **58** (70 mg, 0.16 mmol). The mixture was refluxed for 2 h. The reaction mixture was cooled, and the solvent was evaporated. The residue was chromatographed using 2−10% methanol in dichloromethane to give the title compound (53 mg, 0.12 mmol, 79% yield) as an off-white solid.

LCMS (formic acid): rt = 0.71 min, MH^+ = 430.

^{1}H NMR (DMSO-d_6, 400 MHz): δ 2.14 (s, 3H), 2.31 (s, 3H), 3.46 (s, 3H), 3.62 (s, 3H,), 4.93 (s, 2H), 6.05 (s, 2H), 6.86 (d, 1H, J = 12.0 Hz) 7.23−7.28 (m, 1H), 7.35 (s, 1H), 7.62 (dt, 1H, J = 12.0 Hz, 4.0 Hz), 7.99 (s, 1H), 8.66 (d, 1H, J = 4.0 Hz), 9.24 (s, 1H).

*4-(8-Methoxy-1-(pyridin-2-ylmethyl)-2-(tetrahydro-2H-pyran-4-yl)-1H-imidazo[4,5-c]quinolin-7-yl)-3,5-dimethylisoxazole (**27**).* To 7-(3,5-dimethylisoxazol-4-yl)-6-methoxy-N^4-(pyridin-2-ylmethyl)-quinoline-3,4-diamine **53** (2.0 g, 5.33 mmol) in DCM was added HATU (3.65 g, 9.6 mmol), NEt_3 (excess), and tetrahydro-2*H*-pyran-4-carboxylic acid (693 mg, 9.6 mmol), and the reaction mixture was stirred at room temperature overnight. The reaction mixture was partitioned between saturated aqueous sodium bicarbonate solution and dichloromethane. The organic layer was dried using Na_2SO_4, filtered, and evaporated to dryness to give the intermediate **59** (2.5 g). Acetic acid (30 mL) was added, and the reaction mixture was heated at 90 °C for 6 h. The reaction mixture was evaporated to dryness, resuspended in saturated aqueous sodium bicarbonate solution, and extracted with dichloromethane. The organic layer was dried using Na_2SO_4, filtered, and evaporated to dryness. The material was purified using silica column chromatography, eluted with 5% methanol in

https://doi.org/10.1021/acs.jmedchem.1c00855
J. Med. Chem. 2021, 64, 12200−12227

dichloromethane. Recrystallization in ethanol gave the title compound (1.88 g, 4.0 mmol, 75% yield) as a beige solid.

LCMS (formic acid): rt = 0.64 min, MH^+ = 470.

^{1}H NMR (DMSO-d_6, 400 MHz) δ 1.75−2.10 (m, 7H), 2.27 (s, 3H), 3.29−3.39 (m, 1H), 3.47−3.62 (m, 2H), 3.67 (s, 3H), 3.90−4.01 (m, 2H), 6.17 (s, 2H), 7.21−7.27 (m, 1H), 7.28−7.36 (m, 1H), 7.39 (s, 1H), 7.76−7.83 (m, 1H), 7.91 (s, 1H), 8.49−8.54 (m, 1H), 9.10 (s, 1H).

*4-(8-Methoxy-2-(methoxymethyl)-1-(1-methoxypropan-2-yl)-1H-imidazo[4,5-c]quinoline-7-yl)-3,5-dimethylisoxazole (**28**).* A solution of 2-methoxyacetic acid (43 μL, 0.56 mmol), HATU (229 mg, 0.60 mmol), and DIPEA (243 μL, 1.39 mmol) in DMF (2 mL) was stirred at room temperature for 15 min. 7-(3,5-Dimethylisoxazol-4-yl)-6-methoxy-N^4-(1-methoxypropan-2-yl)quinoline-3,4-diamine **70** (165 mg, 0.463 mmol) was added, and the reaction mixture was stirred at room temperature over the weekend. A solution of 2-methoxyacetic acid (22 μL, 0.28 mmol), HATU (115 mg, 0.30 mmol), and DIPEA (121 μL, 0.69 mmol) in DMF (1 mL) was stirred at room temperature for 15 min. This was added to the reaction mixture, which was then stirred at room temperature for 6 h. The reaction mixture was blown down under a stream of nitrogen. The sample was loaded in DCM and purified by SPE (aminopropyl, 2 g), eluted using 10% MeOH in DCM. The appropriate fractions were combined and blown down under a stream of nitrogen to give a brown gum. The gum was purified by MDAP (high pH). The solvent was blown down under a stream of nitrogen to give a colorless gum. The gum was dissolved in acetic acid (1.5 mL, 0.34 mmol), and the reaction mixture was heated under microwave conditions at 120 °C for 1 h. The reaction mixture was blown down under a stream of nitrogen. The resulting gum was purified by MDAP (high pH). The solvent was blown down under a stream of nitrogen to give the title compound **15** (40 mg, 0.10 mmol, 21% yield) colorless glass.

LCMS (formic acid): rt = 0.75 min, MH^+ = 491.

^{1}H NMR (DMSO-d_6, 393 K, 400 MHz): δ 1.81 (d, J = 7.1 Hz, 3H), 2.16 (s, 3H), 2.35 (s, 3H), 3.31 (s, 2H), 3.43 (s, 2H), 3.94−4.05 (m, 4H), 4.79−4.92 (m, 2H), 5.42−5.56 (m, 1H), 7.83 (s, 1H), 8.00 (s, 1H), 9.06 (s, 1H).

*4-(8-Methoxy-2-(methoxymethyl)-1-((tetrahydro-2H-pyran-4-yl)methyl)-1H-imidazo[4,5-c]quinoline-7-yl)-3,5-dimethylisoxazole (**29**).* A solution of 2-methoxyacetic acid (15 μL, 0.19 mmol), HATU (81 mg, 0.21 mmol), and DIPEA (84 μL, 0.48 mmol) in DMF (2 mL) was stirred at room temperature for 15 min. 7-(3,5-Dimethylisoxazol-4-yl)-6-methoxy-N^4-((tetrahydro-2H-pyran-4-yl)-methyl)quinoline-3,4-diamine **71** (37 mg, 0.097 mmol) was added, and the reaction mixture was stirred at room temperature for 3 h. The reaction mixture was blown down under a stream of nitrogen. The sample was loaded in DCM and purified by SPE (aminopropyl, 2 g), eluted using 10% MeOH in DCM. The appropriate fractions were combined and blown down a stream of nitrogen to give a brown gum. The gum was purified by MDAP (high pH). The solvent was blown down a stream of nitrogen to give a colorless gum (22 mg). To this was added acetonitrile (1.5 mL) and 10 mM aqueous ammonium bicarbonate solution, adjusted to pH 10 using ammonia (1.5 mL), and the reaction mixture stood at room temperature for 4 days. The reaction mixture was blown down under a stream of nitrogen to give the title compound (22 mg, 0.050 mmol, 52% yield) as a colorless glass.

LCMS (formic acid): rt = 0.70 min, MH^+ = 437.

^{1}H NMR (DMSO-d_6, 393 K, 400 MHz): δ 1.51−1.64 (m, 4H), 2.16 (s, 3H), 2.35−2.43 (m, 4H), 3.26−3.32 (m, 2H), 3.45 (s, 3H), 3.85−3.90 (m, 2H), 4.02 (s, 3H), 4.69 (d, J = 7.6 Hz, 2H), 4.84 (s, 2H), 7.73 (s, 1H), 8.00 (s, 1H), 9.06 (s, 1H).

*4-(1-(Cyclopropylmethyl)-8-methoxy-2-(tetrahydro-2H-pyran-4-yl)-1H-imidazo[4,5-c]quinoline-7-yl)-3,5-dimethylisoxazole (**30**).* To a suspension of N-(cyclopropylmethyl)-7-(3,5-dimethylisoxazol-4-yl)-6-methoxy-3-nitroquinolin-4-amine **67** (100 mg, 0.27 mmol) and sodium hydrosulfite (142 mg, 0.81 mmol) in EtOH (0.8 mL) and water (0.4 mL) was added tetrahydro-2H-pyran-4-carbaldehyde (62 mg, 0.54 mmol), and the reaction mixture was heated in under microwave conditions at 100 °C for 1 h. The reaction mixture was blown down under a stream of nitrogen, and the residue was dissolved in DMSO (3 mL) and purified by MDAP (high pH). The solvent was blown down under a stream of nitrogen to give the title compound (32 mg, 0.074 mmol, 27% yield) as a colorless gum.

LCMS (formic acid): rt = 0.78 min, MH^+ = 433.

^{1}H NMR (DMSO-d_6, 393 K, 400 MHz): δ 0.48−0.55 (m, 2H) 0.64−0.68 (m, 2H), 1.38−1.52 (m, 1H), 1.89−1.92 (m, 2H), 2.01−2.10 (m, 2H), 2.15 (s, 3H), 2.34 (s, 3 H), 3.30−3.43 (m, 1H), 3.56−3.68 (m, 2H), 3.99−4.09 (m, 5H), 4.71 (d, J = 6.0 Hz, 2H), 7.89 (s, 1H), 7.97 (s, 1H), 9.04 (s, 1H).

*4-(8-Methoxy-1-(1-methoxypropan-2-yl)-2-(tetrahydro-2H-pyran-4-yl)-1H-imidazo[4,5-c]quinoline-7-yl)-3,5-dimethylisoxazole (**31**).* A solution of 7-(3,5-dimethylisoxazol-4-yl)-6-methoxy-N^4-(1-methoxypropan-2-yl)quinoline-3,4-diamine **70** (9.1 g, 25.5 mmol) in DCM (300 mL) was treated with pyridine (30 mL) and tetrahydro-2H-pyran-4-carbonyl chloride (5.0 mL, 41.1 mmol). The solution was stirred under nitrogen at room temperature for 3.5 h and then left standing overnight. The reaction mixture was concentrated under reduced pressure, and the residue partitioned between DCM and water. The organic phase was washed with water (×2), and the combined aqueous layers were extracted with DCM. The combined organic layers were washed with brine, dried using a hydrophobic frit, and evaporated under reduced pressure. The combined aqueous layers, including the brine wash, were basified with solid sodium bicarbonate, and the aqueous layer was twice extracted with DCM. The organic fractions were dried using a hydrophobic frit, combined with the previously extracted material, and evaporated to dryness under reduced pressure to give a brown foam. This foam was further dried *in vacuo* to give 13.5 g of material. The material was triturated with diethyl ether, the suspension was chilled (ice/water bath), and the solid was isolated by filtration. The solid was washed with a little diethyl ether and air-dried to give a beige solid (11.95 g). This solid and *p*-toluenesulfonic acid (1.2 g, 25.5 mmol) in toluene (250 mL) was heated at reflux, under nitrogen, using a Dean−Stark apparatus for 3 days. Further *p*-toluenesulfonic acid (0.2 g, 4.3 mmol) was added, and heating was continued overnight. The reaction mixture had boiled dry. Water (750 mL) was added, followed by saturated aqueous sodium bicarbonate solution until the pH reached 8. The aqueous layer was extracted with EtOAc (3 × 750 mL). The organic layers were combined, dried using a hydrophobic frit, and evaporated under reduced pressure to give a light brown solid, ∼11 g. The solid was triturated in ether (∼200 mL) and placed briefly in an ultrasonic bath, and the majority of the solid appeared to be a fine powder. The fine powder suspended in the ether was decanted, and the solid was isolated by filtration and dried in a vacuum oven to give 6.3 g of material. This material was triturated in ether (∼100 mL), placed briefly in an ultrasonic bath, and stood overnight at room temperature. The solid was isolated by filtration and dried in a vacuum oven to give the title compound (4.9 g). The clumped solid left over from the decanting was triturated in ether (100 mL), placed in an ultrasonic bath for 15 min, and stood at room temperature for 3 days. The solid was isolated by filtration and dried in a vacuum oven to give the title compound (3.6 g). The total amount of material obtained was 8.5 g, 74% yield.

LCMS (formic acid): rt = 0.76 min, MH+ = 451.

^{1}H NMR (DMSO-d_6, 393 K, 400 MHz): δ 1.80 (d, J = 7.3 Hz, 3H), 1.83−1.96 (m, 2 H), 2.01−2.10 (m, 2H), 2.13 (s, 3H), 2.32 (s, 3H), 3.25 (s, 3H), 3.38−3.48 (m, 1H), 3.54−3.63 (m, 2H), 3.95−4.05 (m, 6H), 4.08−4.14 (m, 1H) 5.32−5.52 (m, 1H), 7.71 (s, 1H), 7.96 (s, 1H), 9.01 (s, 1H).

*4-(8-Methoxy-1-((R)-1-methoxypropan-2-yl)-2-(tetrahydro-2H-pyran-4-yl)-1H-imidazo[4,5-c]quinoline-7-yl)-3,5-dimethylisoxazole (**32**).* The racemic 4-(1-(1-methoxypropan-2-yl)-2-(tetrahydro-2H-pyran-4-yl)-1H-imidazo[4,5-c]quinoline-7-yl)-3,5-dimethylisoxazole **31** (85 mg, 0.19 mmol) was separated by chiral HPLC. The HPLC analysis was carried out on a Chiralpak AD-H column "ADH10029-01" (250 × 30 mm, i.d. 5 μm packing diameter). The purification was run using 15% EtOH in heptane over 35 min, with a flow rate of 45 mL/min. The UV detection was at a wavelength of 300 nm. The second eluting enantiomer was collected, between 28 and 31

https://doi.org/10.1021/acs.jmedchem.1c00855
J. Med. Chem. 2021, 64, 12200−12227

min. Combined fraction solutions were evaporated to dryness under reduced pressure, the residue was transferred to a vial using EtOH, and the solvent was dried under a stream of nitrogen to leave the title compound (39 mg, 0.087 mmol, 46% yield).

LCMS (formic acid): rt = 0.73 min, MH^+ = 451.

^{1}H NMR (DMSO-d_6, 393 K, 400 MHz): δ 1.80 (d, J = 7.3 Hz, 3H), 1.83−1.98 (m, 2H), 2.00−2.10 (m, 2H), 2.13 (s, 3H), 2.32 (s, 3H), 3.26 (s, 3H), 3.39−3.49 (m, 1H), 3.54−3.62 (m, 2H), 3.95−4.05 (m, 6H), 4.08−4.12 (m, 1H) 5.35−5.47 (br.s., 1H), 7.72 (s, 1H), 7.95 (s, 1H), 9.00 (s, 1H).

Chiral HPLC (conditions as for preparative HPLC, except column diameter of 4.6 mm): 97% ee.

^{13}C NMR (DMSO-d_6, 303 K): δ 10.3, 11.3, 17.6, 31.3, 31.7, 33.2, 51.3, 55.6, 58.5, 66.6, 74.0, 101.2, 102.6, 112.1, 117.4, 119.4, 132.1, 133.1, 137.5, 139.5, 142.7, 154.7, 159.1, 166.0.

IR: 2963 (saturated CH_2), 2940 (saturated CH_2), 2852 (ether $COCH_3$), 1618 (aryl), 1583 (aryl), 1221 (aryl ether), 839 (aryl C−H) cm^{-1}.

M.p.: 190−192 °C.

HRMS: ($C_{25}H_{31}N_4O_4$) MH^+ requires 451.2340, found MH^+ 451.2331.

$[\alpha_D]^{23.1\ oC}$ (c 1.0, MeOH): + 2.9°.

*4-(8-Methoxy-1-((S)-1-methoxypropan-2-yl)-2-(tetrahydro-2H-pyran-4-yl)-1H-imidazo[4,5-c]quinoline-7-yl)-3,5-dimethylisoxazole (**33**).* The racemic 4-(1-(1-methoxypropan-2-yl)-2-(tetrahydro-2*H*-pyran-4-yl)-1*H*-imidazo[4,5-*c*]quinolin-7-yl)-3,5-dimethylisoxazole **31** (85 mg, 0.189 mmol) was purified by chiral HPLC. The HPLC analysis was carried out on a Chiralpak AD-H column "ADH10029-01" (250 × 30 mm, i.d. 5 μm packing diameter). The purification was run using 15% EtOH in heptane over 35 min, with a flow rate of 45 mL/min. The UV detection was at a wavelength of 300 nm. The first eluting enantiomer was collected, between 24 and 26.5 min. Combined fraction solutions were evaporated to dryness under reduced pressure, the residue was transferred to a vial using EtOH, and the solvent was dried under a stream of nitrogen to leave the title compound (38 mg, 0.084 mmol, 44% yield).

LCMS (formic acid): rt = 0.73 min, MH^+ = 451.

^{1}H NMR (DMSO-d_6, 393 K, 400 MHz): δ 1.80 (d, J = 7.3 Hz, 3H), 1.82−1.98 (m, 2 H), 2.00−2.10 (m, 2H), 2.13 (s, 3H), 2.32 (s, 3H), 3.26 (s, 3H), 3.54−3.63 (m, 2H), 3.96−4.05 (m, 7H), 5.34−5.49 (br m, 1H), 7.72 (s, 1H), 7.95 (s, 1H), 9.00 (s, 1H).

Chiral HPLC (conditions as for preparative HPLC, except column diameter of 4.6 mm): >99% ee.

*4-(8-Methoxy-2-(tetrahydro-2H-pyran-4-yl)-1-(1-(tetrahydro-2H-pyran-4-yl)ethyl)-1H-imidazo[4,5-c]quinoline-7-yl)-3,5-dimethylisoxazole (**34**).* To a suspension of tetrahydro-2*H*-pyran-4-carboxylic acid (51 mg, 0.39 mmol) and HATU (168 mg, 0.44 mmol) in DMF (2 mL) was added DIPEA (0.136 mL, 0.779 mmol), and the resulting solution was stirred at room temperature for 15 min. 7-(3,5-Dimethylisoxazol-4-yl)-6-methoxy-N^4-(1-(tetrahydro-2*H*-pyran-4-yl)-ethyl)quinoline-3,4-diamine **72** (103 mg, 0.26 mmol) was added, and the reaction mixture was stirred at room temperature overnight. The reaction mixture was blown down under a stream of nitrogen, and the residue was loaded in DCM and purified by SPE (aminopropyl, 5 g), eluted using 10% MeOH in DCM. The appropriate fractions were combined and dried under a stream of nitrogen to give a brown gum. The gum was dissolved in DMSO (2 mL) and purified by MDAP (formic acid). The solvent was dried under a stream of nitrogen to give a light brown solid (45 mg). To the solid was added glacial acetic acid (1 mL, 0.09 mmol), and the reaction mixture was heated under microwave conditions at 120 °C for a total of 29 h. The reaction mixture was blown down under a stream of nitrogen. The resulting gum was dissolved in DMSO (1 mL) and purified by MDAP (high pH). The solvent was blown down under a stream of nitrogen to give the title compound (18.7 mg, 0.038 mmol, 15% yield) as a light pink solid.

LCMS (formic acid): rt = 0.75 min, MH^+ = 491.

^{1}H NMR (DMSO-d_6, 393 K, 400 MHz): δ 0.83−0.96 (m, 1H), 1.19−1.34 (m, 1H), 1.55−1.70 (m, 1H), 1.80−1.97 (m, 6H), 2.01−2.11 (m, 2H), 2.17 (s, 3H), 2.35 (s, 3H), 2.55−2.70 (m, 1H), 3.06−3.19 (m, 1H), 3.39−3.53 (m, 2H) 3.58−3.76 (m, 2H), 3.94−4.13 (m, 7H), 4.69−5.12 (m, 1H), 7.75 (s, 1H), 7.99 (s, 1H), 9.04 (s, 1H).

*7-(3,5-Dimethylisoxazol-4-yl)-8-methoxy-N,N-dimethyl-1-((tetrahydro-2H-pyran-4-yl)methyl)-1H-imidazo[4,5-c]quinoline-2-amine (**35**).* 7-(3,5-Dimethylisoxazol-4-yl)-6-methoxy-N^4-((tetrahydro-2*H*-pyran-4-yl)methyl)quinoline-3,4-diamine **71** (50 mg, 0.13 mmol) and *N*-(dichloromethylene)-*N*-methylmethanaminium chloride (43 mg, 0.26 mmol) were combined in dry acetonitrile (0.5 mL) and heated under microwave conditions at 120 °C for 10 min. The reaction mixture was blown down under a stream of nitrogen, and the residue was dissolved in DMSO (1 mL) and purified by MDAP (high pH). The solvent was blown down under a stream of nitrogen to give the title compound (44 mg, 0.10 mmol, 77% yield) as a yellow gum.

LCMS (formic acid): rt = 0.70 min, MH^+ = 436.

^{1}H NMR (DMSO-d_6, 393 K, 400 MHz): δ 1.31−1.37 (m, 4H), 2.15 (s, 3H), 2.17−2.25 (m, 1H), 2.34 (s, 3H), 2.99 (s, 6H), 3.13−3.26 (m, 2H), 3.74−3.84 (m, 2H), 3.99 (s, 3H), 4.51 (d, J = 7.3 Hz, 2H), 7.60 (s, 1H) 7.91 (s, 1H) 8.90 (s, 1H)

^{13}C NMR (DMSO-d_6, 300 K): δ 10.4, 11.4, 29.6, 35.0, 42.7, 50.8, 55.8, 66.2, 99.4, 112.4, 117.9, 119.6, 131.9, 132.9, 135.8, 138.9, 141.0, 155.0, 159.2, 160.6, 165.9.

IR (neat): 2944 (NCH_3), 2911 (NCH_3), 2853 (NCH_3), 1574 (aryl), 1531 (aryl), 1216 (aryl ether), 845 (aryl C−H) cm^{-1}.

M.p.: 205−207 °C.

HRMS: ($C_{24}H_{30}N_5O_3$) MH^+ requires 436.2343, found MH^+ 436.2335.

*7-(3,5-Dimethyl-4-isoxazolyl)-8-(methyloxy)-2-(4-morpholinyl)-1-(tetrahydro-2H-pyran-4-ylmethyl)-1H-imidazo[4,5-c]quinoline (**36**).* 7-(3,5-Dimethyl-4-isoxazolyl)-8-(methyloxy)-1-(tetrahydro-2*H*-pyran-4-ylmethyl)-1,3-dihydro-2*H*-imidazo[4,5-*c*]quinolin-2-one **13** (220 mg, 0.54 mmol) was dissolved in $POCl_3$ (2 mL, 21.5 mmol), PCl_5 (0.2 g, 0.96 mmol) was added, and the mixture was heated at 120 °C for 24 h. The reaction mixture was evaporated *in vacuo* to give a beige solid. The solid was dissolved in NMP (0.5 mL), and morpholine (0.3 mL, 3.44 mmol) was added, and then the solution was heated in the microwave at 150 °C for 1 h. The solution was loaded onto a 20 g SCX cartridge and washed with methanol (30 mL) and then eluted with 2 M methanolic ammonia (30 mL), and the eluant waa evaporated *in vacuo* to give a beige gum. This was dissolved in DCM (3 mL) , loaded onto a 25 g silica column and then eluted with 0−10% 2 M methanolic ammonia/DCM. Product-containing fractions were evaporated *in vacuo* to give the title compound (4.7 mg, 9.84 μmol, 2% yield) as a beige solid.

LCMS (formic acid): rt = 0.70 min, MH^+ = 478.

^{1}H NMR ($CDCl_3$, 400 MHz) δ 1.33−1.40 (m, 2H), 1.48−1.61 (m, 2H), 2.26 (s, 3H), 2.41 (s, 3H), 3.22−3.37 (m, 6H), 3.95−4.00 (m, 10H), 4.38−4.42 (m, 2H), 7.39 (s, 1H), 8.03 (s, 1H), 9.16 (s, 1H).

*7-(3,5-Dimethylisoxazol-4-yl)-8-methoxy-N-(2-methoxyethyl)-1-((R)-1-(pyridine-2-yl)ethyl)-1H-imidazo[4,5-c]quinoline-2-amine (**37**).* To a solution of 7-(3,5-dimethylisoxazol-4-yl)-6-methoxy-N^4-((*R*)-1-(pyridine-2-yl)ethyl)quinoline-3,4-diamine **74** (538 mg, 1.38 mmol) in EtOH (40 mL) was added 1-isothiocyanato-2-methoxy-ethane (300 μL, 2.76 mmol), and the reaction mixture was heated at 60 °C for 5.5 h. Further, 1-isothiocyanato-2-methoxyethane (150 μL, 1.38 mmol) was added, and the reaction mixture was heated at 60 °C overnight. The solvent was removed under reduced pressure, the residue was dissolved in THF (40 mL), EDC (530 mg, 2.76 mmol) was added, and the mixture was heated at 60 °C for 4 h. The solvent was removed under reduced pressure, and the sample was loaded in MeOH/DCM (and the column dried in a vacuum oven) and purified by SPE (silica, 100 g) using a gradient of 0−10% (2 M ammonia in MeOH) in DCM. The appropriate fractions were combined and evaporated under reduced pressure to give crude product (~600 mg). The crude product was dissolved in DMSO (5 mL) and purified by MDAP (high pH). The samples were blown down under a stream of nitrogen to give the title compound (122 mg, 0.26 mmol, 19% yield) as a white solid.

LCMS (formic acid): rt = 0.73 min, MH^+ = 473.

^{1}H NMR (DMSO-d_6, 393 K, 400 MHz): δ 2.06−2.11 (m, 6H), 2.27 (s, 3H), 3.35 (s, 3H), 3.59 (s, 3H), 3.62−3.73 (m, 4H), 6.32 (q,

https://doi.org/10.1021/acs.jmedchem.1c00855
J. Med. Chem. 2021, 64, 12200−12227

J = 7.1 Hz, 1H), 6.77−6.85 (br m, 1H), 6.96 (s, 1H), 7.30 (d, J = 7.8 Hz, 1H), 7.33−7.39 (m, 1H), 7.75−7.81 (m, 2H), 8.68 (d, J = 4.0 Hz, 1H), 8.82 (s, 1H).

^{13}C NMR (DMSO-d_6, 303 K): δ 10.3, 11.3, 17.7, 42.8, 55.3, 58.1 (br, 2 C), 70.5, 112.3, 113.9, 116.7, 118.3, 121.1, 121.2, 122.9, 132.7, 137.8, 138.5, 139.9, 149.5, 149.6, 154.0, 155.7, 158.9, 159.1, 165.8

IR (neat): 3239 (imine NH), 1591 (aryl), 1556 (aryl), 1219 (aryl ether), 772 (aryl C−H) cm^{-1}.

M.p.: 109−111 °C.

HRMS: ($C_{26}H_{29}N_6O_3$) MH^+ requires 473.2296, found MH^+ 473.2284.

$[\alpha_D]^{23.1\ °C}$ (c 1.0, MeOH): + 118.7°.

*7-(3,5-Dimethyl-4-isoxazolyl)-4-[(1-methylethyl)amino]-6-(methyloxy)-3-quinolinecarboxamide, (**40**).* 4-Chloro-7-(3,5-dimethyl-4-isoxazolyl)-6-(methyloxy)-3-quinolinecarboxamide **39** (500 mg, 1.51 mmol) was taken up in NMP (1.5 mL). DIPEA (0.66 mL, 3.77 mmol) was added, followed by 2-propanamine (0.16 mL, 1.88 mmol). The mixture was stirred at 120 °C for 2 h. Another equivalent of 2-propanamine was added, and the reaction mixture was left to stand for three nights and then reheated to 120 °C for a further 1 h. The brown solution was loaded on to a 20 g SCX cartridge. The cartridge was eluted with methanol and then 2 M NH_3 in methanol. The appropriate fractions were concentrated in vacuo. The crude product was loaded in the minimum amount of DCM and purified by column chromatography (silica), eluted using 1−10% of NH_3/MeOH in DCM. The appropriate fractions were combined and concentrated *in vacuo* to give the title compound (224 mg, 0.57 mmol, 38% yield) as a brown solid.

LCMS (formic acid): rt = 0.66 min, MH^+ = 355.

^{1}H NMR ($CDCl_3$, 400 MHz) δ 1.42 (d, 6H, J = 6.3 Hz) 2.24 (s, 3H) 2.39 (s, 3H) 3.93 (s, 3H) 4.26−4.40 (m, 1H) 5.79−6.07 (m, 2H) 7.51 (s, 1H) 7.74 (s, 1H) 8.69 (s, 2H).

*7-(3,5-Dimethyl-4-isoxazolyl)-6-(methyloxy)-4-[(2-methylpropyl)amino]-3-quinolinecarboxamide (**41**).* 4-Chloro-7-(3,5-dimethyl-4-isoxazolyl)-6-(methyloxy)-3-quinolinecarboxamide **39** (500 mg, 1.51 mmol) was taken up in NMP (1.5 mL). DIPEA (0.66 mL, 3.77 mmol) was added, followed by isobutylamine (0.19 mL, 1.88 mmol). The reaction mixture was stirred at 120 °C for 2 h. The brown solution was purified by SCX, eluted with methanol and then 2 M NH_3 in MeOH. The basic fractions were concentrated *in vacuo*. The methanol fraction was repurified by SCX, eluted with methanol and then 2 M NH_3 in MeOH. The appropriate fractions were concentrated *in vacuo*. NMP was found to be in the product. This mixture was repurified by SCX, eluted with methanol and 2 M NH_3 in MeOH. The appropriate fractions were concentrated *in vacuo*. The NH_3 in MeOH fractions from all the SCX purifications was combined. The crude product was loaded in the minimum amount of DCM and purified by column chromatography (silica), eluted using 1−10% NH_3 in MeOH. The appropriate fractions were combined and concentrated *in vacuo* to give the title compound (879 mg, 1.19 mmol, 79% yield) as an orange solution. Minimum purity was 50% due to residual NMP.

LCMS (formic acid): rt = 0.73 min, MH^+ = 369.

^{1}H NMR ($CDCl_3$, 400 MHz) δ 1.07 (d, 6H, J = 6.8 Hz) 2.21 (s, 3H) 2.38 (s, 3H) 3.62 (dd, 1H, J = 6.4, 5.4 Hz) 3.89 (s, 3H) 6.16 (bs, 2H) 7.57 (s, 1H) 7.69 (s, 1H) 8.68 (s, 1H) 9.36 (br s, 1H).

*7-(3,5-Dimethylisoxazol-4-yl)-6-methoxy-4-(pentan-2-ylamino)-quinoline-3-carboxamide (**42**).* 4-Chloro-7-(3,5-dimethylisoxazol-4-yl)-6-methoxyquinoline-3-carboxamide **39** (500 mg, 1.51 mmol) was taken up in NMP (1.5 mL), pentan-2-amine (0.22 mL, 1.88 mmol) and DIPEA (0.66 mL, 3.77 mmol) were added, and the mixture was stirred at 120 °C for 3 h. The reaction mixture was cooled and purified by SCX, eluted with methanol and then 2 M NH_3 in MeOH. The appropriate fractions were concentrated *in vacuo* and loaded in the minimum amount of DCM and purified by column chromatography (silica), eluted using 1−10% NH_3 in MeOH. The fractions were combined and concentrated *in vacuo* in two batches. Batch 1: the title compound (316 mg, 0.78 mmol, 52% yield) as an orange solid.

LCMS (formic acid): rt = 0.73 min, MH^+ = 383.

^{1}H NMR ($CDCl_3$, 400 MHz) δ 0.86 (t, 3H, J = 7.2 Hz) 1.27−1.49 (m, 5H) 1.52−1.76 (m, 2H) 2.16 (s, 3H) 2.30 (s, 3H) 3.88 (s, 3H) 4.07−4.26 (m, 1H) 6.49−7.02 (m, 1H) 7.47 (s, 1H) 7.67 (s, 1H) 8.71 (d, 1H, J = 9.3 Hz) 8.77 (s, 1H).

Batch 2: the title compound (178 mg, 0.42 mmol, 28% yield) as a yellow solid.

LCMS (formic acid): rt = 0.73 min, MH^+ = 383,

^{1}H NMR ($CDCl_3$, 400 MHz) δ 0.89−0.94 (t, 3H, J = 6.3 Hz), 1.41 (d, 3H, J = 6.3 Hz), 1.42−1.55 (m, 2H), 1.61−1.79 (m, 2H), 2.22 (s, 3H), 2.36 (s, 3H), 3.95 (s, 3H), 4.17−4.24 (m, 1H), 6.5−7.5 (br s, 2H), 7.53 (s, 1H), 7.72 (s, 1H), 8.83−8.88 (m, 2 H).

*4-((Cyclopropylmethyl)amino)-7-(3,5-dimethylisoxazol-4-yl)-6-methoxyquinoline-3-carboxamide (**43**).* To a suspension of 4-chloro-7-(3,5-dimethylisoxazol-4-yl)-6-methoxyquinoline-3-carboxamide **39** (500 mg, 1.51 mmol) in dry NMP (2.5 mL) were added DIPEA (0.658 mL, 3.77 mmol) and cyclopropylmethanamine (0.163 mL, 1.88 mmol). The reaction mixture was heated under nitrogen at 100 °C for 3.5 h. Further cyclopropylmethanamine (0.163 mL, 1.88 mmol) was added, and the reaction mixture was heated under nitrogen at 100 °C overnight. The sample was loaded directly onto and purified by SCX. The column was washed with 10% MeOH in DCM and eluted using 2 M ammonia in MeOH. The appropriate fractions were combined and evaporated under reduced pressure to give a brown gum. The compound was triturated in EtOAc; the solid was removed and dried in a vacuum oven overnight to give the title compound (371 mg, 1.01 mmol, 67% yield) as a yellow solid.

LCMS (formic acid): rt = 0.70 min, MH^+ = 367.

^{1}H NMR (DMSO-d_6, 400 MHz): δ 0.27−0.34 (m, 2H), 0.48−0.56 (m, 2H), 1.12−1.23 (m, 1H), 2.13 (s, 3H) 2.32 (s, 3H), 3.50−3.56 (m, 2H) 3.91 (s, 3H), 7.33−7.44 (br s, 1H), 7.64−7.67 (m, 2H), 7.97−8.07 (br s, 1H), 8.60 (s, 1H) 8.75 (t, J = 5.3 Hz, 1 H).

*7-(3,5-Dimethylisoxazol-4-yl)-6-methoxy-4-((1-methoxypropan-2-yl)amino)quinoline-3-carboxamide (**44**).* 4-Chloro-7-(3,5-dimethylisoxazol-4-yl)-6-methoxyquinoline-3-carboxamide **39** (100 mg, 0.30 mmol), 1-methoxypropan-2-amine (0.04 mL, 0.38 mmol), and DIPEA (0.13 mL, 0.75 mmol) were taken up in *N*-methyl-2-pyrrolidone (0.5 mL). The mixture was stirred at 120 °C for 4 h. Further 1-methoxypropan-2-amine was added (0.016 mL), and the mixture continued to be stirred at 120 °C for another 4 h. The reaction mixture was cooled and purified by SCX, eluted with methanol and then 2 M NH_3 in MeOH. The appropriate fractions were combined and concentrated *in vacuo* to give the crude title compound (116 mg) as a brown solid which was used directly in the next reaction without further purification.

LCMS (formic acid): rt = 0.69 min, MH^+ = 385.

^{1}H NMR ($CDCl_3$, 400 MHz) δ 1.36 (d, 3H, J = 6.6 Hz) 2.23−2.27 (m, 5H) 2.40 (s, 4H) 3.44 (s, 3H) 3.55 (d, 2H, J = 5.6 Hz) 3.95 (s, 3H) 4.25−4.38 (m, 1H) 7.76 (s, 1H) 7.77 (s, 1H) 8.34 (d, 1H, J = 1.0 Hz) 8.73 (s, 1H).

*7-(3,5-Dimethylisoxazol-4-yl)-6-methoxy-4-(((tetrahydrofuran-3-yl)methyl)amino)quinoline-3-carboxamide (**45**).* To a suspension of 4-chloro-7-(3,5-dimethylisoxazol-4-yl)-6-methoxyquinoline-3-carboxamide **39** (1 g, 3.01 mmol) in dry *N*-methyl-2-pyrrolidinone (2.5 mL) was added DIPEA (1.32 mL, 7.54 mmol) and (tetrahydrofuran-3-yl)methanamine (0.381 g, 3.77 mmol). The reaction mixture was heated under nitrogen at 100 °C for 2 h and then stood at room temperature overnight. The solution was added directly onto, and purified by, SCX. The column was washed with 10% MeOH in DCM and eluted with 50% (2 M ammonia in MeOH) in DCM. The appropriate fractions were combined and evaporated under reduced pressure to give a brown gum. The gum was triturated in EtOAc (∼15 mL); the solid was removed by filtration and dried in a vacuum oven for 2 h to give the title compound (671 mg, 1.69 mmol, 56% yield) as a pale brown solid.

LCMS (formic acid): rt = 0.61 min, MH^+ = 397.

^{1}H NMR (DMSO-d_6): δ 1.55−1.65 (m, 1H), 1.96−2.05 (m, 1H), 2.13 (s, 3H), 2.32 (s, 3H), 2.55−2.64 (m, 1H), 3.47 (dd, J = 9.0, 6.0 Hz, 1 H) 3.56−3.66 (m, 3H) 3.71−3.80 (m, 2H), 3.92 (s, 3H), 7.42−7.51 (br s, 1H), 7.66 (s, 1H), 7.67 (s, 1H), 8.00−8.08 (br s, 1H), 8.45 (br t, 1H), 8.57 (s, 1H).

https://doi.org/10.1021/acs.jmedchem.1c00855
J. Med. Chem. 2021, 64, 12200−12227

*7-(3,5-Dimethylisoxazol-4-yl)-6-methoxy-4-(((tetrahydro-2H-pyran-3-yl)methyl)amino)quinoline-3-carboxamide (**46**).* To a suspension of 4-chloro-7-(3,5-dimethylisoxazol-4-yl)-6-methoxyquinoline-3-carboxamide **39** (1 g, 3.01 mmol) in dry *N*-methyl-2-pyrrolidinone (2.5 mL) was added DIPEA (1.32 mL, 7.54 mmol) and (tetrahydro-2*H*-pyran-3-yl)methanamine (0.434 g, 3.77 mmol). The reaction mixture was heated under nitrogen at 100 °C for 2 h and then stood at room temperature overnight. The solution was added directly onto, and purified by, SCX. The column was washed with 10% MeOH in DCM and eluted with 50% (2 M ammonia in MeOH) in DCM. The appropriate fractions were combined and evaporated under reduced pressure to give a brown gum. The gum was triturated in EtOAc (∼15 mL); the solid was removed by filtration and dried in a vacuum oven overnight to give the title compound (614 mg, 1.50 mmol, 50% yield) as a pale brown solid.

LCMS (formic acid): rt = 0.66 min, MH^+ = 411.

^{1}H NMR (DMSO-d_6, 400 MHz): δ 1.23−1.35 (m, 1H), 1.42−1.53 (m, 1H), 1.54−1.63 (m, 1H), 1.81−1.97 (m, 2H), 2.13 (s, 3H), 2.33 (s, 3H), 3.18 (dd, J = 11.1, 9.1 Hz, 1H), 3.49 (t, J = 6.2 Hz, 1H), 3.67−3.75 (m, 1H), 3.79−3.86 (m, 1H), 3.93 (s, 3H), 7.44−7.51 (br s, 1H), 7.67 (s, 2H), 8.02−8.09 (br s, 1H), 8.36 (br t, 1H), 8.55 (s, 1H).

*7-(3,5-Dimethylisoxazol-4-yl)-6-methoxy-4-(((tetrahydro-2H-pyran-4-yl)methyl)amino)quinoline-3-carboxamide (**47**).* To a suspension of 4-chloro-7-(3,5-dimethylisoxazol-4-yl)-6-methoxyquinoline-3-carboxamide **39** (2 g, 6.03 mmol) in *N*-methyl-2-pyrrolidinone (5 mL) was added DIPEA (2.63 mL, 15.07 mmol) and (tetrahydro-2*H*-pyran-4-yl)methanamine (0.868 g, 7.54 mmol), and the reaction mixture was heated at 120 °C for 2 h. The reaction mixture was loaded directly onto and purified by SCX washed with 20% MeOH in DCM and eluted using 2 M ammonia in MeOH. The appropriate fractions were combined and evaporated under reduced pressure. The resulting gum was triturated using EtOAc to give the title compound (1.76 g, 4.29 mmol, 71% yield) as a pale brown solid.

LCMS (formic acid): rt = 0.64 min, MH^+ = 411.

^{1}H NMR (DMSO-d_6, 400 MHz): δ 1.20−1.30 (m, 2H), 1.60−1.72 (m, 2H), 1.84−1.96 (m, 1H), 2.13 (s, 3H), 2.32 (s, 3H), 3.22−3.33 (m, 2H), 3.53 (d, J = 6.1 Hz, 2H), 3.86 (dd, J = 11.2, 3.2 Hz, 2H), 3.92 (s, 3H), 7.39−7.51 (m, 1H), 7.66−7.67 (m, 2H), 7.98−8.09 (br s, 1H), 8.58 (s, 1H), 8.61 (t, J = 5.3 Hz, 1H).

*7-(3,5-Dimethylisoxazol-4-yl)-6-methoxy-4-((1-(tetrahydro-2H-pyran-4-yl)ethyl)amino)quinoline-3-carboxamide (**48**).* 4-Chloro-7-(3,5-dimethylisoxazol-4-yl)-6-methoxyquinoline-3-carboxamide **39** (1 g, 3.01 mmol) was suspended in *N*-methyl-2-pyrrolidinone (5 mL), 1-(tetrahydro-2*H*-pyran-4-yl)ethanamine (0.487 g, 3.77 mmol) and DIPEA (1.32 mL, 7.54 mmol) added, and the reaction mixture was heated at 100 °C for 3.5 h. The sample was loaded directly, and purified by SCX, washed with 50% MeOH in DCM, and eluted using 2 M ammonia in MeOH. The appropriate fractions were combined and evaporated under reduced pressure to give a brown gum. The gum was loaded in MeOH/DCM (and the column dried in a vacuum oven) and purified by SPE (100 g, silica) using a gradient of 0−100% EtOAc in cyclohexane followed by 0−10% (2 M ammonia in MeOH) in DCM. The appropriate fractions were combined and evaporated under reduced pressure to give the title compound (173 mg, 0.41 mmol, 14% yield) as a brown gum.

LCMS (formic acid): rt = 0.68 min, MH^+ = 425, 77% pure by UV.

^{1}H NMR (DMSO-d_6, 400 MHz): δ 1.23−1.29 (m, 5H) 1.27 (d, J = 6.6 Hz, 3H) 1.52−1.62 (m, 1H) 1.62−1.74 (m, 2H) 2.14 (s, 3H) 2.34 (s, 3H) 3.22−3.30 (m, 3H) 3.82−3.90 (m, 2H) 3.93 (s, 3H) 7.54 (s, 1H) 7.70 (s, 1H) 8.38 (d, J = 9.9 Hz, 1H) 8.65 (s, 1H). Compound >70% pure.

*7-(3,5-Dimethyl-4-isoxazolyl)-6-(methyloxy)-4-(tetrahydro-2H-pyran-4-ylamino)-3-quinolinecarboxamide (**49**).* 4-Chloro-7-(3,5-dimethyl-4-isoxazolyl)-6-(methyloxy)-3-quinolinecarboxamide **39** (0.5 g, 1.51 mmol) and 4-aminotetrahydropyran hydrochloride (0.270 g, 1.96 mmol) were heated in a mixture of DIPEA (0.66 mL, 3.77 mmol) and *N*-methyl-2-pyrrolidone (3 mL) for 3 h at 120 °C. The brown solution was cooled and purified by SCX, washed with methanol (200 mL), then eluted with 2 M methanolic ammonia (100 mL), and the eluant was dried *in vacuo*. The residue was dissolved in DCM (10 mL) and loaded onto a 50 g silica column and then eluted with 0−50% 2 M methanolic ammonia/DCM to give the title compound (0.34 g, 0.86 mmol, 57% yield) as a beige crystalline solid.

LCMS (formic acid): rt = 0.59 min, MH^+ = 397.

^{1}H NMR ($CDCl_3$, 400 MHz) δ 1.78−1.88 (m, 2H), 2.07−2.15 (m, 2H), 2.18 (s, 3H), 2.23 (s, 3H), 3.48−3.54 (m, 2H), 3.92 (s, 3H), 4.02−4.07 (m, 2H), 4.11−4.18 (m, 1H), 6.0−6.5 (br s, 2H), 7.43 (s, 1H), 7.76 (s, 1H), 8.73 (s, 1H), 8.70−8.79 (m, 1H).

*tert-Butyl 4-((3-carbamoyl-7-(3,5-dimethylisoxazol-4-yl)-6-methoxyquinolin-4-yl)amino)piperidine-1-carboxylate (**50**).* 4-Chloro-7-(3,5-dimethyl-4-isoxazolyl)-6-(methyloxy)-3-quinolinecarboxamide **39** (0.5 g, 1.51 mmol) and 1,1-dimethylethyl 4-amino-1-piperidinecarboxylate (0.302 g, 1.51 mmol) were combined in NMP (3 mL) and DIPEA (0.7 mL), and the mixture was heated at 120 °C for 3 h, then cooled and added to water (30 mL). The mixture was extracted with EtOAc (30 mL), and the solvent was washed with water (2 × 30 mL), dried, and evaporated to give a brown gum. The gum was dissolved in DCM (5 mL) and loaded onto a 50 g silica column and then eluted with 0−50% 2 M methanolic ammonia/DCM. Product-containing fractions were evaporated *in vacuo* to give the title compound (0.52 g, 1.05 mmol, 70% yield).

LCMS (formic acid): rt = 0.82 min, MH^+ = 496,

1H NMR ($CDCl_3$, 400 MHz) δ 1.49 (s, 9H), 1.65−1.80 (m, 2H), 2.05−2.13 (m, 2H), 2.25 (s, 3H), 2.39 (s, 3H), 2.95−3.07 (m, 2H), 3.92 (s, 3H), 3.93−4.15 (m, 4H), 5.75−6.15 (br s, 2H), 7.44 (s, 1H), 7.78 (s, 1H), 8.71 (s, 1H), 8.74−8.80 (m, 1H).

*7-(3,5-Dimethyl-4-isoxazolyl)-6-(methyloxy)-4-{[(1-methyl-4-piperidinyl)methyl]amino}-3-quinolinecarboxamide (**51**).* 4-Chloro-7-(3,5-dimethyl-4-isoxazolyl)-6-(methyloxy)-3-quinolinecarboxamide **39** (0.37 g, 1.12 mmol) and (1-methylpiperidin-4-yl)methanamine (0.200 g, 1.56 mmol) were combined in NMP (3 mL) and DIPEA (0.7 mL), and the mixture was heated at 120 °C for 3 h and then cooled and dissolved in methanol (20 mL). The brown solution was loaded onto a 50 g SCX cartridge and washed with methanol (100 mL), then eluted with 2 M methanolic ammonia, and the eluant evaporated *in vacuo* to give the title compound (253 mg, 0.60 mmol, 54% yield) as a brown gum.

LCMS (formic acid): rt = 0.43 min, MH^+ = 424.

^{1}H NMR ($CDCl_3$, 400 MHz) δ 1.85−1.99 (m, 4H), 2.24 (s, 3H), 2.26 (s, 3H), 2.88−2.97 (m, 4H), 3.92 (s, 3H), 5.75−5.95 (br s, 2H), 7.58 (s, 1H), 7.74 (s, 1H), 8.65 (s, 1H), 9.31−9.37 (m, 1H). Sample contains unreacted amine starting material that obscures some of the signals.

*4-((2-(Dimethylamino)ethyl)amino)-7-(3,5-dimethylisoxazol-4-yl)-6-methoxyquinoline-3-carboxamide (**52**).* 4-Chloro-7-(3,5-dimethylisoxazol-4-yl)-6-methoxyquinoline-3-carboxamide **39** (500 mg, 1.51 mmol), N^1,N^1-dimethylethane-1,2-diamine (0.206 mL, 1.88 mmol) and DIPEA (0.66 mL, 3.77 mmol) were taken up in *N*-methyl-2-pyrrolidone (1.5 mL). The mixture was stirred at 120 °C for 3 h. The reaction mixture was loaded onto a 70 g SCX cartridge. The cartridge was eluted with methanol and then 2 M NH_3 in MeOH. The appropriate fractions were concentrated *in vacuo* and then loaded onto a 100 g silica cartridge in the minimum amount of DCM. The column was eluted with 1−10% NH_3 in MeOH. The appropriate fractions were combined and concentrated *in vacuo* to give the title compound (501 mg, 1.24 mmol, 82% yield) as a yellow solid.

LCMS (formic acid): rt = 0.41 min, MH^+ = 384.

^{1}H NMR ($CDCl_3$, 400 MHz) δ 2.24 (s, 3H), 2.36 (s, 6H), 2.39 (s, 3H), 2.65 (t, J = 5.9, 2H), 3.79 (q, J = 6.0 Hz, 2H), 3.94 (s. 3H), 5.80−6.50 (br s, 2H), 7.54 (s, 1H), 7.75 (s, 1H), 8.30−8.39 (br t, 1H), 8.71 (s, 1H).

*N-{7-(3,5-Dimethyl-4-isoxazolyl)-6-(methyloxy)-4-[(2-pyridinylmethyl)amino]-3-quinolinyl}acetamide (**54**).* Acetic anhydride (27 mg, 25 μL, 0.26 mmol) was added to a solution of 7-(3,5-dimethylisoxazol-4-yl)-6-methoxy-N^4-(pyridin-2-ylmethyl)quinoline-3,4-diamine **53** (100 mg, 0.26 mmol) in dichloromethane (5 mL) and pyridine (0.5 mL). The reaction mixture was stirred at room temperature for 2 h. The solvent was evaporated, and the residue was chromatographed using 5−10% methanol in dichloromethane to give

https://doi.org/10.1021/acs.jmedchem.1c00855
J. Med. Chem. 2021, 64, 12200−12227

the title compound (80 mg, 0.19 mmol, 72% yield) as a colorless solid after trituration with diethyl ether.

LCMS (formic acid): rt = 0.63 min, MH^+ = 418.

^{1}H NMR (DMSO-d_6, 400 MHz) δ 1.86 (s, 3H), 2.13 (s, 3H), 2.32 (s, 3H), 3.89 (s, 3H), 4.79 (d, J = 6.0 Hz, 2H), 7.01 (t, J = 6.0 Hz, 1H), 7.26−7.29 (m, 1H), 7.34 (d, J = 6.8 Hz, 1H), 7.67 (s, 1H), 7.72 (s, 1H), 7.73−7.77 (m, 1H), 8.16 (s, 1H), 8.54−8.57 (m, 1H), 9.59 (s, 1H).

*N-{7-(3,5-Dimethyl-4-isoxazolyl)-6-(methyloxy)-4-[(2-pyridinylmethyl)amino]-3-quinolinyl}propanamide (**55**).* Propionyl chloride (28 mg, 0.30 mmol) was added to a solution of 7-(3,5-dimethylisoxazol-4-yl)-6-methoxy-N^4-(pyridin-2-ylmethyl)quinoline-3,4-diamine **54** (100 mg, 0.26 mmol) in dichloromethane (5 mL) and pyridine (0.5 mL). The reaction mixture was stirred at room temperature for 2 h. The solvent was evaporated, and the residue was chromatographed using 5−10% methanol in dichloromethane] to give the title compound (68 mg, 0.16 mmol, 59% yield) as a colorless solid after trituration with diethyl ether.

LCMS (formic acid): rt = 0.63 min, MH^+ = 432.

^{1}H NMR (DMSO-d_6, 400 MHz): δ 0.97 (t, 3H, J = 12.0 Hz), 2.13 (s, 3H), 2.16 (q, 2H, J = 12.0 Hz), 2.33 (s, 3H), 3.91 (s, 3H), 4.36 (br s, 2H), 4.84−4.89 (m, 1H), 7.26−7.35 (m, 2H), 7.71 (s, 1H,), 7.73−7.79 (m, 1H), 7.81 (s, 1H), 8.25 (s, 1H), 8.52−8.55 (m, 1H), 9.58 (s, 1H).

*N-{7-(3,5-Dimethyl-4-isoxazolyl)-6-(methyloxy)-4-[(2-pyridinylmethyl)amino]-3-quinolinyl}butanamide (**56**).* *n*-Butanoyl chloride (20 mg, 0.19 mmol) was added to a stirred solution of 7-(3,5-dimethylisoxazol-4-yl)-6-methoxy-N^4-(pyridin-2-ylmethyl)-quinoline-3,4-diamine **53** (70 mg, 0.19 mmol) in dichloromethane (3 mL) and pyridine (0.3 mL). The reaction mixture was stirred at room temperature for 2 h. The solvent was evaporated, and the residue was twice re-evaporated from toluene. The residue was chromatographed using 2−5% methanol in dichloromethane, followed by trituration with diethyl ether, to give the title compound (52 mg, 0.12 mmol, 63% yield) as a pale yellow solid.

LCMS (formic acid): rt = 0.67 min, MH^+ = 446.

^{1}H NMR (DMSO-d_6, 400 MHz): δ 0.88 (t, 3H, J = 12.0 Hz), 1.47−1.55 (m, 2H), 2.10−2.15 (m, 5H), 2.33 (s, 3H), 3.90 (s, 3H), 4.80−4.87 (m, 2H), 7.20−7.30 (m, 2H), 7.69 (s, 1H), 7.73−7.80 (m, 3H), 8.23 (s, 1H), 8.53−8.57 (m, 1H), 9.58 (s, 1H).

*N-{7-(3,5-Dimethyl-4-isoxazolyl)-6-(methyloxy)-4-[(2-pyridinylmethyl)amino]-3-quinolinyl}-2-methylpropanamide (**57**).* Isobutyryl chloride (20 mg, 0.19 mmol) was added to a stirred solution of 7-(3,5-dimethylisoxazol-4-yl)-6-methoxy-N^4-(pyridin-2-ylmethyl)quinoline-3,4-diamine **53** (70 mg, 0.19 mmol) in dichloromethane (3 mL) and pyridine (0.3 mL). The reaction mixture was stirred at room temperature for 2 h. The solvent was evaporated, and the residue was twice re-evaporated from toluene. The residue was chromatographed using 2−5% methanol in dichloromethane and then triturated with diethyl ether to give the title compound (58 mg, 0.13 mmol, 70% yield) as a pale yellow solid.

LCMS (formic acid): rt = 0.68 min, MH^+ = 446.

^{1}H NMR (DMSO-d_6, 400 MHz): δ 1.04 (d, 6H, J = 12.0 Hz), 2.13 (s, 3H), 2.33 (s, 3H), 3.90 (s, 3H), 4.80−4.85 (m, 2H), 6.98−7.05 (m, 1H), 7.25−7.29 (m, 1H), 7.38 (d, 1H, J = 12.0 Hz), 7.68 (s, 1H), 7.70−7.78 (m, 2H), 8.19 (s, 1H), 8.52−8.56 (m, 1H), 9.51 (s, 1H). Methine proton of the isopropyl group was obscured by DMSO.

*N-{7-(3,5-Dimethyl-4-isoxazolyl)-6-(methyloxy)-4-[(2-pyridinylmethyl)amino]-3-quinolinyl}-2-(methyloxy)acetamide (**58**).* A mixture of 7-(3,5-dimethylisoxazol-4-yl)-6-methoxy-N^4-(pyridin-2-ylmethyl)quinoline-3,4-diamine **53** (100 mg, 0.27 mmol), DIPEA (42 mg, 57 μL, 0.33 mmol), 2-methoxyacetic acid (25 mg, 0.28 mmol), and HATU (122 mg, 0.32 mmol) in DMF (2 mL) was stirred at room temperature overnight. Saturated $NaHCO_3$ (5 mL) was added, and the mixture was extracted with ethyl acetate (3 × 5 mL). The combined extracts were washed with water and brine. The organic phase was dried and evaporated. The residue was chromatographed using 2−5% methanol in dichloromethane to give the title compound (73 mg, 0.16 mmol, 61% yield) as a light brown oil.

LCMS (formic acid): rt = 0.61 min, MH^+ = 448.

^{1}H NMR ($CDCl_3$, 400 MHz) δ 2.21 (s, 3H), 2.35 (s, 3H), 3.61 (s, 3H), 3.96 (s, 3H), 4.23 (s, 2H), 4.79 (d, J = 6.1 Hz, 2H), 5.38 (t, J = 6.1 Hz, 1H), 7.19−7.21 (m, 1H), 7.23−7.25 (m, 1H), 7.47 (s, 1H), 7.66−7.70 (m, 1H), 7.79 (s, 1H), 8.65−8.68 (m, 1H), 8.89 (s, 1H), 9.86 (s 1H).

*7-(3,5-Dimethylisoxazol-4-yl)-6-methoxyquinolin-4-ol (**61**).* To refluxing diphenyl ether (120 mL) was added 7-(3,5-dimethylisoxazol-4-yl)-4-hydroxy-6-methoxyquinoline-3-carboxylic acid **60** (6.1 g, 19.3 mmol) in small portions over 8 min. Vigorous bubbling was seen on addition. Safety note: because of the high temperature and volume of gas produced, extreme caution should be taken to add in small portions and to use a wide-necked vessel with capacity for the gas to escape. The reaction mixture was heated at reflux for 16 min and then allowed to cool to room temperature over 2 h. Diethyl ether (100 mL) was added, and the mixture stood at room temperature for 2 h. The solid was removed by filtration, washed on the filter with diethyl ether (2 × 50 mL), and dried in a vacuum oven overnight to give the title compound (4.6 g, 17.0 mmol, 88% yield) as a pale brown powder.

LCMS (formic acid): rt = 0.62 min, MH^+ = 271.

^{1}H NMR (DMSO-d_6, 400 MHz): δ 2.12 (s, 3H), 2.32 (s, 3H), 3.31 (s, 3H), 6.03 (d, J = 7.3 Hz, 1H), 7.43 (s, 1H), 7.62 (s, 1H), 7.86−7.91 (m, 1H), 11.66−11.76 (br s, 1H).

*7-(3,5-Dimethylisoxazol-4-yl)-6-methoxy-3-nitroquinolin-4-ol (**62**).* To a stirred solution of 7-(3,5-dimethylisoxazol-4-yl)-6-methoxyquinolin-4-ol **61** (8.7 g, 32.2 mmol) in propionic acid (88 mL) was added, dropwise, fuming nitric acid (3.16 mL, 70.8 mmol). Safety note: nitration reactions have potential for a runaway exotherm. Maintain close temperature monitoring and control via slow addition of the nitric acid. After addition was complete, the reaction mixture was stirred at 100 °C for 1 h. The reaction mixture was allowed to cool to room temperature. The solid was removed by filtration, washed on the filter with diethyl ether (100 mL), and dried in a vacuum oven to give the title compound (7.3 g, 23.2 mmol, 72% yield) as a mustard yellow solid.

LCMS (formic acid): rt = 0.70 min, MH^+ = 316.

^{1}H NMR (DMSO-d_6, 400 MHz) δ 2.13 (s, 3H), 2.33 (s, 3H), 3.92 (s, 3H), 7.61 (s, 1H), 7.78 (s, 1H), 9.17 (br s, 1H), 12.8−13.01 (br s, 1H).

^{13}C NMR (DMSO-d_6, 303 K): δ 10.3, 11.4, 55.9, 105.6, 111.7, 122.3, 125.2, 129.2, 130.4, 132.4, 141.3, 155.1, 158.8, 166.6, 166.8.

IR: 1613 (aryl), 1536 (aryl), 1536 (NO_2), 1361 (NO_2), 1221 (aryl ether), 786 (aryl C−H) cm^{-1}.

M.p.: 257−267 (decomposition).

HRMS: ($C_{15}H_{15}N_3O_5$) MH^+ requires 316.0933, found MH^+ 316.0937.

*4-(4-Chloro-6-methoxy-3-nitroquinolin-7-yl)-3,5-dimethylisoxazole (**63**).* A solution of 7-(3,5-dimethylisoxazol-4-yl)-6-methoxy-3-nitroquinolin-4-ol **62** (3.5 g, 11.1 mmol) in phosphorus oxychloride (35 mL, 375 mmol) was heated at 120 °C for 2 h. The reaction mixture was allowed to cool to room temperature and evaporated under reduced pressure. Twice, toluene (50 mL) was added, and the mixture was evaporated under reduced pressure. Safety note: Ensure very cautious quenching of the evaporated excess phosphorus oxychloride. The residual brown liquid was dissolved in DCM (250 mL), and the organic layer was washed with saturated aqueous sodium bicarbonate solution (3 × 150 mL), until the aqueous layer removed was neutral. The organic layer was dried using a hydrophobic frit and evaporated under reduced pressure. The sample was loaded in DCM and purified by SPE (silica, 100 g) using 0−50% EtOAc in cyclohexane. The appropriate fractions were combined and evaporated under reduced pressure to give the title compound (2.76 g, 8.27 mmol, 75% yield) as a yellow solid.

LCMS (formic acid): rt = 1.13 min, MH^+ = 334.

^{1}H NMR (DMSO-d_6, 400 MHz): δ 2.16 (s, 3H), 2.36 (s, 3H), 4.05 (s, 3H), 7.74 (s, 1H), 8.15 (s, 1H), 9.27 (s, 1H).

^{13}C NMR (DMSO-d_6, 303 K): δ 10.3, 11.4, 55.9, 105.6, 111.7, 122.3, 125.2, 129.2, 130.4, 132.4, 141.3, 155.1, 158.8, 166.6, 166.8.

IR (neat): 1612 (aryl), 1589 (aryl), 1535 (NO_2), 1361 (NO_2), 1223 (aryl ether), 784 (aryl C−H) cm^{-1}.

https://doi.org/10.1021/acs.jmedchem.1c00855
J. Med. Chem. 2021, 64, 12200−12227

M.p.: 279−>300 °C (decomposition).

HRMS: ($C_{15}H_{14}N_3O_5$ - consistent with hydroxyl replacement of chloro) MH^+ requires 316.0928, found MH^+: 316.0926.

*7-(3,5-Dimethylisoxazol-4-yl)-6-methoxy-N-(1-methoxypropan-2-yl)-3-nitroquinolin-4-amine (**64**).* To a solution of 4-(4-chloro-6-methoxy-3-nitroquinolin-7-yl)-3,5-dimethylisoxazole **63** (20 g, 59.9 mmol) in 1,4-dioxane (200 mL) was added 1-methoxypropan-2-amine (32 mL, 300 mmol) and the reaction mixture heated at 70 °C for 1.5 h. The solvent was removed under reduced pressure and the resulting solid partitioned between EtOAc (3 × 750 mL) and water (750 mL). The organic layers were combined, dried using a hydrophobic frit and evaporated under reduced pressure to give the title compound (25.8 g, 98% yield).

LCMS (formic acid): rt = 0.97 min, MH^+ = 387.

^{1}H NMR (DMSO-d_6, 400 MHz): δ 1.41 (d, J = 6.6 Hz, 3H), 2.15 (s, 3H), 2.34 (s, 3H), 3.29 (s, 3H), 3.55−3.58 (m, 2H), 3.97 (s, 3H), 4.34−4.44 (m, 1H), 7.79 (s, 1H), 7.83 (s, 1H), 8.63 (d, J = 9.1 Hz, 1H), 9.04 (s, 1H).

*7-(3,5-Dimethylisoxazol-4-yl)-6-methoxy-3-nitro-N-((tetrahydro-2H-pyran-4-yl)methyl)quinoline-4-amine (**65**).* To a suspension of 4-(4-chloro-6-methoxy-3-nitroquinolin-7-yl)-3,5-dimethylisoxazole **63** (2 g, 5.99 mmol) in *N*-methyl-2-pyrrolidone (5 mL) was added DIPEA (1.05 mL, 5.99 mmol) and (tetrahydro-2*H*-pyran-4-yl)-methanamine (1.04 g, 8.99 mmol) and the reaction mixture heated at 100 °C overnight. The resulting solid was triturated in EtOAc to give the title compound (2.1 g, 5.09 mmol, 85% yield) as a yellow solid.

LCMS (formic acid): rt = 0.87 min, MH^+ = 413.

^{1}H NMR (DMSO-d_6, 400 MHz): δ 1.18−1.29 (m, 2H), 1.56−1.65 (m, 2H), 1.91−2.04 (m, 1H), 2.14 (s, 3H), 2.33 (s, 3H), 3.23−3.28 (m, 2H), 3.29 (s, 3H), 3.47 (t, J = 6.0 Hz, 2H), 3.85 (dd, J = 11.2, 3.2 Hz, 2H), 3.97 (s, 3H), 7.79 (s, 1H) 7.92 (s, 1H) 8.67−8.72 (m, 1H) 8.93 (s, 1H).

*7-(3,5-Dimethylisoxazol-4-yl)-6-methoxy-3-nitro-N-(1-(tetrahydro-2H-pyran-4-yl)ethyl)quinoline-4-amine (**66**).* 4-(4-Chloro-6-methoxy-3-nitroquinolin-7-yl)-3,5-dimethylisoxazole **63** (520 mg, 1.56 mmol) was dissolved in *N*-methyl-2-pyrrolidinone (5 mL), DIPEA (0.27 mL, 1.56 mmol) and 1-(tetrahydro-2*H*-pyran-4-yl)ethanamine (302 mg, 2.34 mmol) added, and the reaction mixture heated at 100 °C for 3.5 h. The sample was loaded directly, and purified by, SPE (SCX, 50 g). The column was washed with 50% MeOH in DCM and eluted using 2 M ammonia in MeOH. The appropriate fractions were combined and evaporated under reduced pressure to give a brown gum. The gum was loaded in MeOH/DCM (and the column dried in a vacuum oven) and purified by SPE (silica, 25 g) using 0−20% (2 M ammonia in MeOH) in DCM. The appropriate fractions were combined and dried under a stream of nitrogen to give the title compound (124 mg, 0.29 mmol, 19% yield) as a brown gum.

LCMS (formic acid): rt = 0.97 min, MH^+ = 427.

^{1}H NMR (DMSO-d_6, 400 MHz): δ 1.46 (d, J = 6.3 Hz, 3H) 1.53−1.61 (m, 2H) 2.16 (s, 3H) 2.16−2.22 (m, 3H) 2.35 (s, 3H) 3.19−3.29 (m, 1H) 3.81−3.90 (m, 4H) 3.99 (s, 3H) 7.75 (s, 1H) 7.81 (s, 1H) 8.45−8.53 (m, 1H) 8.99 (s, 1H) Compound 60% pure.

*N-(Cyclopropylmethyl)-7-(3,5-dimethylisoxazol-4-yl)-6-methoxy-3-nitroquinolin-4-amine (**67**).* 4-(4-Chloro-6-methoxy-3-nitroquinolin-7-yl)-3,5-dimethylisoxazole **63** (1 g, 3.00 mmol) was dissolved in *N*-methyl-2-pyrrolidinone (4 mL), DIPEA (0.523 mL, 3.00 mmol) and cyclopropylmethanamine (0.378 mL, 4.49 mmol) added, and the reaction mixture heated at 100 °C for 3.5 h. The sample was loaded directly, and purified by, SPE (SCX, 20 g), washed with 50% MeOH in DCM and eluted using (2 M ammonia in MeOH). The appropriate fractions were combined and evaporated under reduced pressure to give a brownish yellow solid. The solid was triturated in EtOAc, filtered, and dried in a vacuum oven to leave the title compound (259 mg, 0.70 mmol, 23% yield) as a yellow solid.

LCMS (formic acid): rt = 0.97 min, MH^+ = 369.

^{1}H NMR (DMS-d_6 400 MHz): δ 0.33−0.39 (m, 2H), 0.53−0.61 (m, 2H), 1.14−1.26 (m, 1H), 2.14 (s, 3H), 2.33 (s, 3H), 3.58 (dd, J = 6.2, 4.9 Hz, 2H), 3.97 (s, 3H), 7.78 (s, 1H), 7.88 (s, 1H), 8.97 (s, 1H), 9.00−9.04 (m, 1H).

*7-(3,5-Dimethylisoxazol-4-yl)-6-methoxy-3-nitro-N-(pyridine-2-ylmethyl)quinoline-4-amine (**68**).* To a suspension of 4-(4-chloro-6-methoxy-3-nitroquinolin-7-yl)-3,5-dimethylisoxazole **63** (3 g, 8.99 mmol) in 1,4-dioxane (20 mL) was added pyridine-2-ylmethanamine (1.40 mL, 13.5 mmol), and the reaction mixture stirred at room temperature for 5 h. Further pyridine-2-ylmethanamine (0.7 mL, 6.74 mmol) was added and the reaction mixture stirred at room temperature overnight. The solvent was removed under reduced pressure and the residue loaded in MeOH/DCM (and the column dried in a vacuum oven) and purified by SPE (silica, 2 × 100 g) using a gradient of 50−100% EtOAc in cyclohexane. The appropriate fractions were combined and evaporated under reduced pressure to give the title compound (2.67 g, 6.59 mmol, 73% yield) as a yellow solid.

LCMS (formic acid): rt = 0.87 min, MH^+ = 406.

^{1}H NMR (DMSO-d_6, 393 K, 400 MHz): δ 2.14 (s, 3H), 2.34 (s, 3H), 3.90 (s, 3H), 5.17 (d, J = 4.8 Hz, 2H), 7.29−7.39 (m, 1H), 7.51 (d, J = 7.8 Hz, 1H), 7.77 (s, 1H), 7.80−7.84 (m, 1H), 7.96 (s, 1H), 8.60 (d, J = 4.5 Hz, 1H), 9.02 (s, 1H), 9.47−9.66 (br s, 1H).

*7-(3,5-Dimethylisoxazol-4-yl)-6-methoxy-3-nitro-N-((R)-1-(pyridine-2-yl)ethyl)quinoline-4-amine (**69**).* To a suspension of 4-(4-chloro-6-methoxy-3-nitroquinolin-7-yl)-3,5-dimethylisoxazole **63** (1 g, 3.00 mmol) in 1,4-dioxane (6.5 mL) was added (*R*)-1-(pyridine-2-yl)ethanamine (0.55 g, 4.5 mmol), and the reaction mixture stirred at room temperature for 5 h. Further (*R*)-1-(pyridine-2-yl)-ethanamine (0.26 g, 2.3 mmol) was added and the reaction mixture stirred at room temperature overnight. The solvent was removed under reduced pressure and the residue loaded in MeOH/DCM (and the column dried in a vacuum oven) and purified by SPE (silica, 2 × 100 g) using a gradient of 50−100% EtOAc in cyclohexane. The appropriate fractions were combined and evaporated under reduced pressure to give the title compound (1.15 g, 2.74 mmol, 92% yield) as an orange solid.

LCMS (formic acid): rt = 0.98 min, MH^+ = 420.

^{1}H NMR (DMSO-d_6, 393 K, 400 MHz): δ 1.74 (d, J = 6.6 Hz, 3H), 2.13 (s, 3H), 2.32 (s, 3H), 3.86 (s, 3H), 5.51−5.58 (m, 1H), 7.29−7.33 (m, 1H), 7.56 (d, J = 7.8 Hz, 1H), 7.77 (s, 1H), 7.78 (s, 1H), 7.79−7.82 (m, 1H), 8.58 (d, J = 4.8 Hz, 1H), 9.05 (s, 1H), 9.24 (d, J = 7.6 Hz, 1H).

*7-(3,5-Dimethylisoxazol-4-yl)-6-methoxy-N4-(1-methoxypropan-2-yl)quinoline-3,4-diamine (**70**).* 7-(3,5-Dimethylisoxazol-4-yl)-6-methoxy-*N*-(1-methoxypropan-2-yl)-3-nitroquinolin-4-amine **64** (25.8 g, 66.8 mmol) was dissolved in a mixture of EtOAc (1000 mL) and dimethyl sulfoxide (50 mL) and the solution was hydrogenated using an H-cube (settings: 20 °C, 1 bar, 1 mL/min flow rate) using 10% Pd/C CatCart 70 cartridges containing the catalyst. The catalyst cartridge was changed whenever it became blocked. The reaction mixture was evaporated under reduced pressure and partitioned between EtOAc (750 mL) and water (3 × 750 mL). The aqueous layers were combined and extracted with EtOAc (750 mL). Both organic layers were combined, dried using a hydrophobic frit, and evaporated under reduced pressure. The residue was loaded in DCM and purified by SPE (silica, 8 × 100 g) using a gradient of 0−4% (2 M ammonia in MeOH) in DCM. The appropriate fractions were combined and evaporated under reduced pressure to give batches of product (13.6 g) and recovered starting material (6.5 g). The recovered starting material was dissolved in EtOAc (250 mL) and the reaction was hydrogenated using an H-cube (settings: 20 °C, 1 bar, 1 mL/min flow rate) using a 10% Pd/C CatCart 70 as the catalyst. The reaction mixture was evaporated under reduced pressure and the residue was loaded in DCM and purified by SPE (silica, 2 × 100 g) using a gradient of 0−4% (2 M ammonia in MeOH) in DCM. The appropriate fractions were combined and evaporated under reduced pressure to give a second batch of product. Both batches of product were combined to give the title compound (15.6 g, 43.8 mmol, 66% yield) as a sticky dark brown gum.

LCMS (formic acid): rt = 0.73 min, MH^+ = 357.

^{1}H NMR (DMSO-d_6, 393 K): δ 1.20 (d, J = 6.6 Hz, 2 H), 2.11 (s, 3 H), 2.30 (s, 3 H), 3.32 (s, 3 H), 3.35−3.43 (m, 2 H) 3.52−3.65 (m, 1

https://doi.org/10.1021/acs.jmedchem.1c00855
J. Med. Chem. 2021, 64, 12200−12227

H), 3.89 (s, 3 H), 4.31 (d, J = 10.1 Hz, 1 H), 4.96 (s, 1 H), 7.45 (s, 1 H), 7.55 (s, 1 H), 8.32 (s, 1 H).

*7-(3,5-Dimethylisoxazol-4-yl)-6-methoxy-N⁴-((tetrahydro-2H-pyran-4-yl)methyl)quinoline-3,4-diamine (**71**).* To a suspension of 7-(3,5-dimethylisoxazol-4-yl)-6-methoxy-3-nitro-*N*-((tetrahydro-2*H*-pyran-4-yl)methyl)quinoline-4-amine **65** (1.1 g, 2.67 mmol) in EtOH (20 mL) was added tin(II) chloride (1.77 g, 9.33 mmol) and the reaction mixture stirred at 40 °C for 1.5 h. The reaction mixture was basified to pH 12 using 2 M aqueous sodium hydroxide solution. Water (50 mL) was added and the aqueous suspension extracted with DCM (3 × 50 mL). The organic layers were combined, dried using a hydrophobic frit and blown down under a stream of nitrogen. The sample was loaded in DCM and purified by SPE (silica, 100 g) using a gradient of 0−10% (2 M ammonia in MeOH) in DCM. The appropriate fractions were combined and blown down under a stream of nitrogen to give the title compound (984 mg, 2.57 mmol, 96% yield) as a brown gum.

LCMS (formic acid): rt = 0.69 min, MH^+ = 383.

^{1}H NMR (DMSO-d_6, 400 MHz): δ 1.20−1.31 (m, 2H), 1.72−1.80 (m, 3H), 2.10 (s, 3H), 2.29 (s, 3H), 3.05 (t, J = 6.6 Hz, 2H), 3.22−3.28 (m, 2H), 3.82−3.93 (m, 5H), 4.74 (t, J = 7.1 Hz, 1H), 5.07 (br s, 2H), 7.39 (s, 1H), 7.55 (s, 1H), 8.27 (s, 1H).

*7-(3,5-Dimethylisoxazol-4-yl)-6-methoxy-N⁴-(1-(tetrahydro-2H-pyran-4-yl)ethyl)quinoline-3,4-diamine (**72**).* 7-(3,5-Dimethylisoxazol-4-yl)-6-methoxy-3-nitro-*N*-(1-(tetrahydro-2*H*-pyran-4-yl)ethyl)-quinoline-4-amine **66** (120 mg, 0.28 mmol) was dissolved in EtOAc (4.5 mL) and EtOH (1.5 mL) and the reaction mixture was hydrogenated using an H-cube (20 °C, 1 bar, 1 mL/min flow rate) with a 10% Pd/C CatCart 30. After the first pass through the H-cube the reaction mixture was recirculated for 60 min. The reaction mixture was blown down under a stream of nitrogen to give the title compound (104 mg, 0.26 mmol, 93% yield) as a brown gum.

LCMS (formic acid): rt = 0.74 min, MH^+ = 397, 69% pure.

*7-(3,5-Dimethylisoxazol-4-yl)-6-methoxy-N⁴-(pyridine-2-ylmethyl)quinoline-3,4-diamine (**73**).* To a suspension of 7-(3,5-dimethylisoxazol-4-yl)-6-methoxy-3-nitro-*N*-(pyridine-2-ylmethyl)-quinoline-4-amine **68** (2.7 g, 6.6 mmol) in EtOH (50 mL) was added tin(II) chloride (4.4 g, 23.0 mmol) and the reaction mixture stirred at 40 °C for 2.5 h. The reaction mixture was basified to pH 12 using 2 M aqueous sodium hydroxide solution. Water (100 mL) was added and the aqueous suspension extracted with DCM (3 × 100 mL). The organic layers were combined, dried using a hydrophobic frit and blown down a stream of nitrogen. The sample was loaded in DCM and purified by SPE (silica, 100 g) using a gradient of 0−10% (2 M ammonia in MeOH) in DCM. The appropriate fractions were combined and blown down a stream of nitrogen to give the title compound (879 mg, 2.34 mmol, 36% yield) as a dark brown gum.

LCMS (formic acid): rt = 0.63 min, MH^+ = 376.

^{1}H NMR (DMSO-d_6, 393 K, 400 MHz): δ 2.10 (s, 3H), 2.29 (s, 3H), 3.82 (s, 3H), 4.52 (d, J = 3.8 Hz, 2H), 4.82−5.01 (br s, 2H) 5.12−5.25 (br s, 1H), 7.24−7.27 (m, 1H), 7.47 (s, 1H), 7.49 (d, J = 7.8 Hz, 1H), 7.55 (s, 1H), 7.72−7.76 (m, 1H), 8.33 (s, 1H), 8.57 (d, J = 4.3 Hz, 1H).

*7-(3,5-Dimethylisoxazol-4-yl)-6-methoxy-N⁴-((R)-1-(pyridine-2-yl)ethyl)quinoline-3,4-diamine (**74**).* To a suspension of 7-(3,5-dimethylisoxazol-4-yl)-6-methoxy-3-nitro-*N*-((*R*)-1-(pyridine-2-yl)-ethyl)quinoline-4-amine **69** (1.1 g, 2.50 mmol) in EtOH (20 mL) was added tin(II) chloride (1.66 g, 8.76 mmol) and the reaction mixture stirred at 40 °C for 2.5 h. The reaction mixture was basified to pH 12 using 2 M aqueous sodium hydroxide solution. Water (100 mL) was added and the aqueous suspension extracted with DCM (3 × 100 mL). The organic layers were combined, dried using a hydrophobic frit and blown down a stream of nitrogen. The sample was loaded in DCM and purified by SPE (silica, 100 g) using a gradient of 0−10% (2 M ammonia in MeOH) in DCM. The appropriate fractions were combined and blown down a stream of nitrogen to give the title compound (543 mg, 1.39 mmol, 56% yield) as a dark brown gum.

LCMS (formic acid): rt = 0.70 min, MH^+ = 390.

^{1}H NMR (DMSO-d_6, 393 K, 400 MHz): δ 1.58 (d, J = 6.8 Hz, 3H), 2.09 (s, 3H), 2.28 (s, 3H), 3.83 (s, 3H), 4.66−4.80 (m, 1H), 4.80−4.97 (m, 2H), 7.18−7.27 (m, 1H), 7.38 (s, 1H), 7.45 (d, J = 7.8 Hz, 1H), 7.53 (s, 1H), 7.67−7.73 (m, 1H), 8.33 (s, 1H), 8.56 (d, J = 4.8 Hz, 1H).

*4-(8-Methoxy-1-((R)-1-methoxypropan-2-yl)-2-(tetrahydro-2H-pyran-4-yl)-1H-imidazo[4,5-c]quinolin-7-yl)-3,5-dimethylisoxazole, methanesulfonic acid salt (**75**).* 4-(8-Methoxy-1-((*R*)-1-methoxypropan-2-yl)-2-(tetrahydro-2*H*-pyran-4-yl)-1*H*-imidazo[4,5-*c*]-quinolin-7-yl)-3,5-dimethylisoxazole **32** (1.02 g, 2.26 mmol) was dissolved in the minimum amount of hot MeOH, and methanesulfonic acid, 70% weight in water, (0.21 mL, 2.26 mmol) added. The solution was blown down under a stream of nitrogen to leave a white gum. The gum was triturated in diethyl ether and then dried in a vacuum oven to give the title compound (1.18 g, 2.16 mmol, 96% yield).

LCMS (formic acid): rt = 0.73 min, MH^+ = 451.

^{1}H NMR (DMSO-d_6, 393 K, 400 MHz): δ 1.83 (d, J = 7.3 Hz, 3H), 1.86−2.01 (m, 2H), 2.03−2.13 (m, 2H), 2.16 (s, 3H), 2.35 (s, 3H), 2.40 (s, 3H), 3.26 (s, 3H), 3.50−3.65 (m, 3H), 3.98−4.08 (m, 6H), 4.11−4.16 (m, 1H), 5.48−5.63 (m, 1H), 7.87 (s, 1H), 8.12 (s, 1H), 9.36 (s, 1H).

IR (neat): 2849 (ether $COCH_3$), 1610 (aryl), 1389 (OSO_2), 1223 (aryl ether), 1163 (OSO_2) 841 (aryl C−H) cm^{-1}.

M.p.: 256−259 °C.

HRMS: ($C_{25}H_{31}N_4O_4$) MH^+ requires 451.2340, found MH^+ 451.2338.

$[\alpha_D]^{23.1\ °C}$ (c 1.0, MeOH): +22.4°.

BRD4 Protein Expression and Purification. Recombinant human bromodomains BRD4 (1−477) (Y390A) (BD2 mutation to monitor binding to BD1) were expressed in *Escherichia coli* cells using a pET15b vector with a 6-His tag at the *N*-terminal. The His-tagged bromodomain pellet was resuspended in 50 mM 4-(2-hydroxyethyl)-piperazine-1-ethanesulfonic acid (HEPES) (pH 7.5), 300 mM NaCl, 10 mM imidazole, and 1 μL/mL protease inhibitor cocktail and extracted from the *E. coli* cells using sonication. Purification was carried out using a nickel sepharose high-performance column, and the proteins were washed and then eluted with a linear gradient of 0−500 mM imidazole with buffer 50 mM HEPES (pH 7.5), 150 mM NaCl, and 500 mM imidazole, over 20 column volumes. Final purification was completed by using a Superdex 200 prep grade size exclusion column. Purified protein was stored at −80 °C in 20 mM HEPES (pH 7.5) and 100 mM NaCl. The protein identity was confirmed by peptide mass fingerprinting, and the predicted molecular weight was confirmed by mass spectrometry.

BRD4 TR-FRET Assay. All assay components were diluted in a buffer composition of 50 mM HEPES (pH 7.4), 150 mM NaCl, 5% glycerol, 1 mM DTT, and 1 mM 3-[(3-cholamidopropyl)-dimethylammonio]-1-propanesulfonate. The final concentration of bromodomain protein was 10 nM. An Alexa Fluor 647 derivative of I-BET762 (**1**) was used as the competing ligand and was used at a concentration equal to the K_d. These components were premixed, and 5 μL of this reaction mixture was added to wells containing 50 nL of various concentrations of the test compound or DMSO vehicle (0.5% DMSO final) in 384-well black low volume microtiter plates and incubated in the dark for 30 min at rt. The bromodomain protein/fluorescent ligand interaction was detected using TR-FRET following 5 μL addition of a 1.5 nM europium chelate-labeled anti-6His antibody in assay buffer. Time-resolved fluorescence (TRF) was then detected on a TRF laser equipped with a PerkinElmer EnVision multimode plate reader (excitation = 337 nm; emission 1 = 615 nm; emission 2 = 665 nm; dual wavelength bias dichroic = 400, 630 nm). The TR-FRET ratio was calculated using the following equation: ratio = ((acceptor fluorescence at 665 nm)/(donor fluorescence at 615 nm)) × 1000. TR-FRET ratio data were normalized to a mean of 16 replicates per microtiter plate of both 10 μM I-BET151 (**5**) and 1% DMSO controls, and IC_{50} values were determined for each of the compounds tested by fitting the fluorescence ratio data to a four parameter model: $y = a + ((b - a)/(1 + (10^x/10^c)^d))$ where "a" is the minimum, "b" is the Hill slope, "c" is the IC_{50}, and "d" is the maximum.

https://doi.org/10.1021/acs.jmedchem.1c00855
J. Med. Chem. 2021, 64, 12200−12227

LPS-Stimulated PBMC Assay. For cell preparation, the plating medium (500 mL of DMEM, 50 mL of heat-inactivated Australian fetal bovine serum, 5 mL penicillin/streptomycin, 5 mL Glutamax) was prewarmed in a 37 °C water bath for at least 20 min prior to thawing frozen peripheral blood mononuclear cells (PBMCs). The compound plates were prepared before commencing cell preparation—two replicates of each master plate are required to account for PBMC donor variability. Sufficient vials of PBMCs from two different donors were selected from the −140 °C freezer and placed in the water bath until the cells were just defrosted. In the primary cell biosafety cabinet, the PBMCs were transferred to 50 mL centrifuge tubes, with each donor being processed separately. Warm medium was added dropwise to each tube of cells, and they were then centrifuged at 1600 rpm for 5 min at ambient temperature. The supernatant was discarded, and the PBMCs were resuspended in a suitable volume of warm media. A total of 300 μL of cell suspension was removed for counting on the Cedex cell counter (Innovatis). The viable cell count and percentage viability for each donor were entered into a spreadsheet which calculated the correct volumes of cell suspension, warm media, and lipopolysaccharide required to make up sufficient plating suspension for the compound plates. A total of 50 μL of cell suspension was added to each well of the compound plates using a Multidrop Combi (Thermo). The seeded plates were then lidded and placed in the humidified primary cell incubator for 18−24 h at 37 °C, 5% CO_2.

The activity of compounds in the IL-6 assay were determined by using Mesoscale Discovery (MSD) technology to measure electrochemiluminescence. Ten microliters of cell supernatant was transferred to a low-profile 384-well MSD plate, precoated with human IL-6 capture antibody using the Biomek FX. The plates were then sealed and placed on a shaker at 600 rpm at room temperature for 2 h. A 1% solution of MSD blocker A was prepared by dissolving solid blocker A in PBS, and this was then used to dilute the antihuman IL-6 antibody labeled with MSD SULFO-TAG reagent to a working solution of 1 μg/mL (a 1 in 50 dilution). Ten microliters of the working antibody solution was then added to each well of the MSD plates using a Multidrop Combi. The plates were then resealed and returned to the shaker for another 2 h at 600 rpm at room temperature. The plates were then washed three times with PBS, ensuring there was no liquid remaining in the plate after washing. A total of 35 μL of 2× MSD Read Buffer T (stock 4× MSD Read Buffer T was diluted 50:50 with deionized water) was then added to each well using a Multidrop Combi, and the plates were then read on the MSD Sector Imager 6000. The resulting data were used for data analysis.

LPS-Stimulated HWB Assay. Compounds diluted to 4.2 mM in 100% DMSO were serially diluted (1:3) in DMSO and 1 μL stamped into 96-well flat-bottomed tissue culture plates. A total of 130 μL of human whole blood (containing 10 IU/mL sodium heparin) was added to the compound wells, the plates were incubated (37 °C, 5% CO_2) for 30 min, and 10 μL of 2.8 μg/mL LPS (diluted in 1% BSA) was added. The plates were incubated (37 °C, 5% CO_2) for 24 h. A total of 140 μL of PBS was added, and the plate was shaken for 1 min. The plates were centrifuged at either 2000 or 2500 rpm for 10 min, and 100 μL of supernatant was removed. Twenty-five microliters of supernatant (diluted 1 in 40 in MSD diluent) was added to IL-6 MSD assay plates (MSD MA6000 96-well plate), and the plates were shaken for 2 h. Twenty-five microliters of Sulfo-tag anti-IL-6 antibody (1 mg/mL dilution in MSD antibody diluent) was added, and the plates were shaken for 2 h. A total of 150 μL of MSD read buffer T (diluted 1:1 in distilled water) was added, and the plates were read on an MSD 6000 plate reader.

FaSSIF Solubility. FaSSIF GI medium (pH 6.5) was added to a sample of compound in order to produce a known concentration of suspension. The samples were left on a roller mixer for 30 min or 4 hm at which point a 200 μL aliquot was removed. The samples were filtered and centrifuged (Durapore PVDF 0.45 μm filters, 10 000 rpm), and then 100 μL of the supernatant was diluted in 1:1 MeCN/H_2O. Samples were analyzed by gradient HPLC

Three-Month Accelerated Storage. One milligram and 100 mg of I-BET282E were stored under the following conditions for three months: 40 °C, 75% relative humidity, open; 50 °C, ambient humidity, closed; 30 °C, 65% relative humidity, closed. PXRD diffractograms of the closed samples were concordant with the input material. Additional peaks were visible in the PXRD diffractograms of the open samples showing that some degradation of the material was observed.

Cocrystallization and Structure Determination. One microliter of 200 mM of I-BET282 **32** was dissolved in DMSO and added to 100 μL of BRD4 (44-168). This solution was incubated for 3 h on ice before crystallization was performed using four diverse screens (PACT, PEGI, PEGII, INDEX). 150 nL + 150 nL drops of the protein complex and well solution were used for crystallization on Innoadyne SD2 96-well plates. The crystallization plates were stored at 20 °C. Data were collected from a single crystal grown in 200 mM $CaCl_2$ 25% PEG4K, 100 mM trisHCl pH8.5 on a house RIGAKU FRE+ SUPERBRIGHT/A200 system. The crystal had been briefly transferred into well solution with the addition of 20% ethylene glycol as a cryoprotectant prior to flash freezing in liquid nitrogen. The diffraction images were processed and scaled using D*Trek to give a 1.7 Å data set. The $P2_12_12_1$ orthorhombic cell ($\alpha = \beta = \gamma = 90°$, a = 42.55 Å, b = 46.29 Å, c = 61.41 Å) has one molecule in the ASU. After rigid body refinement using a previously determined in-house structure, model building was performed using Coot[48] and refined using refmac.[49] There was clear difference density for the ligand at the acetyl lysine binding site, allowing I-BET282 **32** to be unambiguously placed. The statistics for the data collection and refined coordinates are given in Table S1. The final refined model (Rfac/Rfree = 18.1%/21.5%) showed excellent density for the ligand and an unambiguous binding mode for this molecule. The chirality of this compound was also unambiguously determined.

***In Vitro* DMPK Studies.** The human biological samples were sourced ethically, and their research use was in accordance with the terms of the informed consents under an IRB/EC approved protocol.

Metabolic Stability in Hepatocytes. Cryopreserved hepatocytes from mouse, rat, dog, and human were obtained from Invitrogen UK and stored in liquid nitrogen prior to use. A 5 mM stock solution of I-BET282 32 was prepared and diluted to 100 μM with DMSO. An aliquot was taken and further diluted to 1 μM with Williams Medium E (WME) and prewarmed at 37 °C. The cryopreserved hepatocytes for each species were thawed in the manner recommended by the supplier. Cell concentration and viability were ascertained using the Trypan blue exclusion method. The cell suspension was then diluted to 1.4 million cells per mL with prewarmed (37 °C) WME. A total of 300 μL of cell suspension was added to each well of a 12-well plate to which 300 μL of 1 μm I-BET282 32 was also added to give a final incubation concentration of 0.5 μM I-BET282 32 and 0.7 million cells/mL. The incubations were maintained at 37 °C for the duration of the experiment. At set intervals (0, 10, 20, 30, 45, 60, 75, 90, 105, and 120 min), 25 μL of cell suspension was transferred to a 96-well block containing 100 μL of stopping solution containing an internal standard. No compound controls, replacing I-BET282 32 with 300 μL of WME, were performed, with samples being taken at 120 min only. No hepatocyte controls, replacing 300 μL of cell suspension with 300 μL of WME, were also performed, with samples being taken at 0 and 120 min only. Incubations were repeated with 0.05 μM I-BET282 32 using mouse, rat, dog, and human hepatocytes. Samples were analyzed by LCMS/MS. The peak area of I-BET282 32 was quantified at each time point, and the ratio of this relative to internal standard peak area over a time course was plotted. The intrinsic clearance (CLi) was determined from the first-order elimination rate constant by nonlinear regression using Grafit v 5.0.8 (Erithacus Software Ltd.).

Fraction Unbound in Blood. Control male Balb/C mouse, male Wistar Han rat, and male Beagle dog blood was obtained on the day of experimentation from in-house GSK stock animals. Control human blood from a single nonmedicated donor was obtained from a GSK blood donation unit on the day of the experiment (gender unknown). A nominal 10 mg/mL DMSO stock solution of I-BET282 32 was diluted to 4 mg/mL and further diluted to 200 μg/mL and 20 μg/mL in 50:50 acetonitrile/water, and a 5 μL aliquot of each was spiked into 995 μL of whole blood from each species to achieve nominal

https://doi.org/10.1021/acs.jmedchem.1c00855
J. Med. Chem. 2021, 64, 12200−12227

concentrations of 1000 ng/mL and 100 ng/mL respectively. The fraction unbound of I-BET282 32 at nominal concentrations of 1000 ng/mL and 100 ng/mL in the blood was determined using a rapid equilibrium dialysis technology (RED) plate. Spiked blood was incubated at 37 °C on a roller for 10 min, prior to being dialyzed against phosphate buffered saline solution by incubating the dialysis units at 37 °C for 4 h on an orbital shaker operating at 100 rpm. Following incubation, aliquots of blood and buffer were matrix matched and extracted using acetonitrile containing an analytical internal standard. The samples were shaken for 20 min on a vortex mixer and centrifuged for 30 min at 1600*g*, prior to analysis by LC−MS/MS. The unbound fraction was determined using the peak area ratios between analyte and internal standard in buffer and in blood (mean of $n = 6$ replicates).

Potential for Inhibition of P450 Enzymes CYP1A2, CYP2C9, CYP2C19, CYP2D6, and CYP3A4. Bactosomes expressing CYP450 enzymes were obtained from Cypex Ltd. and were stored at approximately −80 °C prior to experimental use. The inhibition of CYP450-mediated NADPH-dependent mono-oxygenase metabolism of profluorescent probe substrates by test compounds was assessed in a fluorometric assay, with the following recombinant human cytochrome P450s coexpressed in *E. coli* with human NADPH reductase: CYP1A2 with the substrate ethoxyresorufin (ER); CYP2C9 with the substrate 7-methoxy-4-trifluoromethylcoumarin-3-acetic acid (FCA); CYP2C19 with the substrate 3-butyryl-7-methoxycoumarin (BMC); CYP2D6 with the substrate 4-methyl-aminomethyl-7-methoxycoumarin (MMC); and CYP3A4 with the substrates VividGreen and VividRed. For the fluorometric IC_{50} determination assay, DMSO stock solutions of test compounds were incubated for 15−60 min at room temperature (22 ± 0.5 °C) over 11 successive 3-fold dilutions of 50 μM, with bactosomes expressing recombinant human CYP1A2, 2C9, 2C19, 2D6, or 3A4 (Cypex Ltd., Dundee; 0.1 mg protein/mL) in the presence of a profluorescent substrate for the specific CYP isoform under test. At the end of the incubation, the fluorescent intensity of each sample was read on a plate reader (EnVision or ViewLux, PerkinElmer), and pIC_{50} values were determined by automated curve-fitting using ActivityBase (IDBS).

Time-Dependent Inhibition of P450 Enzymes CYP2D6 and CYP3A4. Bactosomes expressing CYP3A4 or CYP2D6 were obtained from Cypex Ltd. and were stored at approximately −80 °C prior to experimental use. A 5 mM stock solution of I-BET282 32 was prepared in methanol and serially diluted to give 1.65, 0.5, 0.165, 0.05, 0.0165, and 0.005 mM solutions, and aliquots of each concentration were incubated with probe substrate (either diethoxyfluorescein, DEF; 7-benzyloxyquinoline, 7-BQ; or 4-methylaminomethyl-7-methoxycoumarin, MMC) and CYP3A4 or CYP2D6 bactosomes in 50 mM phosphate buffer, pH7.4, for 10 min at 37 °C. Reactions were initiated by the addition of a cofactor (an NADPH-regenerating system), and the fluorescent products of metabolism were measured at 1 min intervals over a 30 min time course in a Cytofluor series 4000 fluorescent plate reader. Final incubation concentrations were 0.1−100 μM I-BET282 32, 1 μM DEF or 25 μM, 7-BQ or 10 μM of MMC and 0.1 mg/mL bactosomal protein. Control incubations, containing methanol only, and incubations with the positive control CYP3A4 inhibitor, troleandomycin or the CYP2D6 inhibitor, MDMA at a concentration range 0.01−10 μM were also performed. The rates of fluorescent metabolite production in each well, over each successive 5 min interval, were expressed as a percentage of the uninhibited control rates (in wells containing methanol only), and plotted against I-BET282 32 concentration to determine the IC50. Graphical analysis of data was performed using GraFit v 5.0 (Erithacus Software Ltd.).

***In Vivo* DMPK Studies.** All animal studies were ethically reviewed and carried out in accordance with The Animals (Scientific Procedures) Act 1986 and the GSK Policy on the Care, Welfare and Treatment of Laboratory Animals. For all *in vivo* studies, the temperature and humidity were nominally maintained at 21 °C ± 2 °C and 55% ± 10%, respectively. The diet for rodents was 5LF2 Eurodent Diet 14% (PMI Labdiet, Richmond, IN) and for dogs was Harlan Teklad 2021C (HarlanTeklad, Madison, WI). There were no known contaminants in the diet or water at concentrations that could interfere with the outcome of the studies.

Mouse Surgical Preparation for IV Infusion Study. Male CD1 mice (supplied by Charles River UK Ltd.) were surgically prepared at GSK with cannulae implanted into the jugular vein (for drug administration) while under isoflurane anesthesia. The mice received ampicillin and carprofen (both administered subcutaneously) as a preoperative antibiotic and analgesic, respectively. The mice were allowed to recover for at least 4 days prior to dosing and had free access to food and water throughout.

Mouse IV n = 3 PK Study. Three surgically prepared male CD1 mice received a 1 h intravenous (iv) infusion of I-BET282 32 as a discrete dose formulated in DMSO and 10% (w/v) Kleptose HPB in 0.9% (w/v) saline (2%:98% (v/v)) at a concentration of 0.2 mg/mL, administered at a constant rate of 5 mL/kg/h to achieve a target dose of 1 mg/kg/h. Serial blood samples (20 μL) were collected via the tail vein up to 24 h after the start of the iv infusion and an additional terminal blood sample via cardiac puncture at 26 h after the start of the iv infusion. Diluted blood samples were analyzed for parent compound using a specific LC−MS/MS assay (LLQ = 5 ng/mL). At the end of the study the mice were euthanized by a Schedule 1 method.

Mouse PO n = 3 PK Study. Three naïve male CD1 mice (supplied by Charles River UK Ltd.) with no surgical preparation each received an oral gavage administration of I-BET282 32 as a discrete dose suspended in 1% (w/v) methylcellulose 400 *aq.* at a concentration of 0.6 mg/mL to achieve a target dose of 3 mg/kg. Serial blood samples (20 μL) were collected via direct venipuncture of the tail vein up to 8 h after oral dosing and an additional terminal blood sample via cardiac puncture at 12 h after oral dosing. Diluted blood samples were analyzed for parent compound using a specific LC−MS/MS assay (LLQ = 5 ng/mL). At the end of the study the mice were euthanized by a Schedule 1 method.

Rat Surgical Preparation for IV Infusion Study. Male Wistar Han rats (supplied by Charles River UK Ltd.) were surgically prepared at GSK with cannulae implanted into the vena cava via the femoral vein (for drug administration) and jugular vein (for blood sampling) while under isoflurane anesthesia. The rats received ampicillin (100 mg/kg) and carprofen (7.5 mg/kg), both administered subcutaneously, as a preoperative antibiotic and analgesic, respectively. The rats were allowed to recover for at least 6 days prior to dosing and had free access to food and water throughout.

Rat IV PO n = 3 Crossover PK Study. This study was conducted as a crossover design over two dosing occasions with at least 3 days between dose administrations, in three surgically prepared male Wistar Han Rats. On the first dosing occasion, each rat received a 1 h intravenous (iv) infusion of I-BET282 32 as a discrete dose formulated in DMSO and 10% (w/v) Kleptose HPB in 0.9% (w/v) saline (2%:98% (v/v)) at a concentration of 0.2 mg/mL, administered at a constant rate of 5 mL/kg/h to achieve a target dose of 1 mg/kg/h. On the second dosing occasion, the same three rats received an oral gavage administration of I-BET282 32 as a discrete dose suspended in 1% (w/v) methylcellulose 400 aq. at a concentration of 0.6 mg/mL to achieve a target dose of 3 mg/kg. Serial blood samples (60 μL) were collected predose and up to 26 h after the start of the iv infusion and after oral dosing. Diluted blood samples were analyzed using a specific LC−MS/MS assay (LLQ = 10 ng/mL). At the end of the study the rats were euthanized by a Schedule 1 method.

Rat PO n = 6 PK Study. Six naïve male Wistar Han rats (supplied by Charles River UK Ltd.) with no surgical preparation received an oral gavage administration of I-BET282 32 ($n = 3$) or I-BET282E 75 ($n = 3$) as a discrete dose suspended in 1% hydroxypropylmethyl cellulose (w/v), at a concentration of 0.1 mg/mL to achieve a target dose of 1 mg/kg. Serial blood samples (200 μL) were collected up to 24 h after oral dosing and were centrifuged to obtain plasma. Plasma samples were analyzed for parent compound using a specific HPLC−MS/MS assay (LLQ = 0.5 ng/mL). At the end of the study the rats were euthanized by a Schedule 1 method.

Dog IV PO n = 3 Crossover PK Study. Three healthy, laboratory-bred, male Beagle dogs (supplied by Harlan Laboratories, U.K.) were

https://doi.org/10.1021/acs.jmedchem.1c00855
J. Med. Chem. 2021, 64, 12200−12227

used. The dogs were fasted overnight prior to each dose administration and fed approximately 4 h after the start of dosing and had free access to water throughout the study. This study was conducted as a crossover design, with 7 days between dose administrations. On the first dosing occasion, each dog received a 1 h intravenous (iv) infusion of I-BET282 32 as a discrete dose via cannulation of the saphenous vein. I-BET282 32 was formulated in DMSO and 10% (w/v) Kleptose HPB in 0.9% (w/v) saline (2%:98% (v/v)) at a concentration of 0.2 mg/mL, and administered at a rate of 5 mL/kg/h to achieve a target dose of 1 mg/kg/h. On the second dosing occasion, the same dogs received an oral gavage administration of I-BET282 32 as a discrete dose suspended in 1% (w/v) methylcellulose 400 aq. at a concentration of 1.5 mg/mL to achieve a target dose of 3 mg/kg. A temporary cannula was inserted into the cephalic vein from which serial blood samples (200 μL) were collected predose and up to 2 h after the start of dosing. After collection of the 2 h sample, the cannula was removed and serial blood samples (200 μL) were taken via direct venipuncture of the jugular vein up to 28 h after the start of dosing. Diluted blood samples were analyzed for parent drug concentration using a specific LC−MS/MS assay (LLQ = 1 ng/mL). At the end of the study, the dogs were returned to the colony.

Dog PO n = 4 Crossover PK Study. Four healthy, laboratory-bred, male Beagle dogs (supplied by Harlan Laboratories, U.K.) were used. The dogs were fasted overnight prior to each dose administration and fed approximately 4 h after the start of dosing and had free access to water throughout the study. This study was conducted as a crossover design, with 7 days between dose administrations. On the first dosing occasion, each dog received an oral gavage administration of I-BET282 32 as a discrete dose suspended in 1% hydroxypropylmethyl cellulose (w/v) at a concentration of 0.5 mg/mL to achieve a target dose of 5 mg/kg. On the second dosing occasion, the same dogs received an oral gavage administration of I-BET282E 75 as a discrete dose suspended in 1% hydroxypropylmethyl cellulose (w/v) at a concentration of 0.5 mg/mL to achieve a target dose of 5 mg/kg. Serial blood samples (500 μL) were collected via direct venipuncture of the jugular vein predose and up to 24 h after the start of dosing and centrifuged to obtain plasma. Plasma samples were analyzed for parent drug concentration using a specific HPLC−MS/MS assay (LLQ = 0.5 ng/mL). At the end of the study, the dogs were returned to the colony.

Sample Analysis. Diluted blood samples (1:1 with water) were extracted using protein precipitation with acetonitrile containing an analytical internal standard. An aliquot of the supernatant was analyzed by reverse phase LC−MS/MS using a heat assisted electrospray interface in positive ion mode. Samples were assayed against calibration standards prepared in control blood. Plasma samples were analyzed for I-BET282 32 concentrations using a method based on extraction of plasma by addition of acetonitrile, followed by HPLC-MS/MS analysis.

PK Data Analysis from PK Studies. PK parameters were obtained from the blood or plasma concentration−time profiles using noncompartmental analysis with WinNonlin Professional 6 (Pharsight, Mountain View, CA).

Rat Collagen-Induced Arthritis (CIA). Female Lewis rats (5−6 weeks age) were obtained from Charles River Laboratories UK, housed in groups of 4 according to treatment (n = 8 per group) and acclimatized for 14 days to the laboratory environment. Animals received food and water *ad libitum*. On day 0, arthritis was induced by intradermal injection at the base of the tail of 100 μL containing 200 μg bovine type II collagen (MD Bioproducts, Switzerland) and Incomplete Freund's Adjuvant (IFA; Sigma-Aldrich, UK) emulsion. On day 7 a booster injection containing 200 μg collagen, 3 μg MDP and IFA was given. All rats were dosed orally (p.o.) with 1% methylcellulose (vehicle) once daily from day 0 until day 11. Vehicle or I-BET282E **75** (0.3, 1, or 3 mg/kg) were administered p.o. once daily from day 12 (at onset of symptoms) until day 28, i.e. for 16 days. A further group of rats were orally dosed daily with I-BET151 **5** (3 mg/kg) over the same dosing period. Disease onset is typically 5 days following boost (D12), and is defined as the first day that swelling or erythema of the paws is observed. CIA was assessed visually as a clinical score of hind limbs on days 12−28 and by measurement of paw volume on days 12−26. Body weights were measured daily for the entire duration of the study. Arthritis was assessed blinded by clinical score of hind limbs. Clinical score was recorded on a 0−4 scale per paw according to the following criteria: 0 = no signs of arthritis; 1 = slight edema and erythema on the foot or ankle; 2 = slight edema and erythema to the entire paw; 3 = moderate edema and erythema to the entire paw; 4 = severe edema and ankylosis (the maximum clinical score attainable per animal being 8). Paw swelling was measured using a plethysmometer (Linton Instrumentation, UK) on day 6, 12, 13, 14, 15, 18, 19, and 21 and recorded as the mean paw volume of both hind paws. On day 21, blood was collected via cardiac puncture under terminal anesthesia. Blood was assessed for antirat collagen IgG1 antibodies by ELISA (Chondrex; AMS Biotechnology, UK).

Rats were culled by cervical dislocation and both hind limbs were removed, skinned and fixed in 4% paraformaldehyde, prior to obtaining Micro Computed Tomography (CT) scans processing for histological analysis. After a minimum of 24 h of fixation, the hind limbs were removed from fixative and analyzed (Skyscan 1176 microCT scanner, Bruker). Projection images were acquired through 180° with source voltages and current of 50 kV and 500 mA respectively. Individual 3D reconstructions were generated with individual voxel dimensions of 35 × 35 × 35 μm. A subjective scoring technique examining new bone growth, erosion/uneven bone surface and apparent reduction in joint space was applied to determine the degree of arthritic changes seen in the ankle joints. All scoring was blinded to the treatment group. The number of affected bones per hind limb (maximum of 14 per hind limb: 5 metatarsals, 5 main tarsals, calcaneus, talus, tibia and fibula), and an overall severity between 0 and 4 (none, minimal, mild, moderate, marked) were determined. The severity for each hind limb was calculated as the total number of affected bones multiplied by the severity with a maximum possible score per animal of 112 (sum of both hind limbs).

Following 7 days fixation the hind paws and knees were decalcified in 10% EDTA for 14 days at 4 °C, then embedded in paraffin. Serial paraffin sections (4 μm) were stained with hematoxylin and eosin (H&E). All sections were evaluated histologically by two independent observers, and the gradation of arthritis was scored as described. H&E-stained hind limb sections were examined by light microscopy. Each section was assigned a qualitative score for the severity of arthritic changes; 0 = normal joint architecture, 1 = inflammation virtually absent, minimal synovial thickening, no bone remodeling or fibrosis, 2 = minimal mononuclear cell inflammation, some bone remodeling with rare new bone formation and fibrosis, synovial thickening present, 3 = moderate inflammatory changes and fibrosis with bone remodeling; lesion usually focal, 4 = marked remodeling of the bones, with degeneration/necrosis and new bone formation, chronic active inflammation and fibrosis, extensive lesions, involving all the joints/bones and 5 = severe remodeling of the bones, with degeneration/necrosis and new bone formation, chronic active inflammation, fibrosis and cyst formation, extensive lesions, involving all the joints/bones. Statistical analysis was performed using GraphPad Prism v5.0.4, with an ANOVA test followed by a Dunnett's multiple comparisons test.

■ ASSOCIATED CONTENT

Supporting Information

The Supporting Information is available free of charge at https://pubs.acs.org/doi/10.1021/acs.jmedchem.1c00855.

Crystallography data collection and coordinates, BET bromodomain FRET potency data for I-BET282 (**32**), ITC of I-BET282 (**32**) with BRD4 and CBP, T_m selectivity determination, Powder X-ray diffraction (PXRD), HPLC traces of key compounds, ^{1}H NMR, ^{13}C NMR, and chiral HPLC traces for I-BET282 (**32**) (PDF)

https://doi.org/10.1021/acs.jmedchem.1c00855
J. Med. Chem. 2021, 64, 12200−12227

Molecular formula strings (CSV)

Accession Codes

7O18 (**32**); authors will release the atomic coordinates and experimental data upon article publication.

AUTHOR INFORMATION

Corresponding Author

Katherine L. Jones − *GlaxoSmithKline, Medicines Research Centre, Stevenage, Hertfordshire SG1 2NY, U.K.*; orcid.org/0000-0003-4853-8283; Email: katherine.jones@crl.com

Authors

Dominic M. Beaumont − *GlaxoSmithKline, Medicines Research Centre, Stevenage, Hertfordshire SG1 2NY, U.K.*

Sharon G. Bernard − *GlaxoSmithKline, Medicines Research Centre, Stevenage, Hertfordshire SG1 2NY, U.K.*

Rino A. Bit − *GlaxoSmithKline, Medicines Research Centre, Stevenage, Hertfordshire SG1 2NY, U.K.*

Simon P. Campbell − *GlaxoSmithKline, Medicines Research Centre, Stevenage, Hertfordshire SG1 2NY, U.K.*

Chun-wa Chung − *GlaxoSmithKline, Medicines Research Centre, Stevenage, Hertfordshire SG1 2NY, U.K.*; orcid.org/0000-0002-2480-3110

Leanne Cutler − *GlaxoSmithKline, Medicines Research Centre, Stevenage, Hertfordshire SG1 2NY, U.K.*

Emmanuel H. Demont − *GlaxoSmithKline, Medicines Research Centre, Stevenage, Hertfordshire SG1 2NY, U.K.*; orcid.org/0000-0001-7307-3129

Kate Dennis − *GlaxoSmithKline, Medicines Research Centre, Stevenage, Hertfordshire SG1 2NY, U.K.*

Laurie Gordon − *GlaxoSmithKline, Medicines Research Centre, Stevenage, Hertfordshire SG1 2NY, U.K.*

James R. Gray − *GlaxoSmithKline, Medicines Research Centre, Stevenage, Hertfordshire SG1 2NY, U.K.*

Michael V. Haase − *GlaxoSmithKline, Medicines Research Centre, Stevenage, Hertfordshire SG1 2NY, U.K.*

Antonia J. Lewis − *GlaxoSmithKline, Medicines Research Centre, Stevenage, Hertfordshire SG1 2NY, U.K.*

Scott McCleary − *GlaxoSmithKline, Medicines Research Centre, Stevenage, Hertfordshire SG1 2NY, U.K.*

Darren J. Mitchell − *GlaxoSmithKline, Medicines Research Centre, Stevenage, Hertfordshire SG1 2NY, U.K.*

Susanne M. Moore − *GlaxoSmithKline, Medicines Research Centre, Stevenage, Hertfordshire SG1 2NY, U.K.*

Nigel Parr − *GlaxoSmithKline, Medicines Research Centre, Stevenage, Hertfordshire SG1 2NY, U.K.*

Olivia J. Robb − *GlaxoSmithKline, Medicines Research Centre, Stevenage, Hertfordshire SG1 2NY, U.K.*

Nicholas Smithers − *GlaxoSmithKline, Medicines Research Centre, Stevenage, Hertfordshire SG1 2NY, U.K.*

Peter E. Soden − *GlaxoSmithKline, Medicines Research Centre, Stevenage, Hertfordshire SG1 2NY, U.K.*

Colin J. Suckling − *Department of Pure & Applied Chemistry, University of Strathclyde, Glasgow G1 1XL, U.K.*

Simon Taylor − *GlaxoSmithKline, Medicines Research Centre, Stevenage, Hertfordshire SG1 2NY, U.K.*

Ann L. Walker − *GlaxoSmithKline, Medicines Research Centre, Stevenage, Hertfordshire SG1 2NY, U.K.*; orcid.org/0000-0002-1027-2099

Robert J. Watson − *GlaxoSmithKline, Medicines Research Centre, Stevenage, Hertfordshire SG1 2NY, U.K.*

Rab K. Prinjha − *GlaxoSmithKline, Medicines Research Centre, Stevenage, Hertfordshire SG1 2NY, U.K.*

Complete contact information is available at: https://pubs.acs.org/10.1021/acs.jmedchem.1c00855

Notes

The authors declare no competing financial interest.

ACKNOWLEDGMENTS

We thank Frédéric Donche, Amanda Emmons, Hannah Fleetwood, and Alex Phillipou for supporting laboratory contributions, and Inma Rioja for her assistance with manuscript preparation.

ABBREVIATIONS USED

ATAD2, ATPase family AAA domain-containing protein 2; AUC, area under the curve; BAZ2A, bromodomain adjacent to zinc finger domain protein 2A; BD1, first (*N*-terminal) bromodomain; BD2, second (*C*-terminal) bromodomain; BET, bromodomain and extraterminal; CBP, CREB-binding protein; CIA, collagen-induced arthritis; CYP, cytochrome P450; DIPEA, diisopropylethylamine; DMPK, drug metabolism and pharmacokinetic; EDC, N^1-((ethylimino)methylene)-N^3,N^3-dimethylpropane-1,3-diamine; FaSSIF, fasted state simulated intestinal fluid; HATU, 1-[bis(dimethylamino)-methylene]-1*H*-1,2,3-triazolo[4,5-*b*]-pyridinium 3-oxide hexafluorophosphate; HEPES, 4-(2-hydroxyethyl) piperazine-1-ethanesulfonic acid; hERG, human ether-à-go-go-related gene; HPV, human papillomavirus; HPLC, high-performance liquid chromatography; HWB, human whole blood; IL-6, interleukin 6; ITC, isothermal titration calorimetry; LLE, lipophilic ligand efficiency; LPS, lipopolysaccharide; MDAP, mass-directed autopreparative high-performance liquid chromatography; MDCK, Madin-Darby canine kidney; NMC, nuclear protein in testis midline carcinoma; PBMC, peripheral blood mononuclear cell; PCAF, P300/CBP-associated factor; SAR, structure activity relationship; SP140, nuclear body protein SP140; TRF, time-resolved fluorescence; PXRD, powder X-ray diffraction

REFERENCES

(1) Tamkun, J. W.; Deuring, R.; Scott, M. P.; Kissinger, M.; Pattatucci, A. M.; Kaufman, T. C.; Kennison, J. A. Brahma: a regulator of Drosophila homeotic genes structurally related to the yeast transcriptional activator SNF2/SWI2. *Cell* **1992**, *68*, 561−72.

(2) Haynes, S. R.; Dollard, C.; Winston, F.; Beck, S.; Trowsdale, J.; Dawid, I. B. The bromodomain: a conserved sequence found in human, Drosophila and yeast proteins. *Nucleic Acids Res.* **1992**, *20*, 2603−2603.

(3) Brownell, J. E.; Allis, C. D. Special HATs for special occasions: linking histone acetylation to chromatin assembly and gene activation. *Curr. Opin. Genet. Dev.* **1996**, *6*, 176−84.

(4) Turner, B. M. Histone acetylation and an epigenetic code. *BioEssays* **2000**, *22* (9), 836−45.

(5) Filippakopoulos, P.; Picaud, S.; Mangos, M.; Keates, T.; Lambert, J.-P.; Barsyte-Lovejoy, D.; Felletar, I.; Volkmer, R.; Müller, S.; Pawson, T.; Gingras, A.-C.; Arrowsmith, C. H.; Knapp, S. Histone recognition and large-scale structural analysis of the human bromodomain family. *Cell* **2012**, *149*, 214−231.

(6) Wu, S. Y.; Chiang, C. M. The double bromodomain-containing chromatin adaptor Brd4 and transcriptional regulation. *J. Biol. Chem.* **2007**, *282*, 13141−13145.

(7) Nakamura, Y.; Umehara, T.; Nakano, K.; Jang, M. K.; Shirouzu, M.; Morita, S.; Uda-Tochio, H.; Hamana, H.; Terada, T.; Adachi, N.;

Matsumoto, T.; Tanaka, A.; Horikoshi, M.; Ozato, K.; Padmanabhan, B.; Yokoyama, S. Crystal structure of the human BRD2 bromodomain: insights into dimerization and recognition of acetylated histone H4. *J. Biol. Chem.* **2007**, *282*, 4193−4201.
(8) Filippakopoulos, P.; Qi, J.; Picaud, S.; Shen, Y.; Smith, W. B.; Fedorov, O.; Morse, E. M.; Keates, T.; Hickman, T. T.; Felletar, I.; Philpott, M.; Munro, S.; McKeown, M. R.; Wang, Y.; Christie, A. L.; West, N.; Cameron, M. J.; Schwartz, B.; Heightman, T. D.; La Thangue, N.; French, C. A.; Wiest, O.; Kung, A. L.; Knapp, S.; Bradner, J. E. Selective inhibition of BET bromodomains. *Nature* **2010**, *468*, 1067−1073.
(9) Delmore, J. E.; Issa, G. C.; Lemieux, M. E.; Rahl, P. B.; Shi, J.; Jacobs, H. M.; Kastritis, E.; Gilpatrick, T.; Paranal, R. M.; Qi, J.; Chesi, M.; Schinzel, A. C.; McKeown, M. R.; Heffernan, T. P.; Vakoc, C. R.; Bergsagel, P. L.; Ghobrial, I. M.; Richardson, P. G.; Young, R. A.; Hahn, W. C.; Anderson, K. C.; Kung, A. L.; Bradner, J. E.; Mitsiades, C. S. BET bromodomain inhibition as a therapeutic strategy to target c-Myc. *Cell* **2011**, *146*, 904−917.
(10) Mertz, J. A.; Conery, A. R.; Bryant, B. M.; Sandy, P.; Balasubramanian, S.; Mele, D. A.; Bergeron, L.; Sims, R. J. Targeting MYC dependence in cancer by inhibiting BET bromodomains. *Proc. Natl. Acad. Sci. U. S. A.* **2011**, *108*, 16669−16674.
(11) Asangani, I. A.; Dommeti, V. L.; Wang, X.; Malik, R.; Cieslik, M.; Yang, R.; Escara-Wilke, J.; Wilder-Romans, K.; Dhanireddy, S.; Engelke, C.; Iyer, M. K.; Jing, X.; Wu, Y.-M.; Cao, X.; Qin, Z. S.; Wang, S.; Feng, F. Y.; Chinnaiyan, A. M. Therapeutic targeting of BET bromodomain proteins in castration-resistant prostate cancer. *Nature* **2014**, *510*, 278−282.
(12) Puissant, A.; Frumm, S. M.; Alexe, G.; Bassil, C. F.; Qi, J.; Chanthery, Y. H.; Nekritz, E. A.; Zeid, R.; Gustafson, W. C.; Greninger, P.; Garnett, M. J.; McDermott, U.; Benes, C. H.; Kung, A. L.; Weiss, W. A.; Bradner, J. E.; Stegmaier, K. Targeting MYCN in neuroblastoma by BET bromodomain inhibition. *Cancer Discovery* **2013**, *3*, 308−323.
(13) Dawson, M. A.; Prinjha, R. K.; Dittmann, A.; Giotopoulos, G.; Bantscheff, M.; Chan, W.-I.; Robson, S. C.; Chung, C.-w.; Hopf, C.; Savitski, M. M.; Huthmacher, C.; Gudgin, E.; Lugo, D.; Beinke, S.; Chapman, T. D.; Roberts, E. J.; Soden, P. E.; Auger, K. R.; Mirguet, O.; Doehner, K.; Delwel, R.; Burnett, A. K.; Jeffrey, P.; Drewes, G.; Lee, K.; Huntly, B. J. P.; Kouzarides, T. Inhibition of BET recruitment to chromatin as an effective treatment for MLL-fusion leukaemia. *Nature* **2011**, *478*, 529−533.
(14) Shi, J.; Vakoc, C. R. The mechanisms behind the therapeutic activity of BET bromodomain inhibition. *Mol. Cell* **2014**, *54*, 728−736.
(15) Nicodeme, E.; Jeffrey, K. L.; Schaefer, U.; Beinke, S.; Dewell, S.; Chung, C. W.; Chandwani, R.; Marazzi, I.; Wilson, P.; Coste, H.; White, J.; Kirilovsky, J.; Rice, C. M.; Lora, J. M.; Prinjha, R. K.; Lee, K.; Tarakhovsky, A. Suppression of inflammation by a synthetic histone mimic. *Nature* **2010**, *468*, 1119−1123.
(16) Wu, S.-Y.; Lee, A. Y.; Hou, S. Y.; Kemper, J. K.; Erdjument-Bromage, H.; Tempst, P.; Chiang, C.-M. Brd4 links chromatin targeting to HPV transcriptional silencing. *Genes Dev.* **2006**, *20*, 2383−2396.
(17) Morse, M. A.; Balogh, K. K.; Brendle, S. A.; Campbell, C. A.; Chen, M. X.; Furze, R. C.; Harada, I. L.; Holyer, I. D.; Kumar, U.; Lee, K.; Prinjha, R. K.; Rüdiger, M.; Seal, J. T.; Taylor, S.; Witherington, J.; Christensen, N. D. BET bromodomain inhibitors show anti-papillomavirus activity in vitro and block CRPV wart growth in vivo. *Antiviral Res.* **2018**, *154*, 158−165.
(18) Wang, F.; Liu, H.; Blanton, W. P.; Belkina, A.; Lebrasseur, N. K.; Denis, G. V. Brd2 disruption in mice causes severe obesity without Type 2 diabetes. *Biochem. J.* **2010**, *425*, 71−83.
(19) Theodoulou, N. H.; Tomkinson, N. C.; Prinjha, R. K.; Humphreys, P. G. Clinical progress and pharmacology of small molecule bromodomain inhibitors. *Curr. Opin. Chem. Biol.* **2016**, *33*, 58−66.
(20) Alqahtani, A.; Choucair, K.; Ashraf, M.; Hammouda, D. M.; Alloghbi, A.; Khan, T.; Senzer, N.; Nemunaitis, J. Bromodomain and extra-terminal motif inhibitors: a review of preclinical and clinical advances in cancer therapy. *Future Sci. OA* **2019**, *5* (3), FSO372−FSO372.
(21) Mirguet, O.; Gosmini, R.; Toum, J.; Clement, C. A.; Barnathan, M.; Brusq, J. M.; Mordaunt, J. E.; Grimes, R. M.; Crowe, M.; Pineau, O.; Ajakane, M.; Daugan, A.; Jeffrey, P.; Cutler, L.; Haynes, A. C.; Smithers, N. N.; Chung, C. W.; Bamborough, P.; Uings, I. J.; Lewis, A.; Witherington, J.; Parr, N.; Prinjha, R. K.; Nicodeme, E. Discovery of epigenetic regulator I-BET762: lead optimization to afford a clinical candidate inhibitor of the BET bromodomains. *J. Med. Chem.* **2013**, *56*, 7501−7515.
(22) Herait, P. E.; Berthon, C.; Thieblemont, C.; Raffoux, E.; Magarotto, V.; Stathis, A.; Thomas, X.; Leleu, X.; Gomez-Roca, C.; Odore, E.; Roumier, C.; Bourdel, F.; Quesnel, B.; Zucca, E.; Michallet, M.; Recher, C.; Cvitkovic, E.; Rezai, K.; Preudhomme, C.; Facon, T.; Palumbo, A.; Dombret, H. Abstract CT231: BET-bromodomain inhibitor OTX015 shows clinically meaningful activity at nontoxic doses: interim results of an ongoing phase I trial in hematologic malignancies. *Cancer Res.* **2014**, *74* (19 Supplement), CT231.
(23) McDaniel, K. F.; Wang, L.; Soltwedel, T.; Fidanze, S. D.; Hasvold, L. A.; Liu, D.; Mantei, R. A.; Pratt, J. K.; Sheppard, G. S.; Bui, M. H.; Faivre, E. J.; Huang, X.; Li, L.; Lin, X.; Wang, R.; Warder, S. E.; Wilcox, D.; Albert, D. H.; Magoc, T. J.; Rajaraman, G.; Park, C. H.; Hutchins, C. W.; Shen, J. J.; Edalji, R. P.; Sun, C. C.; Martin, R.; Gao, W.; Wong, S.; Fang, G.; Elmore, S. W.; Shen, Y.; Kati, W. M. Discovery of N-(4-(2,4-difluorophenoxy)-3-(6-methyl-7-oxo-6,7-dihydro-1H-pyrrolo[2,3-c]pyridin-4-yl)phenyl)ethanesulfonamide (ABBV-075/Mivebresib), a potent and orally available bromodomain and extraterminal domain (BET) family bromodomain inhibitor. *J. Med. Chem.* **2017**, *60*, 8369−8384.
(24) McLure, K. G.; Gesner, E. M.; Tsujikawa, L.; Kharenko, O. A.; Attwell, S.; Campeau, E.; Wasiak, S.; Stein, A.; White, A.; Fontano, E.; Suto, R. K.; Wong, N. C. W.; Wagner, G. S.; Hansen, H. C.; Young, P. R. RVX-208, an inducer of ApoA-I in humans, is a BET bromodomain antagonist. *PLoS One* **2013**, *8*, e83190.
(25) Van der Feen, D. E.; Kurakula, K.; Tremblay, E.; Boucherat, O.; Bossers, G. P. L.; Szulcek, R.; Bourgeois, A.; Lampron, M. C.; Habbout, K.; Martineau, S.; Paulin, R.; Kulikowski, E.; Jahagirdar, R.; Schalij, I.; Bogaard, H. J.; Bartelds, B.; Provencher, S.; Berger, R. M. F.; Bonnet, S.; Goumans, M. J. Multicenter preclinical validation of BET inhibition for the treatment of pulmonary arterial hypertension. *Am. J. Respir. Crit. Care Med.* **2019**, *200*, 910−920.
(26) Petretich, M.; Demont, E. H.; Grandi, P. Domain-selective targeting of BET proteins in cancer and immunological diseases. *Curr. Opin. Chem. Biol.* **2020**, *57*, 184−193.
(27) Stock, D.; Molinoff, P. The value of backup compounds to drug development programs. *Drug Inf. J.* **2002**, *36*, 95−113.
(28) Mirguet, O.; Lamotte, Y.; Donche, F.; Toum, J.; Gellibert, F.; Bouillot, A.; Gosmini, R.; Nguyen, V. L.; Delannee, D.; Seal, J.; Blandel, F.; Boullay, A. B.; Boursier, E.; Martin, S.; Brusq, J. M.; Krysa, G.; Riou, A.; Tellier, R.; Costaz, A.; Huet, P.; Dudit, Y.; Trottet, L.; Kirilovsky, J.; Nicodeme, E. From ApoA1 upregulation to BET family bromodomain inhibition: discovery of I-BET151. *Bioorg. Med. Chem. Lett.* **2012**, *22*, 2963−2967.
(29) Bamborough, P.; Diallo, H.; Goodacre, J. D.; Gordon, L.; Lewis, A.; Seal, J. T.; Wilson, D. M.; Woodrow, M. D.; Chung, C. W. Fragment-based discovery of bromodomain inhibitors part 2: optimization of phenylisoxazole sulfonamides. *J. Med. Chem.* **2012**, *55*, 587−596.
(30) Hewings, D. S.; Wang, M.; Philpott, M.; Fedorov, O.; Uttarkar, S.; Filippakopoulos, P.; Picaud, S.; Vuppusetty, C.; Marsden, B.; Knapp, S.; Conway, S. J.; Heightman, T. D. 3,5-Dimethylisoxazoles act as acetyl-lysine-mimetic bromodomain ligands. *J. Med. Chem.* **2011**, *54*, 6761−6770.
(31) Jennings, L. E.; Schiedel, M.; Hewings, D. S.; Picaud, S.; Laurin, C. M. C.; Bruno, P. A.; Bluck, J. P.; Scorah, A. R.; See, L.; Reynolds, J. K.; Moroglu, M.; Mistry, I. N.; Hicks, A.; Guzanov, P.; Clayton, J.; Evans, C. N. G.; Stazi, G.; Biggin, P. C.; Mapp, A. K.; Hammond, E. M.; Humphreys, P. G.; Filippakopoulos, P.; Conway, S. J. BET

bromodomain ligands: probing the WPF shelf to improve BRD4 bromodomain affinity and metabolic stability. *Bioorg. Med. Chem.* **2018**, *26*, 2937−2957.
(32) Xue, X.; Zhang, Y.; Wang, C.; Zhang, M.; Xiang, Q.; Wang, J.; Wang, A.; Li, C.; Zhang, C.; Zou, L.; Wang, R.; Wu, S.; Lu, Y.; Chen, H.; Ding, K.; Li, G.; Xu, Y. Benzoxazinone-containing 3,5-dimethylisoxazole derivatives as BET bromodomain inhibitors for treatment of castration-resistant prostate cancer. *Eur. J. Med. Chem.* **2018**, *152*, 542−559.
(33) Zhao, Y.; Zhou, B.; Bai, L.; Liu, L.; Yang, C.-Y.; Meagher, J. L.; Stuckey, J. A.; McEachern, D.; Przybranowski, S.; Wang, M.; Ran, X.; Aguilar, A.; Hu, Y.; Kampf, J. W.; Li, X.; Zhao, T.; Li, S.; Wen, B.; Sun, D.; Wang, S. Structure-based discovery of CF53 as a potent and orally bioavailable bromodomain and extra-terminal (BET) bromodomain inhibitor. *J. Med. Chem.* **2018**, *61*, 6110−6120.
(34) Denny, R. A.; Flick, A. C.; Coe, J.; Langille, J.; Basak, A.; Liu, S.; Stock, I.; Sahasrabudhe, P.; Bonin, P.; Hay, D. A.; Brennan, P. E.; Pletcher, M.; Jones, L. H.; Chekler, E. L. P. Structure-based design of highly selective inhibitors of the CREB binding protein bromodomain. *J. Med. Chem.* **2017**, *60*, 5349−5363.
(35) Ritchie, T. J.; Macdonald, S. J. The impact of aromatic ring count on compound developability–are too many aromatic rings a liability in drug design? *Drug Discovery Today* **2009**, *14*, 1011−1020.
(36) Hughes, J. D.; Blagg, J.; Price, D. A.; Bailey, S.; Decrescenzo, G. A.; Devraj, R. V.; Ellsworth, E.; Fobian, Y. M.; Gibbs, M. E.; Gilles, R. W.; Greene, N.; Huang, E.; Krieger-Burke, T.; Loesel, J.; Wager, T.; Whiteley, L.; Zhang, Y. Physiochemical drug properties associated with in vivo toxicological outcomes. *Bioorg. Med. Chem. Lett.* **2008**, *18*, 4872−4875.
(37) Wellaway, C. R.; Bamborough, P.; Bernard, S. G.; Chung, C.-w.; Craggs, P. D.; Cutler, L.; Demont, E. H.; Evans, J. P.; Gordon, L.; Karamshi, B.; Lewis, A. J.; Lindon, M. J.; Mitchell, D. J.; Rioja, I.; Soden, P. E.; Taylor, S.; Watson, R. J.; Willis, R.; Woolven, J. M.; Wyspiańska, B. S.; Kerr, W. J.; Prinjha, R. K. Structure-based design of a bromodomain and extraterminal domain (BET) inhibitor selective for the N-terminal bromodomains that retains an anti-inflammatory and antiproliferative phenotype. *J. Med. Chem.* **2020**, *63*, 9020−9044.
(38) Leeson, P. D.; Springthorpe, B. The influence of drug-like concepts on decision-making in medicinal chemistry. *Nat. Rev. Drug Discovery* **2007**, *6*, 881−890.
(39) Goodwin, J. T.; Conradi, R. A.; Ho, N. F. H.; Burton, P. S. Physicochemical determinants of passive membrane permeability: role of solute hydrogen-bonding potential and volume. *J. Med. Chem.* **2001**, *44*, 3721−3729.
(40) Prakash, O.; Batra, H.; Kaur, H.; Sharma, P. K.; Sharma, V.; Singh, S. P.; Moriarty, R. M. Hypervalent iodine oxidative rearrangement of anthranilamides, salicylamides and some β-substituted amides: a new and convenient synthesis of 2-benzimidazolones, 2-benzoxazolones and related compounds. *Synthesis* **2001**, *2001*, 541−543.
(41) Katavolos, P.; Cain, G.; Farman, C.; Romero, F. A.; Magnuson, S.; Ly, J. Q.; Choo, E. F.; Katakam, A. K.; Andaya, R.; Maher, J. Preclinical safety assessment of a highly selective and potent dual small-molecule inhibitor of CBP/P300 in rats and dogs. *Toxicol. Pathol.* **2020**, *48*, 465−480.
(42) Chemburkar, S. R.; Bauer, J.; Deming, K.; Spiwek, H.; Patel, K.; Morris, J.; Henry, R.; Spanton, S.; Dziki, W.; Porter, W.; Quick, J.; Bauer, P.; Donaubauer, J.; Narayanan, B. A.; Soldani, M.; Riley, D.; McFarland, K. Dealing with the impact of ritonavir polymorphs on the late stages of bulk drug process development. *Org. Process Res. Dev.* **2000**, *4*, 413−417.
(43) Vertzoni, M.; Dressman, J.; Butler, J.; Hempenstall, J.; Reppas, C. Simulation of fasting gastric conditions and its importance for the in vivo dissolution of lipophilic compounds. *Eur. J. Pharm. Biopharm.* **2005**, *60*, 413−417.
(44) Serajuddin, A. T. Salt formation to improve drug solubility. *Adv. Drug Delivery Rev.* **2007**, *59*, 603−616.
(45) ClinicalTrials.gov. Dose Escalation Study of GSK2820151 in Subjects With Advanced or Recurrent Solid Tumors. https://clinicaltrials.gov/ct2/show/NCT02630251 (accessed 23 July).
(46) Mita, M. M.; Mita, A. C. Bromodomain inhibitors a decade later: a promise unfulfilled? *Br. J. Cancer* **2020**, *123*, 1713−1714.
(47) Postel-Vinay, S.; Herbschleb, K.; Massard, C.; Woodcock, V.; Soria, J.-C.; Walter, A. O.; Ewerton, F.; Poelman, M.; Benson, N.; Ocker, M.; Wilkinson, G.; Middleton, M. First-in-human phase I study of the bromodomain and extraterminal motif inhibitor BAY 1238097: emerging pharmacokinetic/pharmacodynamic relationship and early termination due to unexpected toxicity. *Eur. J. Cancer* **2019**, *109*, 103−110.
(48) Emsley, P.; Cowtan, K. Coot: model-building tools for molecular graphics. *Acta Crystallogr., Sect. D: Biol. Crystallogr.* **2004**, *60*, 2126−2132.
(49) Collaborative Computational Project, No. 4. The CCP4 suite: programs for protein crystallography. *Acta Crystallogr., Sect. D: Biol. Crystallogr.* **1994**, *50*, 760−763.

https://doi.org/10.1021/acs.jmedchem.1c00855
J. Med. Chem. 2021, 64, 12200−12227